

PROJECT REPORT
ON
A DUAL-BAND CIRCULARLY POLARISED PATCH ARRAY ANTENNA
FOR
PHASE-ONLY BEAM SHAPING WITH ELEMENT ROTATION.

A project report submitted in partial fulfilment of the requirements for award of the Degree of
BACHELOR OF TECHNOLOGY
In
ELECTRONICS AND COMMUNICATION ENGINEERING
IS A BONAFIED RECORD OF WORK DONE BY

D. NARASIMHARAO	20KP1A0425
D. KAVITHA	20KP1A0426
G.SIRISHA	20KP1A0441
A. SANGEETHA	21KP5A0401

Under the Esteemed Guidance of
CH.V.S.N.MURTHY



DEPARTMENT OF ELECTRONICS AND COMMUNICATIONENGINEERING
NRI INSTITUTE OF TECHNOLOGY
(Approved by AICTE, Affiliated to JNTU, Kakinada.)
VISADALA (P.O.), MEDIKONDURU MANDAL, GUNTUR-522 438 ANDHRA PRADESH.
2020-2024

NRI INSTITUTE OF TECHNOLOGY

(Approved by AICTE, Affiliated to JNTU, KAKINADA) VISADALA
(P.O.), MEDIKONDURU MANDAL, GUNTURANDHRA PRADESH.



CERTIFICATE

This is to certify that the project report entitled "**A DUAL- BAND CIRCULARLY POLARISED PATCH ARRAY ANTENNA FOR PHASE-ONLY BEAM SHAPING WITH ELEMENT ROTATION**" Is a bonafied record of work out by the members. **D.NARASIMHA RAO(20KP1A0425), D.KAVITHA (20KP1A0426), G.SIRISHA(20KP1A0441), A.SANGEETHA(21KP5A0401)** who carried out the research under the super vision .Certified further ,that to the best of knowledge the work reported here in does not form part of any other Project report or dissertation on the basis of which a degree of award was conferred on an earlier occasionon this or any other candidates.

This work is done under the supervision and guidance.

Signature of the Guide
CH.V.S.N.MURTHY

Signature of Head of Dept
Dr. K.SRIHARI RAO
PROFESSOR & HOD

ACKNOWLEDGEMENT

We are highly indebted to our **guide CH.V.S.N.MURTHY, Department of ELECTRONICS AND COMMUNICATION ENGINEERING, NRI INSTITUTE OF TECHNOLOGY, VISADALA, MEDIKONDURU, GUNTUR** for his valuable guidance in the successful completion of our project work. We are very much indebted to her for suggesting this interesting topic and helping us at every stage for its successful completion.

It is a great pleasure to convey our sincere thanks to our Hon'ble **Chairman Dr. Alapati Ravindra garu** and Hon'ble **Secretary and Correspondent SriAlapati Rajendra Prasad garu** for providing excellent facilities and everything for our success.

Our sincere thanks to respected **Principal, Dr. KOTA.SRINIVASU garu** for his co-operation and valuable suggestions during our stay in this institute.

We thank our respected **Executive director, Chief Executive Officer, Chief Finance Officer and Administrative Officer** for their co-operation and valuable support during our stay in this institute. We thank respected **Vice Principal** for his valuable suggestions and motivation during our stay.

Our heartfelt thanks to beloved **HOD of our department Dr. K. SRI HARI RAO** for his motivation, care and valuable guidance at every step of our project work and in every aspect for our success.

We thank wholeheartedly our **project coordinators Dr. Kalaiselvan, Professor and Dr. Saidaiyah, Professor** For their special care towards completion of our project in smooth manner.

It's our pleasure to thank all the **faculty members of ECE department** for extending their constant co-operation and support during our stay in NRIIT.

Our heartiest thanks to our **beloved parents** who are well behind us for all our success as well as achievements.

Finally, we thank all our **friends** who helped either directly or indirectly to achieve of Goal

- | | |
|-------------------|-------------|
| 1. D.NARASIMHARAO | -20KP1A0425 |
| 2. D.KAVITHA | -20KP1A0426 |
| 3. G.SIRISHA | -20KP1A0441 |
| 4. A.SANGEETHA | -21KP5A0401 |

DECLARATION

We hereby declare that the work which is being presented in the Dissertation Entitled "**A DUAL-BAND CIRCULARLY POLARIZED PATCH ARRAY ANTENNA FOR PHASE-ONLY BEAM SHAPING WITH ELEMENT ROTATION**" submitted towards the partial fulfilment of requirements for the award of the degree in Bachelor of Technology and authentic record in Department of Electronics and Communication Engineering at NRIInstitute of Technology, Guntur.

The matter embodied in this dissertation report has not been submitted by us for the award of any other degree. Further the technical details furnished in the various chapters in this report are purely relevantto the above project and there is no deviation from the theoretical point ofview for design, development and implementation.

PROJECT MEMBERS:

D.NARASIMHARAO	-20KP1A0425
D.KAVITHA	-20KP1A0426
G.SIRISHA	-20KP1A0441
A.SANGEETHA	-21KP5A0401

INSTITUTE OF TECHNOLOGY

(Approved by AICTE, Approved by JNTU, Kakinada)
Visdala (P.O), Medikonduru (M), Guntur-522438, Andhra Pradesh

INSTITUTE VISION:

To become reputed institution of Engineering & Management programs, producing competitive, ethical & socially responsible professionals.

INSTITUTE MISSION:

IM1: Provide quality education through best teaching and learning practices of committed staff.

NRI

IM2: Establish a continuous interaction, participation and collaboration with industry to provide solutions.

IM3: Provide the facilities that motivate/encourage faculty and students in research and development activities.

IM4: Develop human values, professional ethics, and interpersonal skills amongst the individuals.



(Alapati Rajendra Prasad)

Secretary & Correspondent



(Dr. Kota Srinivasu)

PRINCIPAL

NRI INSTITUTE OF TECHNOLOGY
DEPARTMENT OF ELECTRONICS & COMMUNICATION ENGINEERING

PROGRAMME SPECIFIC OUTCOMES

PSO1: Professional Knowledge: Apply the concepts of electronics and communications to arrive at cost effective and appropriate solutions.

PSO2: Problem-solving skills: Apply the principles of analog, digital and signal processing systems for consumer electronics, medical and radar systems.

PSO3: Software usage: Use Computer Simulation Technology, and to design integrated circuits and analyse signals.

**SIGNATURE OF
HOD**

NRI INSTITUTE OF TECHNOLOGY

DEPARTMENT OF ELECTRONICS & COMMUNICATION ENGINEERING

Program Outcomes (PO's)

- 1. Engineering knowledge:** Apply the knowledge of mathematics, science, engineering fundamentals, and an engineering specialization to the solution of complex engineering problems.
- 2. Problem analysis:** Identify, formulate, research literature, and analyse complex engineering problems reaching substantiated conclusions using first principles of mathematics, natural sciences, and engineering sciences.
- 3. Design/development of solutions:** Design solutions for complex engineering problems and design system components or processes that meet the specified needs with appropriate consideration for the public health and safety, and the cultural, societal, and environmental considerations.
- 4. Conduct investigations of complex problems:** Use research-based knowledge and research methods including design of experiments, analysis and interpretation of data, and synthesis of the information to provide valid conclusions.
- 5. Modern tool usage:** Create, select, and apply appropriate techniques, resources, and modern engineering and IT tools including prediction and modelling to complex engineering activities with an understanding of the limitations.
- 6. The engineer and society:** Apply reasoning informed by the contextual knowledge to assess societal, health, safety, legal and cultural issues and the consequent responsibilities relevant to the professional engineering practice.
- 7. Environment and sustainability:** Understand the impact of the professional engineering solutions in societal and environmental contexts, and demonstrate the knowledge of, and need for sustainable development.
- 8. Ethics:** Apply ethical principles and commit to professional ethics and responsibilities and norms of the engineering practice.
- 9. Individual and team work:** Function effectively as an individual, and as a member or leader in diverse teams, and in multidisciplinary settings.
- 10. Communication:** Communicate effectively on complex engineering activities with the engineering community and with society at large, such as, being able to comprehend and write effective reports and design documentation, make effective presentations, and give and receive clear instructions.
- 11. Project management and finance:** Demonstrate knowledge and understanding of the engineering and management principles and apply these to one's own work, as a member or leader in a team, to manage projects and in multidisciplinary environments.
- 12. Life-long learning:** Recognize the need for, and have the preparation and ability to engage in independent and life-long learning in the broadest context of technological change.

ABSTRACT

Wireless technology is one of the main areas of research in the world of communication systems today and a study of communication systems is incomplete without an understanding of the operation and fabrication of antennas. This was the main reason for our selecting a project focusing on this field.

The field of antenna study is an extremely vast one, so, to grasp the fundamentals we used a two pronged approach by dividing ourselves into groups.

The first group focused on the fabrication and testing of a slotted waveguide omni directional antenna and a biquad directional antenna.

The second group focused on the design and simulation of patch antennas (which are widely used in cell phones today) with an emphasis on optimization of a 1.9 GHz rectangular probe fed patch antenna. A dual band antenna and a microstrip fed patch antenna, used in the communication lab were also simulated.

Contents

Chapter 1 - Introduction to Antennas	1
1.1 Antenna Parameters	1
1.2 Types of Antennas	9
Chapter 2 – Hardware Aspects – Fabrication and Testing of RF Antennas	13
2.1 Introduction	13
2.2 Slotted Waveguide Antenna	13
2.3 Biquad Antenna	16
2.4 Testing of the Antennas	20
Chapter 3 – Software Aspects – Design and Simulation of Microstrip Patch Antennas	26
3.1 Introduction	26
3.2 Applications of Microstrip Patch Antennas	28
3.3 Advantages and Disadvantages of Patch Antennas	29
3.4 Feed Techniques	29
3.5 Methods of Analysis	34
3.6 Simulation Software – IE3D	40

3.7 Design of a Simple Rectangular Patch Antenna	41
3.8 Simulation of 1.9 GHz Patch Antenna	43
3.9 Simulation of 5GHz Patch Antenna	70
3.10 Simulation of Dual Band Patch Antennas	74
Chapter 4 – Conclusions and Scope for Improvement	85
4.1 Conclusions	85
4.2 Scope for Improvement	85
Appendix A - MATLAB Codes	86
Appendix B - Data on Equipment used for Antenna Analysis	88
References	92

Chapter 1

Introduction to Antennas

Our project focuses on the hardware fabrication and software simulation of several antennas. In order to completely understand the above it is necessary to start off by understanding various terms associated with antennas and the various types of antennas. This is what is covered in this introductory chapter.

1.1 Antenna parameters

An antenna is an electrical conductor or system of conductors

Transmitter - Radiates electromagnetic energy into space

Receiver - Collects electromagnetic energy from space

The IEEE definition of an antenna as given by Stutzman and Thiele is, “That part of a transmitting or receiving system that is designed to radiate or receive electromagnetic waves”. The major parameters associated with an antenna are defined in the following sections.

1.1.1 Antenna Gain

Gain is a measure of the ability of the antenna to direct the input power into radiation in a particular direction and is measured at the peak radiation intensity. Consider the power density radiated by an isotropic antenna with input power P_0 at a distance R which is given by $S = P_0/4\pi R^2$. An isotropic antenna radiates equally in all directions, and its radiated power density S is found by dividing the radiated power by the area of the sphere $4\pi R^2$. An isotropic radiator is considered to be 100% efficient. The gain of an actual antenna increases the power density in the direction of the peak radiation:

$$S = \frac{P_0 G}{4\pi R^2} = \frac{|\mathbf{E}|^2}{\eta} \quad \text{or} \quad |\mathbf{E}| = \frac{1}{R} \sqrt{\frac{P_0 G \eta}{4\pi}} = \sqrt{S \eta}$$

Equation 1.1

Gain is achieved by directing the radiation away from other parts of the radiation sphere. In general, gain is defined as the gain-biased pattern of the antenna.

$$S(\theta, \phi) = \frac{P_0 G(\theta, \phi)}{4\pi R^2} \quad \text{power density}$$

$$U(\theta, \phi) = \frac{P_0 G(\theta, \phi)}{4\pi} \quad \text{radiation intensity}$$

Equation 1.2

1.1.2 Antenna Efficiency

The surface integral of the radiation intensity over the radiation sphere divided by the input power P_0 is a measure of the relative power radiated by the antenna, or the antenna efficiency.

$$\frac{P_r}{P_0} = \int_0^{2\pi} \int_0^\pi \frac{G(\theta, \phi)}{4\pi} \sin \theta d\theta d\phi = \eta_e \quad \text{efficiency}$$

Equation 1.3

where P_r is the radiated power. Material losses in the antenna or reflected power due to poor impedance match reduce the radiated power.

1.1.3 Effective Area

Antennas capture power from passing waves and deliver some of it to the terminals. Given the power density of the incident wave and the effective area of the antenna, the power delivered to the terminals is the product.

$$P_d = S A_{\text{eff}}$$

Equation 1.4

For an aperture antenna such as a horn, parabolic reflector, or flat-plate array, effective area is physical area multiplied by aperture efficiency. In general, losses due to material, distribution, and mismatch reduce the ratio of the effective area to the physical area. Typical estimated aperture efficiency for a parabolic reflector is 55%. Even antennas with infinitesimal physical areas, such as dipoles, have effective areas because they remove power from passing waves.

1.1.4 Directivity

Directivity is a measure of the concentration of radiation in the direction of the maximum.

$$\text{directivity} = \frac{\text{maximum radiation intensity}}{\text{average radiation intensity}} = \frac{U_{\max}}{U_0}$$

Equation 1.5

Directivity and gain differ only by the efficiency, but directivity is easily estimated from patterns. Gain—directivity times efficiency—must be measured. The average radiation intensity can be found from a surface integral over the

radiation sphere of the radiation intensity divided by 4π , the area of the sphere in steradians:

$$\text{average radiation intensity} = \frac{1}{4\pi} \int_0^{2\pi} \int_0^{\pi} U(\theta, \phi) \sin \theta d\theta d\phi = U_0$$

Equation 1.6

This is the radiated power divided by the area of a unit sphere. The radiation intensity $U(\theta, \phi)$ separates into a sum of co- and cross-polarization components:

$$U_0 = \frac{1}{4\pi} \int_0^{2\pi} \int_0^{\pi} [U_C(\theta, \phi) + U_X(\theta, \phi)] \sin \theta d\theta d\phi$$

Both co- and cross-polarization directivities can be defined:

$$\text{directivity}_C = \frac{U_{C,\max}}{U_0} \quad \text{directivity}_X = \frac{U_{X,\max}}{U_0}$$

Equation 1.7

Directivity can also be defined for an arbitrary direction $D(\theta, \phi)$ as radiation intensity divided by the average radiation intensity, but when the coordinate angles are not specified, we calculate directivity at U_{\max} .

1.1.5 Path Loss

We combine the gain of the transmitting antenna with the effective area of the receiving antenna to determine delivered power and path loss. The power density at the receiving antenna is given by equation 1.2 and the received power is given by equation 1.4. By combining the two, we obtain the path loss as given below.

$$\frac{P_d}{P_t} = \frac{A_2 G_1(\theta, \phi)}{4\pi R^2}$$

Equation 1.8

Antenna 1 transmits, and antenna 2 receives. If the materials in the antennas are linear and isotropic, the transmitting and receiving patterns are identical. When we consider antenna 2 as the transmitting antenna and antenna 1 as the receiving antenna, the path loss is

$$\frac{P_d}{P_t} = \frac{A_1 G_2(\theta, \phi)}{4\pi R^2}$$

Equation 1.9

We make quick evaluations of path loss for various units of distance R and for frequency f in megahertz using the formula

$$\text{path loss(dB)} = K_U + 20 \log(fR) - G_1(\text{dB}) - G_2(\text{dB})$$

where K_U depends on the length units as shown in table 1.1

Unit	K_U
km	32.45
nm	37.80
miles	36.58
m	-27.55
ft	-37.87

Table 1.1

1.1.6 Input Impedance

The input impedance of an antenna is defined as “the impedance presented by an antenna at its terminals or the ratio of the voltage to the current at the pair of terminals or the ratio of the appropriate components of the electric to magnetic fields at a point”. Hence the impedance of the antenna can be written as given below.

$$Z_{in} = R_{in} + jX_{in}$$

Equation 1.10

where Z_{in} is the antenna impedance at the terminals

R_{in} is the antenna resistance at the terminals

X_{in} is the antenna reactance at the terminals

The imaginary part, X_{in} of the input impedance represents the power stored in the near field of the antenna. The resistive part, R_{in} of the input impedance consists of two components, the radiation resistance R_r and the loss resistance R_L . The power associated with the radiation resistance is the power actually radiated by the antenna, while the power dissipated in the loss resistance is lost as heat in the antenna itself due to dielectric or conducting losses.

1.1.7 Antenna Factor

The engineering community uses an antenna connected to a receiver such as a spectrum analyzer, a network analyzer, or an RF voltmeter to measure field strength E . Most of the time these devices have a load resistor Z_L that matches the antenna impedance.

The incident field strength E_i equals antenna factor AF times the received voltage V_{rec} . We relate this to the antenna effective height:

$$AF = \frac{E_i}{V_{\text{rec}}} = \frac{2}{h}$$

Equation 1.11

AF has units meter⁻¹ but is often given as dB(m⁻¹). Sometimes, antenna factor is referred to the open-circuit voltage and it would be one-half the value given by equation 1.11. We assume that the antenna is aligned with the electric field; in other words, the antenna polarization is the electric field component measured:

$$AF = \sqrt{\frac{\eta}{Z_L A_{\text{eff}}}} = \frac{1}{\lambda} \sqrt{\frac{4\pi}{Z_L G}}$$

Equation 1.12

This measurement may be corrupted by a poor impedance match to the receiver and any cable loss between the antenna and receiver that reduces the voltage and reduces the calculated field strength.

1.1.8 Return Loss

It is a parameter which indicates the amount of power that is “lost” to the load and does not return as a reflection. Hence the RL is a parameter to indicate how well the matching between the transmitter and antenna has taken place. Simply put it is the S11 of an antenna. A graph of s11 of an antenna vs frequency is called its return loss curve. For optimum working such a graph must show a dip at the operating frequency and have a minimum dB value at this frequency. This parameter was found to be of crucial importance to our project as we sought to adjust the antenna dimensions for a fixed operating frequency (say 1.9 GHz). A simple RL curve is shown in figure 1.1.

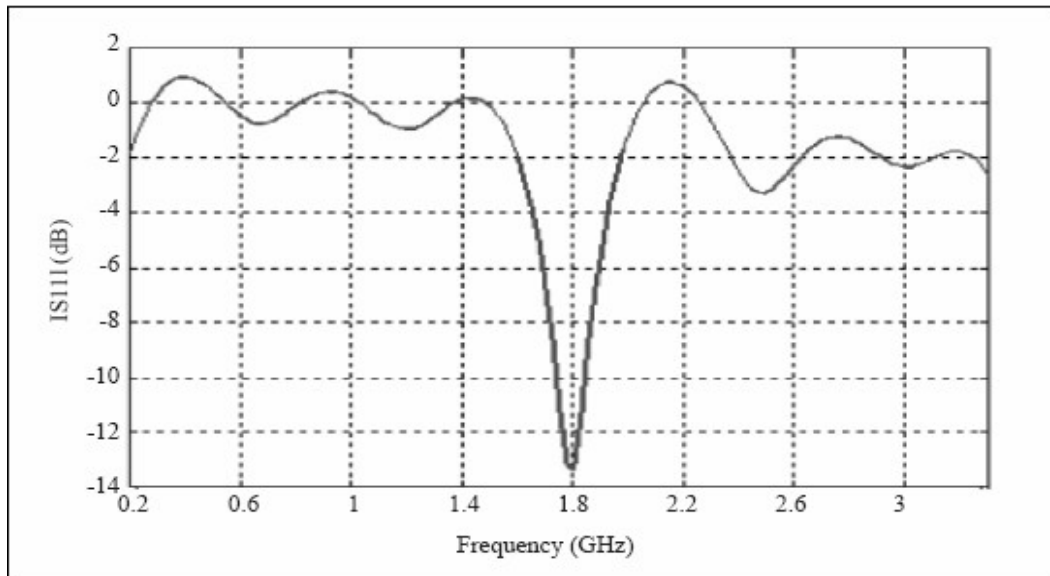


Figure 1.1 – RL curve of an antenna

1.19 Radiation Pattern

The radiation pattern of an antenna is a plot of the far-field radiation properties of an antenna as a function of the spatial co-ordinates which are specified by the elevation angle (θ) and the azimuth angle (ϕ). More specifically it is a plot of the power radiated from an antenna per unit solid angle which is nothing but the radiation intensity. It can be plotted as a 3D graph or as a 2D polar or Cartesian slice of this 3D graph. It is an extremely important parameter as it shows the antenna's directivity as well as gain at various points in space. It serves as the signature of an antenna and one look at it is often enough to realize the antenna that produced it.

Because this parameter was so important to our software simulations we needed to understand it completely. For this purpose we obtained the 2D polar plots of radiation patterns for a few antennas in our lab using a ScienTech antenna trainer kit shown in figure 1.2.



Figure 1.2 – ScienTech Antenna Trainer Kit

The transmitter of the kit was rotated through 360 degrees in 20 degree intervals and the received power was measured (in μV – converted to dB) by a receiver to plot the radiation patterns of a few antennas. A simple MATLAB code written by us to obtain the 2D Polar Plots is given in Appendix A. The main disadvantage of this trainer kit is that it works only at 750MHz. However, it helped us to visualize the radiation patterns of some antennas shown in the following pages.

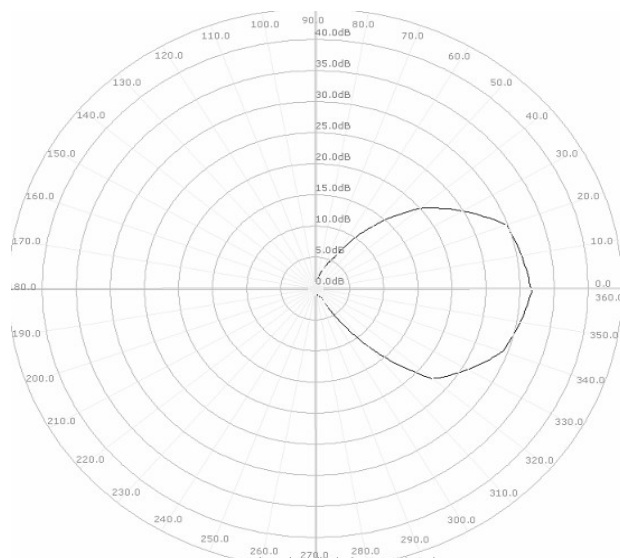


Figure 1.3 – 2D Polar Plot for a Yagi Antenna

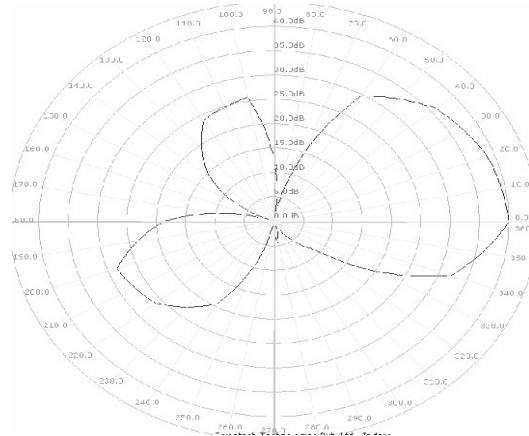


Figure 1.4 – 2D Polar Plot for a Helical Antenna

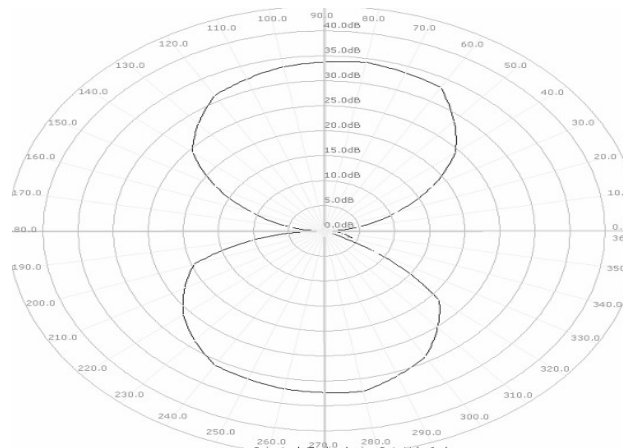


Figure 1.5 – 2D Polar Plot for a Rhombus Patch Antenna

A general 3D radiation pattern is also shown in figure 1.6

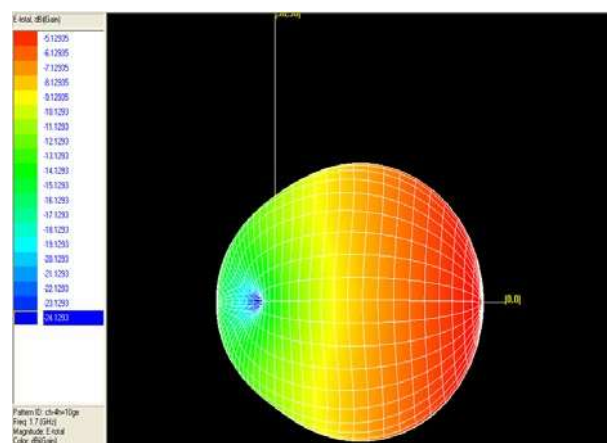


Figure 1.6 – 3D Radiation Pattern for a rectangular patch

1.20 Beamwidth

Beamwidth of an antenna is easily determined from its 2D radiation pattern and is also a very important parameter. Beamwidth is the angular separation of the half-power points of the radiated pattern. The way in which beamwidth is determined is shown in figure 1.7.

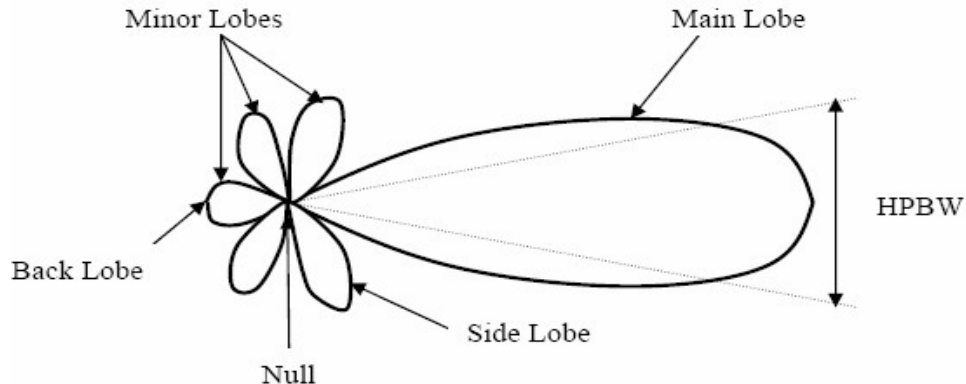


Figure 1.7 – Determination of HPBW from radiation pattern

1.2 Types of Antennas

Antennas can be classified in several ways. One way is the frequency band of operation. Others include physical structure and electrical/electromagnetic design. Most simple, non-directional antennas are basic dipoles or monopoles. More complex, directional antennas consist of arrays of elements, such as dipoles, or use one active and several passive elements, as in the Yagi antenna. New antenna technologies are being developed that allow an antenna to rapidly change its pattern in response to changes in direction of arrival of the received signal. These antennas and the supporting technology are called adaptive or “smart” antennas and may be used for the higher frequency bands in the future. A few commonly used antennas are described in the following sections.

1.2.1 Dipoles and Monopoles

The vertical dipole—or its electromagnetic equivalent, the monopole—could be considered one of the best antennas for LMR applications. It is omni directional (in azimuth) and, if it is a half-wavelength long, has a gain of 1.64 (or $G = 2.15 \text{ dBi}$) in the horizontal plane. A center-fed, vertical dipole is illustrated in figure 1.8 (a). Although this is a simple antenna, it can be difficult to mount on a mast or vehicle. The ideal vertical monopole is illustrated in figure 1.8 (b). It is half a dipole placed in half space, with a perfectly conducting, infinite surface at the boundary.

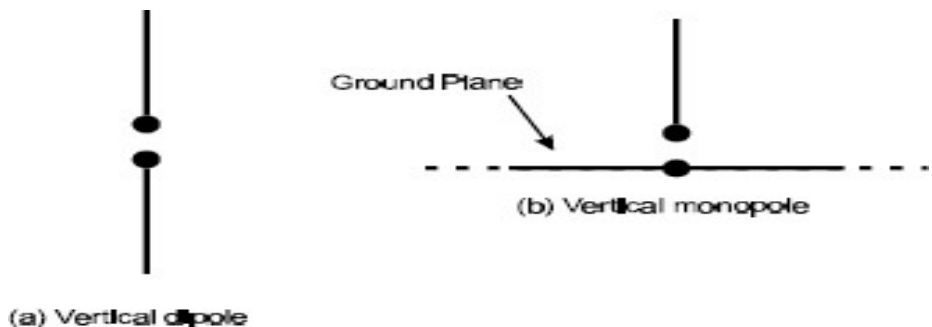


Figure 1.8 - The vertical dipole and its electromagnetic equivalent, the vertical monopole

A monopole over an infinite ground plane is theoretically the same (identical gain, pattern, etc., in the half-space above the ground plane) as the dipole in free space. In practice, a ground plane cannot be infinite, but a ground plane with a radius approximately the same as the length of the active element, is an effective, practical solution. The flat surface of a vehicle's trunk or roof can act as an adequate ground plane. Figure 1.9 shows typical monopole antennas for base-station and mobile applications.

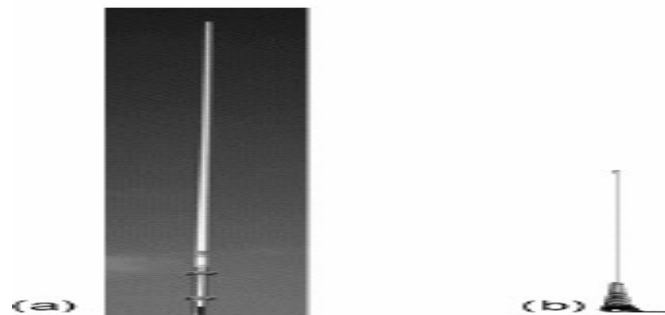


Figure 1.9 - Typical monopole antennas for (a) base-station applications and (b) mobile applications

1.2.2 Corner Reflector

An antenna comprised of one or more dipole elements in front of a corner reflector, called the corner-reflector antenna, is illustrated in figure 1.10.

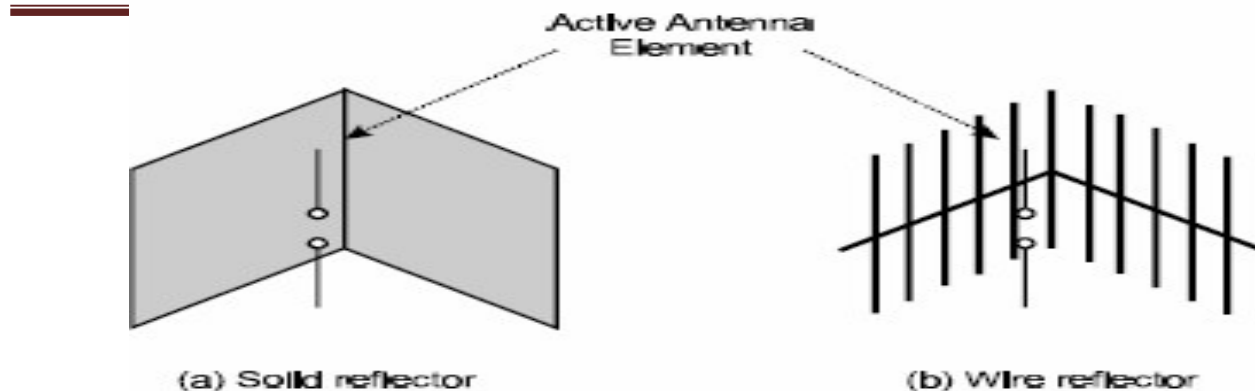


Figure 1.10 - Corner-reflector antennas

This antenna has moderately high gain, but its most important pattern feature is that the forward (main beam) gain is much higher than the gain in the opposite direction. This is called the front-to-back ratio and is evident from its radiation pattern shown in figure 1.11.

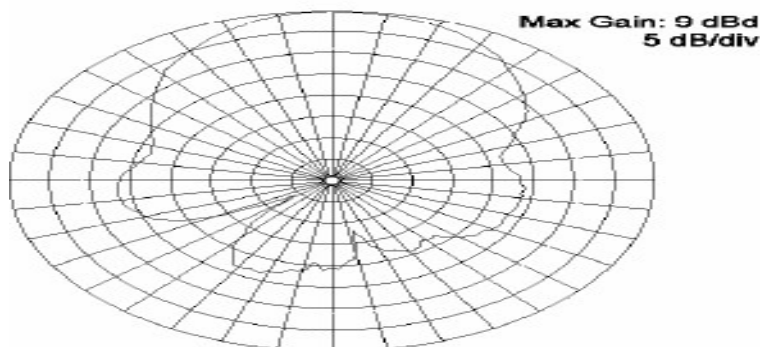


Figure 1.11 - A corner-reflector antenna horizontal-plane pattern

1.2.3 Yagi Antenna

Another antenna design that uses passive elements is the Yagi antenna. This antenna, illustrated in figure 1.12, is inexpensive and effective. It can be constructed with one or more (usually one or two) reflector elements and one or more (usually two or more) director elements. Figure 1.1.3 shows a Yagi antenna with one reflector, a folded-dipole active element, and seven directors, mounted for horizontal polarization.

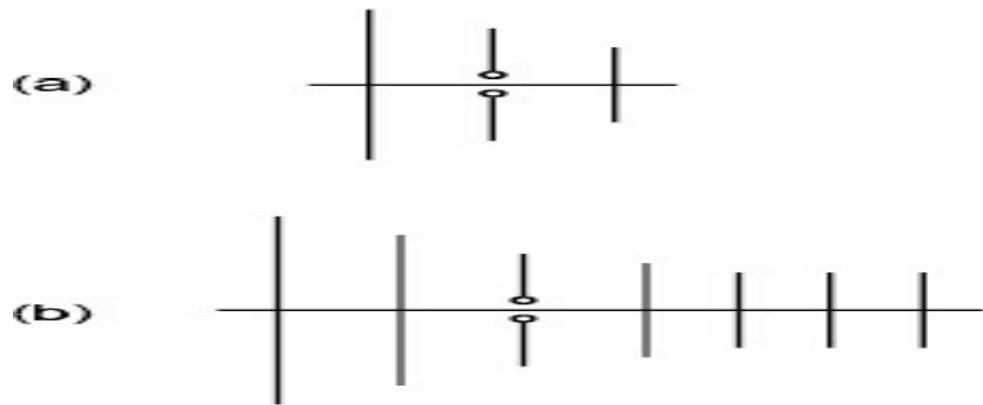


Figure 1.12 - The Yagi antenna — (a) three elements and (b) multiple elements

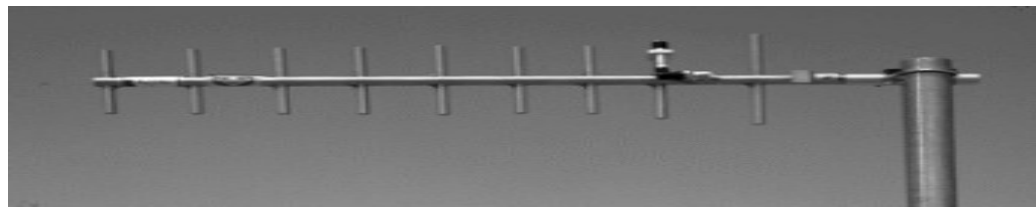


Figure 1.13 - A typical Yagi antenna

Figure 1.14 is the typical radiation pattern obtained for a three element (one reflector, one active element, and one director) Yagi antenna. Generally, the more elements a Yagi has, the higher the gain, and the narrower the beamwidth. This antenna can be mounted to support either horizontal or vertical polarization and is often used for point-to-point applications, as between a base station and repeater-station sites.

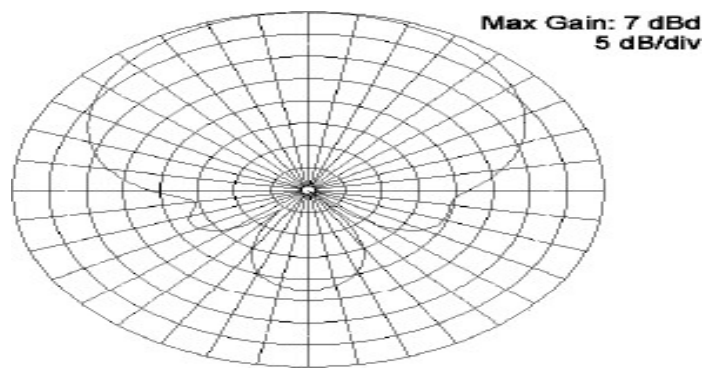


Figure 1.14 - A Yagi antenna horizontal plane pattern

Chapter 2

Hardware Aspects - Fabrication and Testing of RF Antennas

2.1 Introduction

For the project we constructed two RF antennas and tested them in our lab.

The antennas that we constructed were: 1) Slotted Waveguide Antenna. (Omni directional)

2) Biquad antenna. (Directional)

Working central frequency of these antennas is 2.4GHz. 2.4GHz comes under the unlicensed wireless band usually used in WLAN.

2.1.1 Significance of 2.4 GHz

Since 1986, FCC rules have provided for unlicensed spread-spectrum operation in the 915 MHz (902–928 MHz), 2.4 GHz (2400–2483.5 MHz), and 5.7 GHz (5725–5850 MHz) bands. But a vast number of RF devices currently operate in the 2.4 GHz band (like microwave ovens, cordless telephones, medical devices etc.). Recently there has been proliferation of "Wi-Fi" hotspots and wireless computers permitting undeterred internet access by the public and RF identification (RFID) technology.

2.2 Slotted Waveguide Antenna

2.2.1 Introduction

Slotted waveguides are resonant antennas and have a relatively narrow operating frequency range. A slotted waveguide is a waveguide that is used as an antenna in microwave radar applications. Prior to its use in surface search radar, such systems used a parabolic segment reflector.

A slotted waveguide has no reflector but emits directly through the slots. The spacing of the slots is critical and is a multiple of the wavelength used for transmission and reception. The antenna's vertical focus is usually enhanced by the application of a microwave lens attached to the front of the antenna. As this, like the companion slotted waveguide, is a one-dimensional device, it too may be made relatively cheaply as compared to a parabolic reflector and feed horn. In a related application, so-called leaky waveguides are also used in the determination of railcar positions in certain rapid transit applications. They are primarily used to determine the precise position of a train when it is being brought to a halt at a station, so that the doorway positions will align correctly with queuing points on the platform or with a second set of safety doors should such be provided.

2.2.2 Working

A waveguide is a very low loss transmission line. It allows propagation of signals to a number of smaller antennas (slots). The signal is coupled into the waveguide with a simple coaxial probe and as it travels along the guide it traverses the slots. Each of these slots allows a little of the energy to radiate. The slots are in a linear array pattern, and the total of all the radiated signals adds up to a very significant power gain over a small range of angles close to the horizon. In other words, the waveguide antenna transmits almost all of its energy at the horizon, usually exactly where we want it to go. Its exceptional directivity in the elevation plane gives it quite high power gain. Additionally, unlike vertical co-linear antennas, the slotted waveguide transmits its energy using horizontal polarization, the best type for distance transmission.

2.2.3 Construction

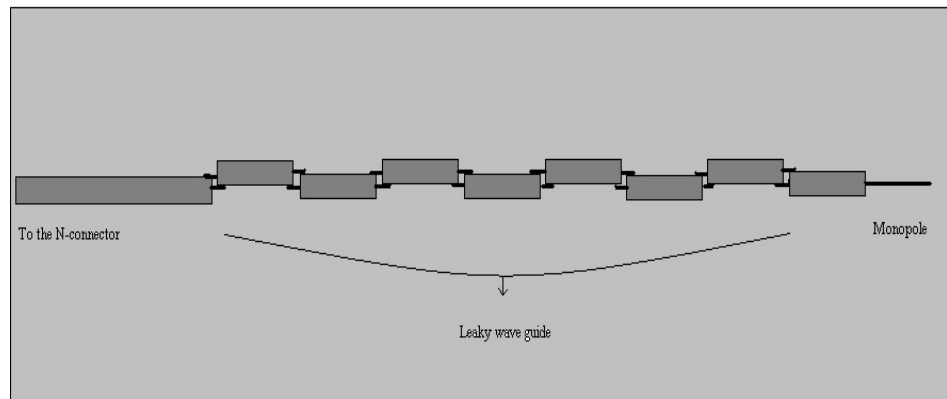


Figure – 2.1 – A Slotted Waveguide Antenna

The components we used to construct this antenna are given below

- i) 1m RG-213U cable (coaxial cable)
- ii) N connectors (BNC-female)
- iii) Plastic casing

Each sector of the antenna needs to be a 1/2 wavelength long multiplied by the velocity factor of the cable. The velocity factor of RG-213 is 0.66. If a different cable (such as LMR-400) is used then the velocity factor of that cable needs to be determined and all the dimensions will need to be recalculated.

$$\frac{V * C}{2 * F} = \frac{0.66 * 299792458}{2 * 2441000000} = 0.0405\text{m} = 40.5\text{mm}$$

Equation 2.1

V = Velocity Factor of RG213 = 0.66

C = Velocity of light = 299792458 m/s

F = Frequency of Signal = 2441000000 Hz (middle of the 2.4GHz range)

The 1/4 wave element is not adjusted by the velocity factor, as it is in the open, so it works out at just 31mm long giving a total antenna length of 355mm + fly-lead. Each sector consists of a short length of RG-213 cable, with the central core sticking out each end. When building the antenna, the exact length of each piece of RG-213 is not that important, it is the overall length of each sector that counts.



Figure -2.2 – Sectors of the antenna

We found that cutting the cable to 37mm with 6mm of core sticking out each end, got enough overlap to easily solder the segments together. If 1mm is allowed for the width of the hacksaw when cutting the sectors apart, it means that $37 + 6 + 6 + 1 = 50$ mm of cable was required for each sector. For making 8sectors + 1/4wave section, 420 mm of cable length for the antenna + cable for the fly lead was required, as illustrated by figure - 2.2.

For making the first segment with the monopole, the sheath, shielding and central insulator of length 31mm was stripped with out damaging the inner conductor which would act as monopole. Leaving 43mm from the star of monopole i.e. 77mm from the monopole's tip the coaxial cable was completely cut. Then leaving 6mm from the other end, sheath, shielding, and central insulator were removed leaving the inner conductor exposed so that it could be connected to other segments.

The other seven segments of the antenna were symmetrical and of 50mm length. So, seven 50mm segments were cut from the coaxial cable. For each segment 6mm of sheath, shielding and central insulator were removed leaving the central conductor for connecting it to other segments. After making all the segments, all eight sectors were checked round the end to make sure that none of the shielding was touching the central cable, as odd strands can get left.

A gentle V shaped cut was made with a knife, at each end of the sectors, to expose the shielding, which is where the central core of the next sector would be soldered. This was done to all sectors which had to be soldered, including the fly-lead part.



Figure – 2.3 – V cut at sector ends

V cuts at each end of the sector lined up; otherwise, when the antenna is soldered together, the whole thing will be twisted all around. All the eight segments and the fly lead were soldered taking care that the wire would not get twisted.

Once the antenna was ready, it was tested with a multimeter to check if the connections were correct. The center of the fly lead should form a circuit to the 1/4 wave section, and the shield of the fly lead to the shield of the top section. The antenna was now tested to ensure that there were no crossed connections, by ensuring there was no circuit between the center of the fly lead and the shielding of the top sector and no circuit between the 1/4 wave section and the shielding of the flyleaf. The slotted waveguide antenna that we constructed is shown below.



Figure – 2.4 – Slotted Waveguide Antenna Constructed

2.3 Biquad Antenna

2.3.1 Introduction

A biquad antenna is a wide band antenna. These antennas are fairly directive, cheap and simple to make. A Biquad is nothing but two single turn loop antennas forming an array where each one is a driven component. The array improves the directivity and bandwidth. The working of a biquad is the same as a folded dipole antenna. It generates the same radiation pattern as a dipole with more directivity and bandwidth. A biquad antenna can be considered as a modified form of a folded dipole antenna. More specifically its elements come under the category of small loop single turn antennas.

2.3.2 Working

A small loop is the dual of an ideal dipole. Pattern and radiation resistance of a loop are insensitive to the loop shape and depend only on the loop area. Radiation from a small loop is highest in the plane of loop and zero along its axis. As the perimeter of a loop antenna becomes a sizeable fraction of a wavelength, the current amplitude and phase will vary over the wire extent. So, a loop antenna with a perimeter that is of the order of half-wavelength or larger will display performance variation with loop size and shape.

The biquad antenna that we made is a combination of two one wavelength square loop antennas.

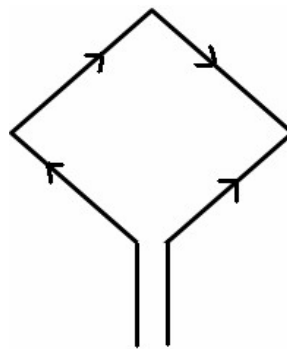


Figure – 2.5 - Square loop

It has one quarter wavelength sides. For one wavelength perimeter it is reasonable to assume that current distribution is sinusoidal and continuous around the loop.

2.3.3 Construction

The components we used to construct the antenna were

- i) 123x123mm square section of blank PCB
- ii) 50mm length of 1/2" copper pipe
- iii) Short length of CNT-400 or LMR-400 low loss coax (~300mm long)
- iv) 250mm of 2.5mm² copper wire (approx 1.5mm diameter)
- v) N connector

We cut a square piece of blank printed circuit board, 123x123mm. 50mm section of copper pipe was taken and filed both ends smooth. Using sandpaper the copper pipe was polished up including the inside of the copper pipe, to ensure a good connection with the coax braid. A notch was cut into one end of the copper pipe, removing approx 2mm from half the circumference.

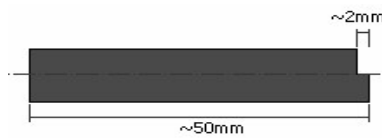


Figure – 2.6 – Copper Pipe

A hole was drilled in the centre of the blank PCB so that the copper pipe was a tight fit in the hole. We drilled a small hole and then widened it using file for making it precisely fit for inserting the copper pipe.

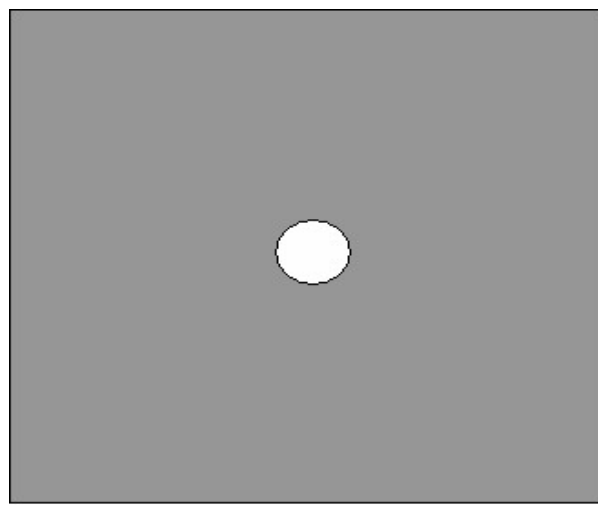


Figure – 2.7 – Square PCB used for construction

Copper pipe was inserted into the hole, with the notched end on the copper side of the blank PCB. The copper pipe protruded approx 16mm through the hole, measured on the copper side of the PCB. The copper pipe was soldered to the PCB to ensure better electrical connectivity. It is not possible to solder the two elements with normal 25W solder gun. We used a high power solder to connect these two elements.

244 mm of copper wire was taken and is bent in as shown in the figure. All the bents are of 90 degrees.

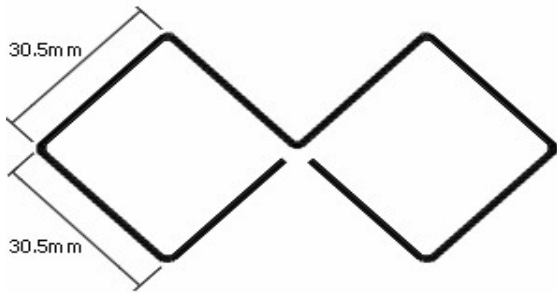


Figure – 2.8 – Biquad Antenna Loop

The element was now attached to the reflector. Only the two "ends" of the copper wire were to be attached to the copper pipe - the centre of the copper wire must not touch the copper pipe (hence the notch which was cut into the end of the copper pipe). Assembling everything as mentioned, our antenna looked as shown below.

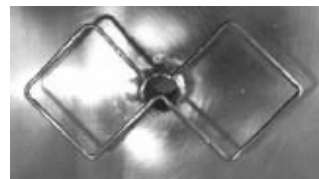


Figure 2.9 – Biquad Loop Constructed

For feeding antenna we stripped approx 30mm of the outer sheath from the end of the coaxial cable. The braid was folded back over the outer sheath the centre conductor was trimmed, so that about 4mm protruded. The outer braid was to be shorted to reflector (ground plane).

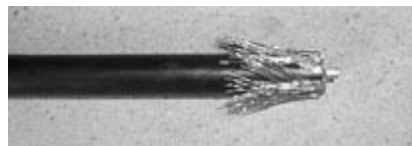


Figure – 2.10 – Stripping of Sheath

We inserted the braid into the copper pipe, so that the end of the centre conductor lined up with the extreme end of the copper pipe, and we then soldered the centre of the element to it, ensuring the centre of the element was not in contact with the copper pipe. At this stage we had completely constructed the biquad antenna shown below.

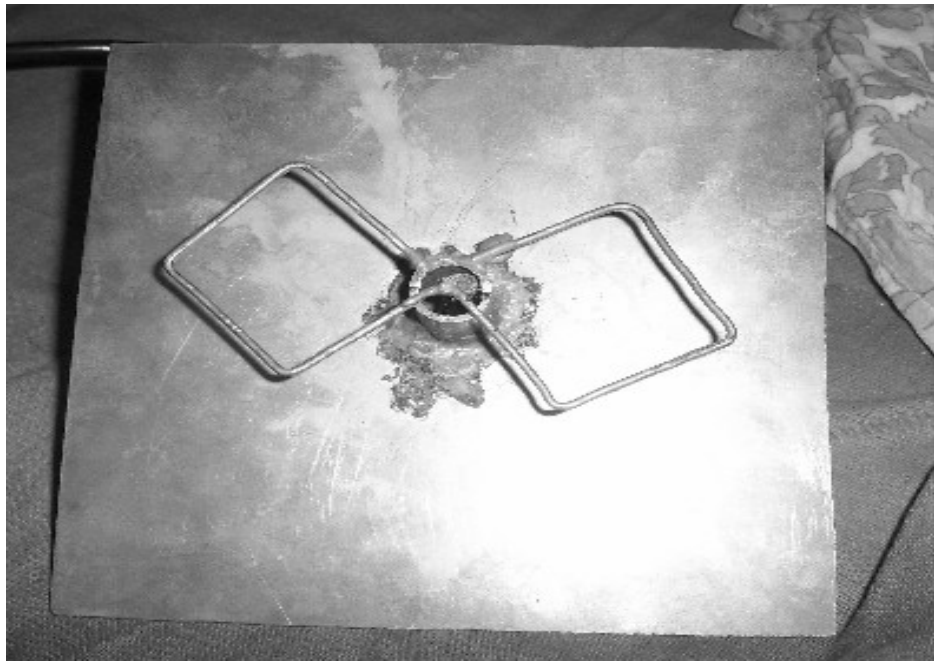


Figure 2.11 – Biquad Antenna Constructed

2.4 Testing of the Antennas

For testing our antennas we used the equipment available in our lab. Equipment like network analyzer, spectrum analyzer and signal generator, which are recent additions to our lab, were studied and then used to determine S_{11} (insertion loss), transmitting power, received power etc. Details about these equipment are available in Appendix B. We first found out insertion loss parameter of each antenna using network analyzer. Then we determined the receiving power of antennas using one as a transmitter and the other as a receiver.

2.4.1 S_{11} parameter

S_{11} gives us the insertion loss of antennas. Insertion loss is proportional to the ratio of reflected to the input power of the antenna. Antennas generally radiate efficiently for particular range of frequencies. At these frequencies the radiated power should be almost equal to input power, i.e., reflected power should very small. So the expected plot of S_{11} for an antenna would be a flat line through out the frequency scale with deep dip in the operating frequency range.

2.4.2 S₁₁ Curve of the Slotted Waveguide Antenna

The S₁₁ curve of the slotted waveguide antenna obtained using vector analyzer is shown in figure 2.12.

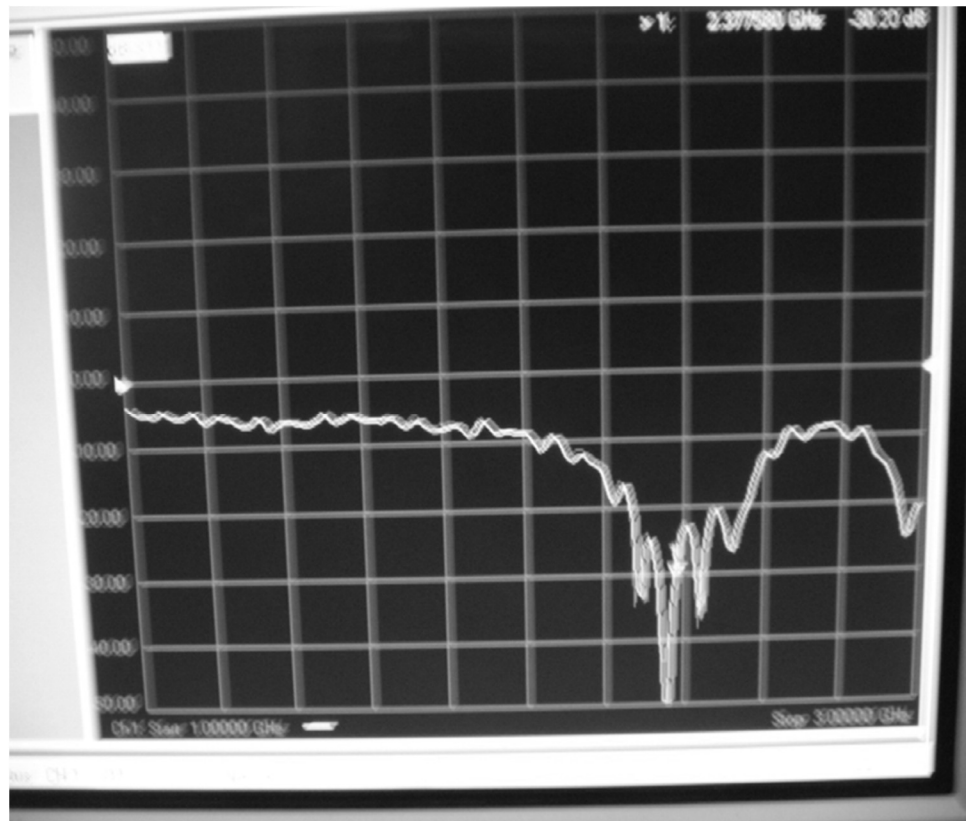


Figure – 2.12 – S₁₁ curve obtained for the Slotted Waveguide Antenna

The dip is the central operating frequency of the antenna. The operating frequency of the antenna was found to be 2.3 GHz. The S₁₁ measured at this frequency was -45 dB.

For the antenna we got more than one dip. The reason for this was that our antenna, being an array of slots, was radiating at different frequencies which were very close by.

2.4.3 S₁₁ Curve of the Biquad Antenna

The S₁₁ vs frequency curve of the biquad antenna obtained using a vector analyzer is shown in figure 2.13.

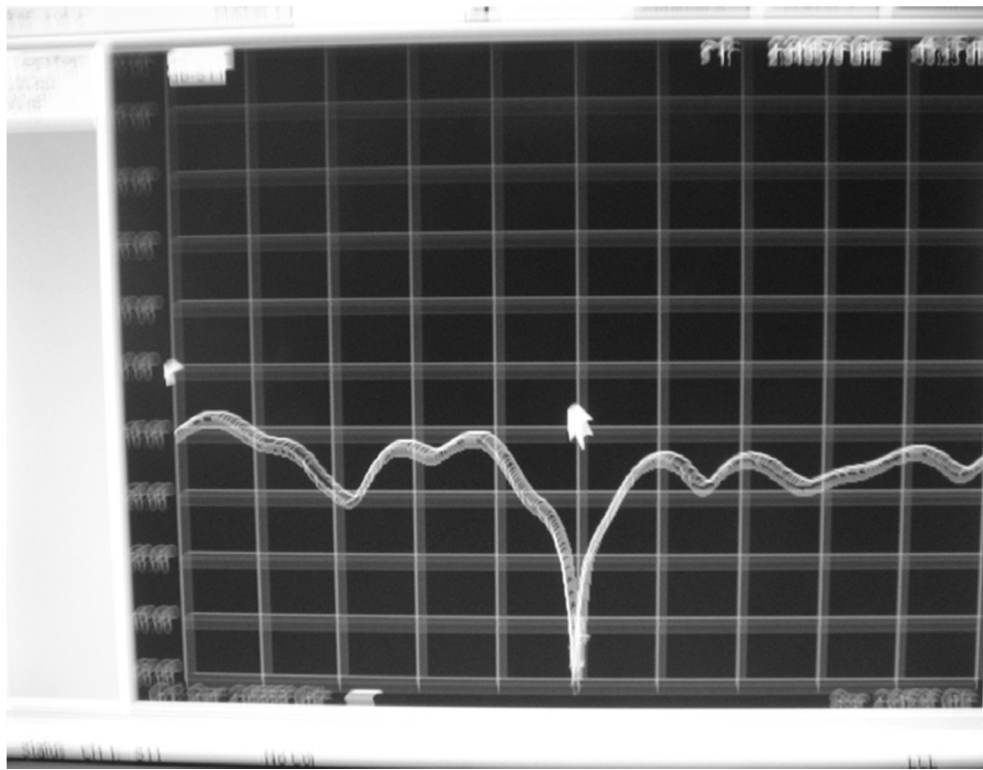


Figure – 2.13 – S₁₁ Curve obtained for the Biquad Antenna

The dip indicates the central operating frequency of the antenna. The operating frequency of the antenna was found to be 2.34 GHz. S₁₁ measured at this frequency was -38 dB.

2.4.4 Problems faced during Testing

We have used BNC connectors for feeding the signal to the antennas. But these connectors were found to be very unreliable for S₁₁ measurement using network analyzer. Even a slight movement in the antenna or the connectors had a significant effect on the results. The S₁₁ measurement which we made could only give us the frequency of operation. For proper measurement of S₁₁, SMA connectors are highly recommended. These connectors are very rugged and results obtained with these connectors are very reliable.

We were also unable to obtain the radiation patterns of the constructed antennas. The theoretical radiation patterns, though, are shown in the following figures.

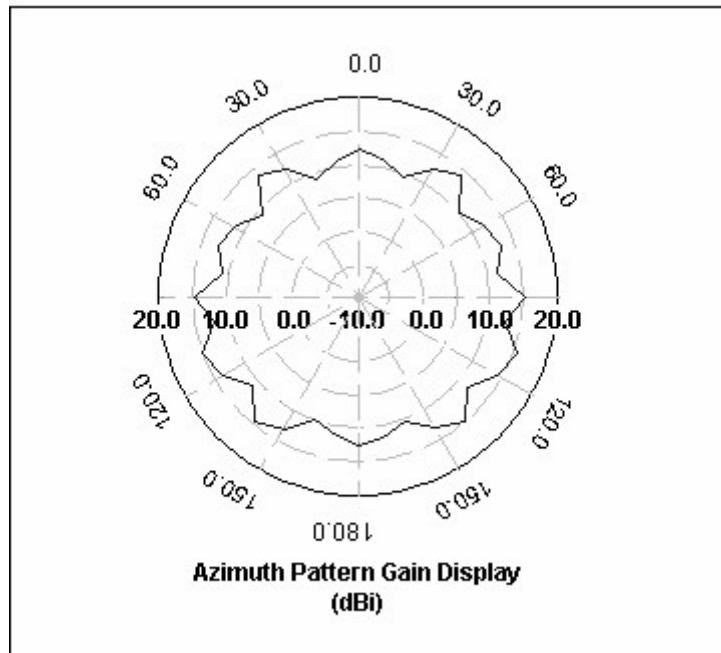


Figure – 2.14 – 2D Radiation Pattern of a Slotted Antenna

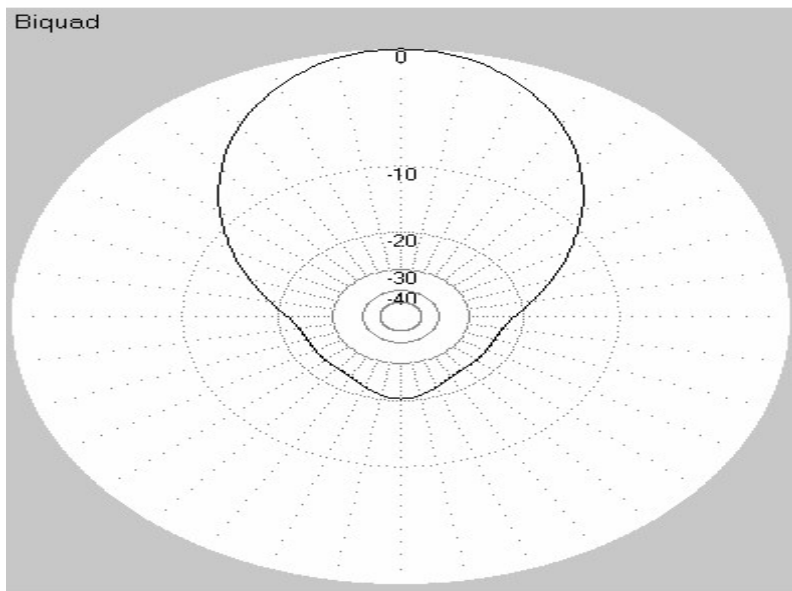


Figure – 2.15 – 2D Radiation Pattern (Polar Plot) of a Biquad Antenna

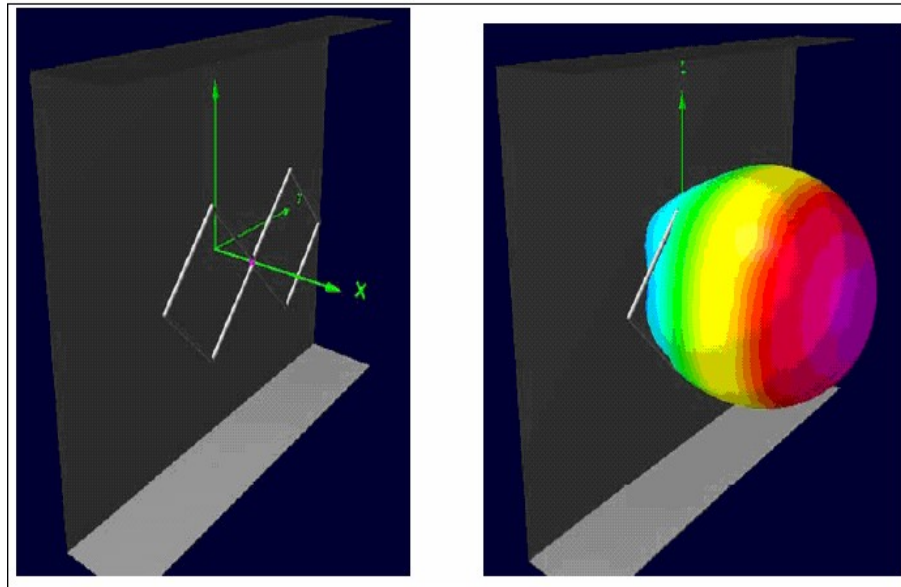


Figure – 2.16 – Orientation and 3D Radiation Pattern of a Biquad Antenna

2.4.5 Power Measurement Arrangement

For power measurement we made an arrangement where one of the antennas was made a transmitter and the antenna, a receiver. The arrangement is as shown below:



Figure – 2.17 – Arrangement for determining power received

Here the slotted waveguide omni-directional antenna is acting as probe antenna so it was our transmitter and the biquad antenna is acted as a receiver.

We fed a continuous signal of different frequency and power to the transmitting antenna from the signal generator (can be seen in the diagram) and on other end we connected the biquad antenna to the spectrum analyzer through a coaxial cable.). On the receiver end we traced out the received signal frequency and power. We found that when a signal of 2.4GHz with a power level of 10 dBm was fed there was a signal of same frequency with lower power level (near -30 dBm received). We even interchanged the setup (i.e. biquad was made transmitter and slotted waveguide antenna was made receiver) and performed our testing. Power received in this case, at same frequency and power level, was bit lower nearly -35 dBm. The values displayed by the signal generator and the receiver (spectrum analyzer) for first the case are shown in the following figures.



Figure – 2.18– Signal Generator Display

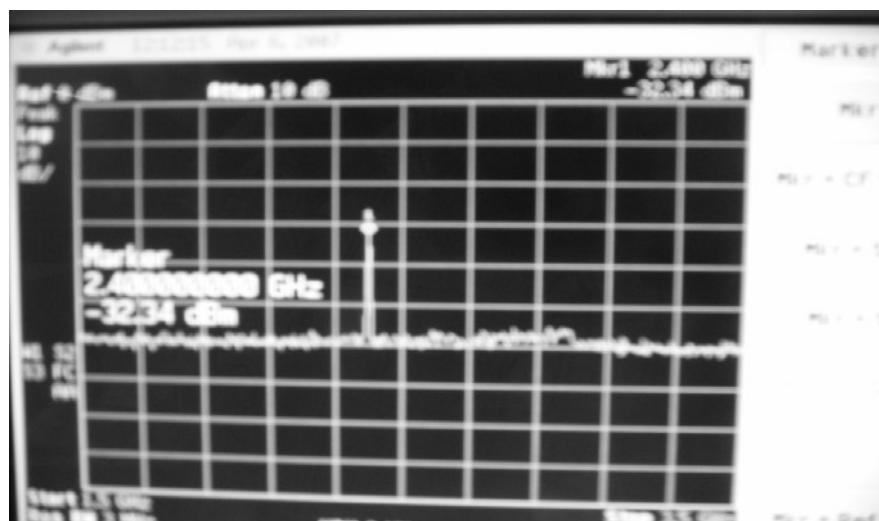


Figure – 2.19– Spectrum Analyzer Display

Chapter 3

Software Aspects – Design and Simulation of Microstrip Patch Antennas

The software simulations of our project focused on designing and testing of patch antennas using software called IE3D (described later on in this chapter). Before the software results are presented the theory behind patch antennas is elucidated.

3.1 Introduction

Microstrip antennas are planar resonant cavities that leak from their edges and radiate. Printed circuit techniques can be used to etch the antennas on soft substrates to produce low-cost and repeatable antennas in a low profile. The antennas fabricated on compliant substrates withstand tremendous shock and vibration environments. Manufacturers for mobile communication base stations often fabricate these antennas directly in sheet metal and mount them on dielectric posts or foam in a variety of ways to eliminate the cost of substrates and etching. This also eliminates the problem of radiation from surface waves excited in a thick dielectric substrate used to increase bandwidth.

In its most basic form, a Microstrip patch antenna consists of a radiating patch on one side of a dielectric substrate which has a ground plane on the other side as shown in Figure 3.1. The patch is generally made of conducting material such as copper or gold and can take any possible shape. The radiating patch and the feed lines are usually photo etched on the dielectric substrate. Arrays of antennas can be photoetched on the substrate, along with their feeding networks. Microstrip circuits make a wide variety of antennas possible through the use of the simple photoetching techniques.

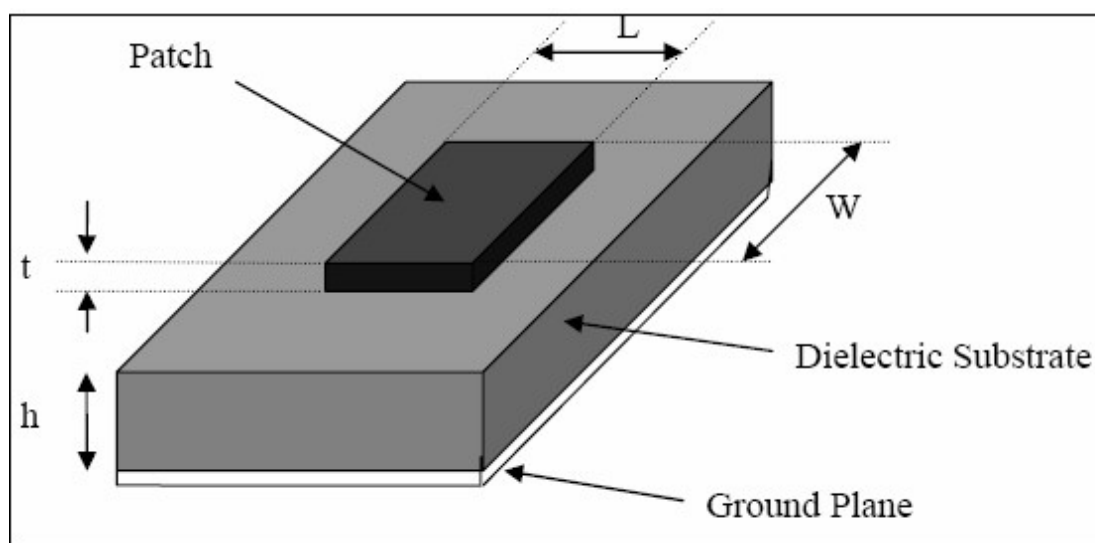


Figure -3.1 – A Typical Microstrip Patch Antenna

In order to simplify analysis and performance prediction, the patch is generally square, rectangular, circular, triangular, elliptical or some other common shape as shown in Figure 2. For a rectangular patch, the length L of the patch is usually $0.333\lambda_o < L < 0.5\lambda_o$, where λ_o is the free-space wavelength. The patch is selected to be very thin such that $t \ll \lambda_o$ (where t is the patch thickness). The height h of the dielectric substrate is usually $0.003\lambda_o \leq h \leq 0.05\lambda_o$. The dielectric constant of the substrate (ϵ_r) is typically in the range $2.2 \leq \epsilon_r \leq 12$.

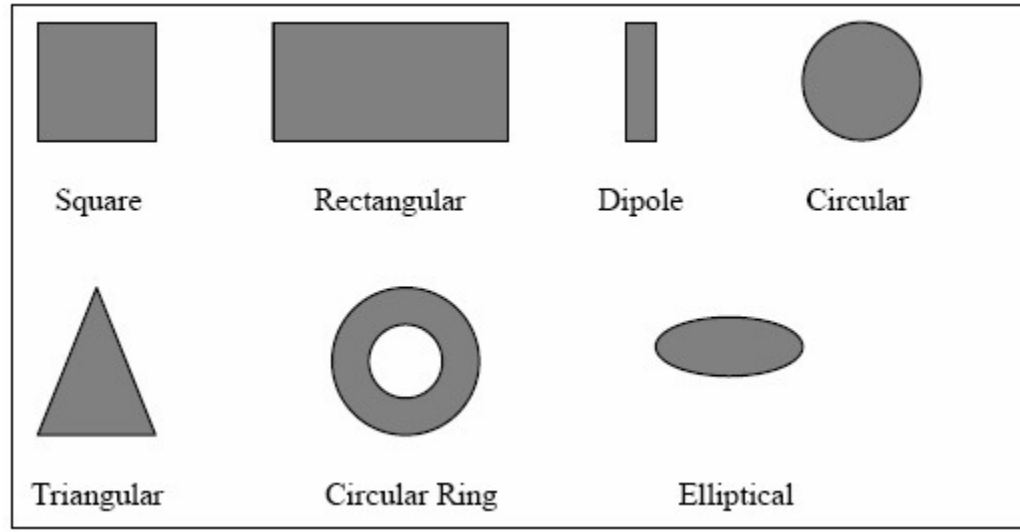


Figure -3.2 – Typical patch shapes

A patch radiates from fringing fields around its edges. The situation is shown in figure 3.3. Impedance match occurs when a patch resonates as a resonant cavity. When matched, the antenna achieves peak efficiency. A normal transmission line radiates little power because the fringing fields are matched by nearby counteracting fields. Power radiates from open circuits and from discontinuities such as corners, but the amount depends on the radiation conductance load to the line relative to the patches. Without proper matching, little power radiates. The edges of a patch appear as slots whose excitations depend on the internal fields of the cavity. A general analysis of an arbitrarily shaped patch considers the patch to be a resonant cavity with metal (electric) walls of the patch and the ground plane and magnetic or impedance walls around the edges.

For good antenna performance, a thick dielectric substrate having a low dielectric constant is desirable since this provides better efficiency, larger bandwidth and better radiation. However, such a configuration leads to a larger antenna size. In order to design a compact Microstrip patch antenna, higher dielectric constants must be used which are less efficient and result in narrower bandwidth. Hence a compromise must be reached between antenna dimensions and antenna performance.

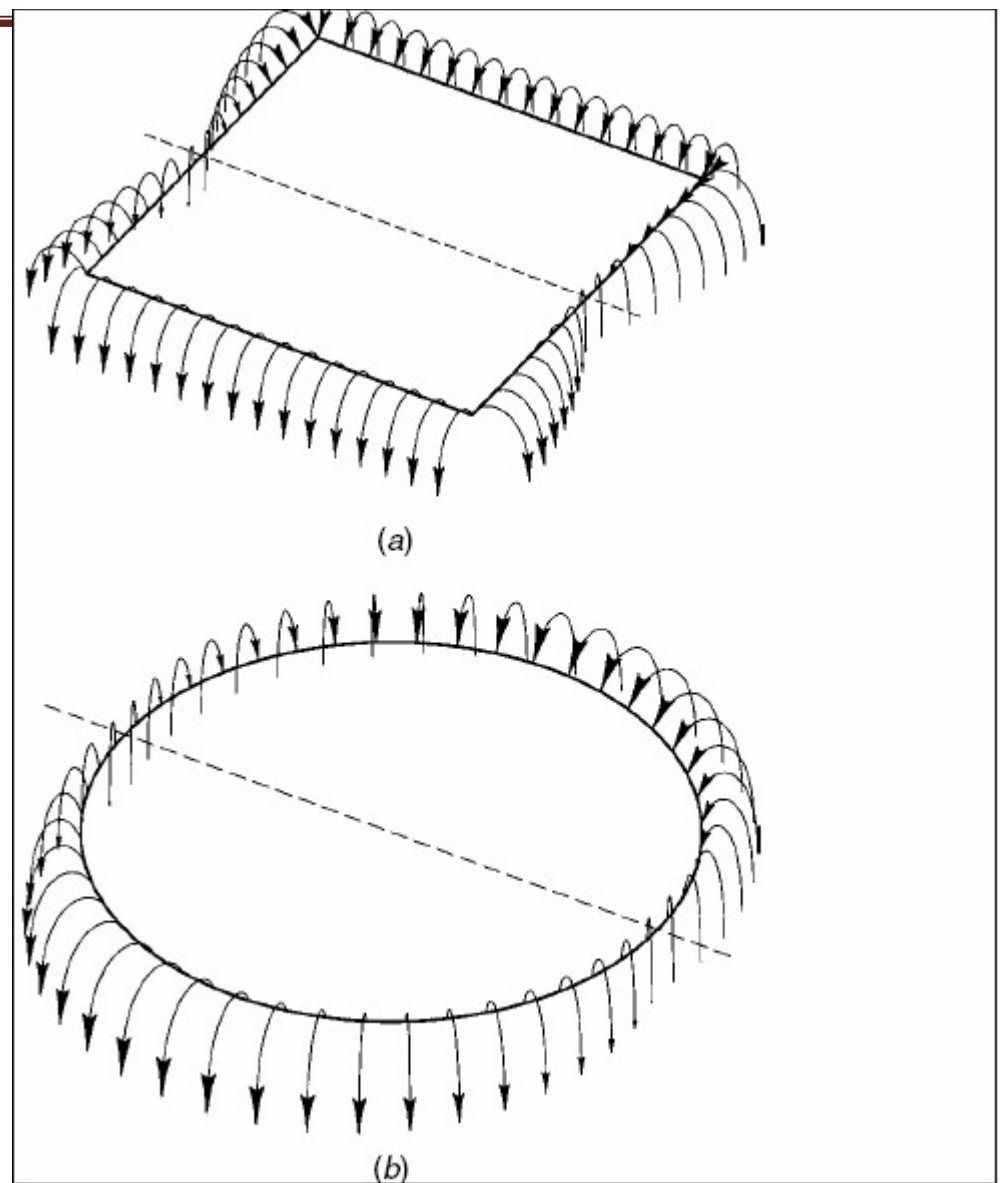


Figure – 3.3 – Fringing Fields in Patch Antennas

3.2 Applications of Microstrip Patch Antennas

Microstrip patch antennas are increasing in popularity for use in wireless applications due to their low-profile structure. Therefore they are extremely compatible for embedded antennas in handheld wireless devices such as cellular phones, pagers etc. The telemetry and communication antennas on missiles need to be thin and conformal and are often microstrip patch antennas. Another area where they have been used successfully is in satellite communication.

3.3 Advantages and Disadvantages of Patch Antennas

Some of their principal advantages of microstrip patch antennas are given below:

- Light weight and low volume.
- Low profile planar configuration which can be easily made conformal to host surface.
- Low fabrication cost, hence can be manufactured in large quantities.
- Supports both, linear as well as circular polarization.
- Can be easily integrated with microwave integrated circuits (MICs).
- Capable of dual and triple frequency operations.
- Mechanically robust when mounted on rigid surfaces.

Microstrip patch antennas suffer from a number of disadvantages as compared to conventional antennas. Some of their major disadvantages are given below:

- Narrow bandwidth
- Low efficiency
- Low Gain
- Extraneous radiation from feeds and junctions
- Poor end fire radiator except tapered slot antennas
- Low power handling capacity.
- Surface wave excitation

Microstrip patch antennas have a very high antenna quality factor (Q). Q represents the losses associated with the antenna and a large Q leads to narrow bandwidth and low efficiency. Q can be reduced by increasing the thickness of the dielectric substrate. But as the thickness increases, an increasing fraction of the total power delivered by the source goes into a surface wave. This surface wave contribution can be counted as an unwanted power loss since it is ultimately scattered at the dielectric bends and causes degradation of the antenna characteristics. However, surface waves can be minimized by use of photonic bandgap structure. Other problems such as low gain and low power handling capacity can be overcome by using an array configuration for the elements.

3.4 Feed Techniques

Microstrip patch antennas can be fed by a variety of methods. These methods can be classified into two categories- contacting and non-contacting. In the contacting method, the RF power is fed directly to the radiating patch using a connecting element such as a microstrip line. In the non-contacting scheme, electromagnetic field coupling is done to transfer power between the microstrip line and the radiating patch. The four most popular feed techniques used are the microstrip line, coaxial probe (both contacting schemes), aperture coupling and proximity coupling (both non-contacting schemes).

3.4.1 Microstrip Line Feed

In this type of feed technique, a conducting strip is connected directly to the edge of the microstrip patch as shown in Figure 3.4. The conducting strip is smaller in width as compared to the patch and this kind of feed arrangement has the advantage that the feed can be etched on the same substrate to provide a planar structure.

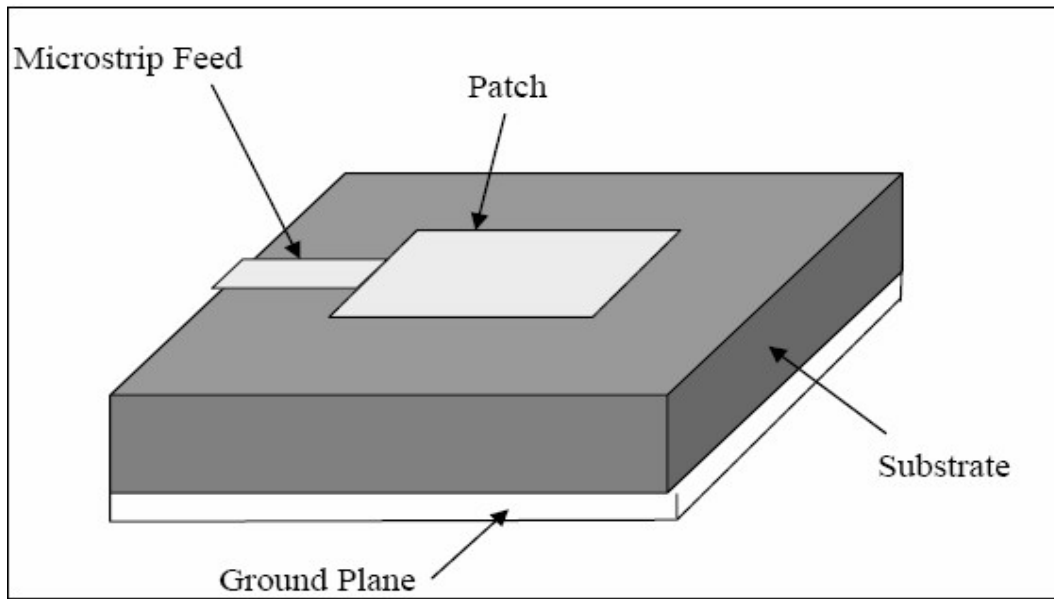


Figure – 3.4 - Microstrip Line Feed

The purpose of the inset cut in the patch is to match the impedance of the feed line to the patch without the need for any additional matching element. This is achieved by properly controlling the inset position. Hence this is an easy feeding scheme, since it provides ease of fabrication and simplicity in modeling as well as impedance matching. However as the thickness of the dielectric substrate being used, increases, surface waves and spurious feed radiation also increases, which hampers the bandwidth of the antenna. The feed radiation also leads to undesired cross polarized radiation.

3.4.2 Coaxial Feed

The Coaxial feed or probe feed is a very common technique used for feeding Microstrip patch antennas. As seen from Figure 3.5, the inner conductor of the coaxial connector extends through the dielectric and is soldered to the radiating patch, while the outer conductor is connected to the ground plane.

The main advantage of this type of feeding scheme is that the feed can be placed at any desired location inside the patch in order to match with its input impedance. This feed method is easy to fabricate and has low spurious radiation. However, its major disadvantage is that it provides narrow bandwidth and is difficult to model since a hole has to be drilled in the substrate and the connector protrudes outside the ground plane, thus not making it completely planar for thick substrates ($h > 0.02\lambda_0$). Also, for thicker substrates, the increased probe length makes the input impedance more inductive, leading to matching problems. It is seen above that for a thick dielectric substrate, which provides broad bandwidth, the microstrip line feed and the coaxial feed suffer from numerous disadvantages. The non-contacting feed techniques discussed below, solve these problems.

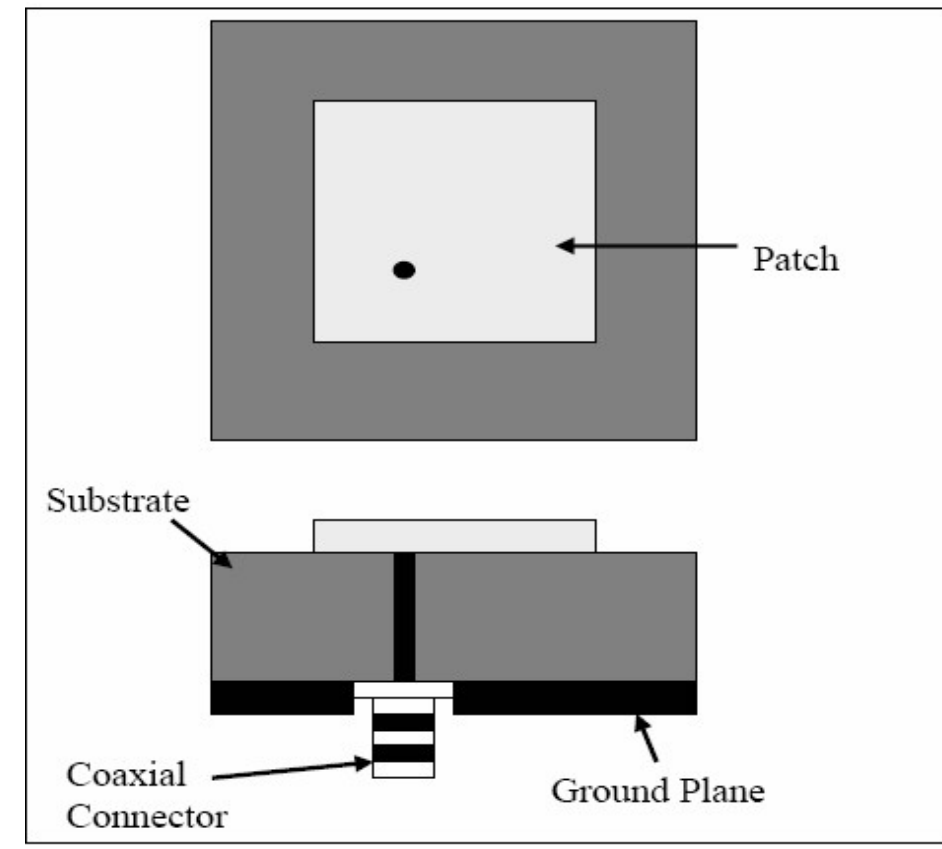


Figure – 3.5 – Coaxial Feed

3.4.3 Aperture Coupled Feed

In this type of feed technique, the radiating patch and the microstrip feed line are separated by the ground plane as shown in Figure 3.6. Coupling between the patch and the feed line is made through a slot or an aperture in the ground plane.

The coupling aperture is usually centered under the patch, leading to lower cross polarization due to symmetry of the configuration. The amount of coupling from the feed line to the patch is determined by the shape, size and location of the aperture. Since the ground plane separates the patch and the feed line, spurious radiation is minimized. Generally, a high dielectric material is used for the bottom substrate and a thick, low dielectric constant material is used for the top substrate to optimize radiation from the patch. The major disadvantage of this feed technique is that it is difficult to fabricate due to multiple layers, which also increases the antenna thickness. This feeding scheme also provides narrow bandwidth.

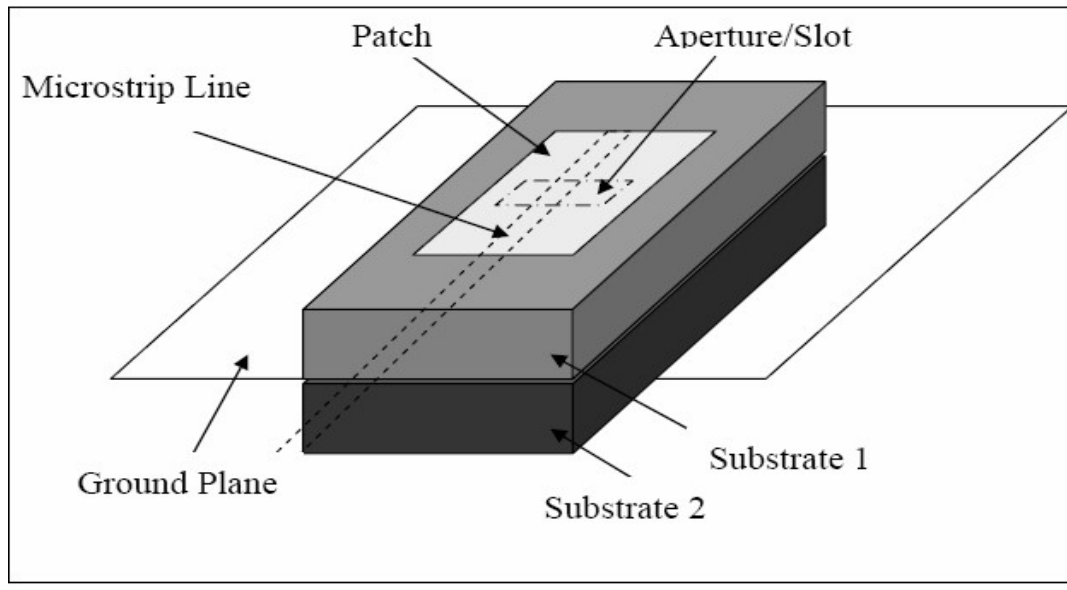


Figure – 3.6 – Aperture Feed

3.4.4 Proximity Coupled Feed

This type of feed technique is also called as the electromagnetic coupling scheme. As shown in Figure 3.7, two dielectric substrates are used such that the feed line is between the two substrates and the radiating patch is on top of the upper substrate. The main advantage of this feed technique is that it eliminates spurious feed radiation and provides very high bandwidth (as high as 13%), due to overall increase in the thickness of the microstrip patch antenna. This scheme also provides choices between two different dielectric media, one for the patch and one for the feed line to optimize the individual performances.

Matching can be achieved by controlling the length of the feed line and the width-to-line ratio of the patch. The major disadvantage of this feed scheme is that it is difficult to fabricate because of the two dielectric layers which need proper alignment. Also, there is an increase in the overall thickness of the antenna.

Table 3.1 summarizes the characteristics of the different feed techniques.

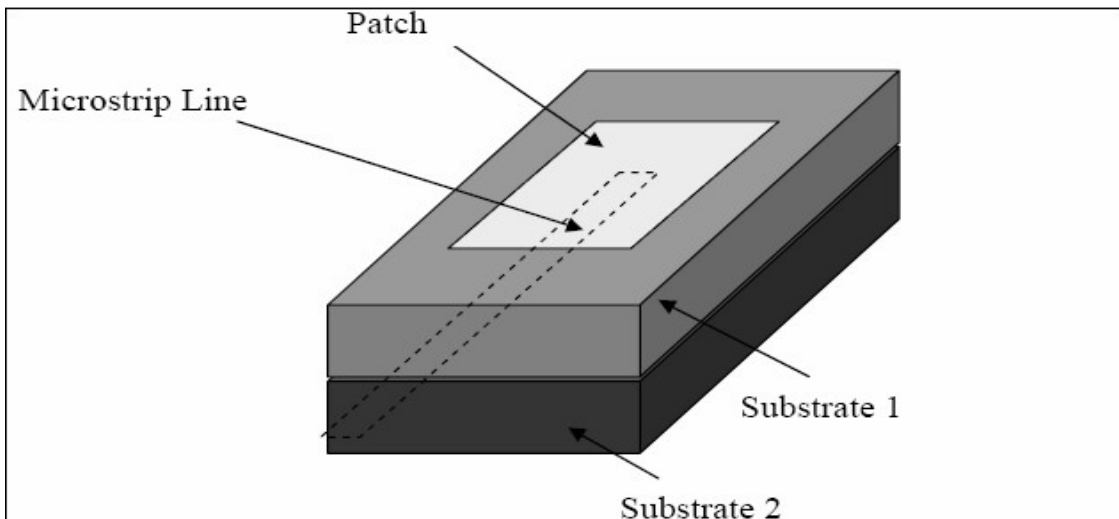


Figure – 3.7 – Proximity Coupled Feed

Characteristics	Microstrip Line Feed	Coaxial Feed	Aperture coupled Feed	Proximity coupled Feed
Spurious feed radiation	More	More	Less	Minimum
Reliability	Better	Poor due to soldering	Good	Good
Ease of fabrication	Easy	Soldering and drilling needed	Alignment required	Alignment required
Impedance Matching	Easy	Easy	Easy	Easy
Bandwidth (achieved with impedance matching)	2-5%	2-5%	2-5%	13%

Table – 3.1 – Comparison of different Feed Methods

It is to be noted that in our project simulations we have used microstrip feed and co-axial feed techniques.

3.5 Methods of Analysis

The most popular models for the analysis of Microstrip patch antennas are the transmission line model, cavity model, and full wave model (which include primarily integral equations/Moment Method). The transmission line model is the simplest of all and it gives good physical insight but it is less accurate. The cavity model is more accurate and gives good physical insight but is complex in nature. The full wave models are extremely accurate, versatile and can treat single elements, finite and infinite arrays, stacked elements, arbitrary shaped elements and coupling.

It must be noted that our project is centered on the transmission line model and uses all of the empirical equations this model is based on for simulations. The cavity model is not at the centre of our project and is hence explained very briefly. The method of moments is explained in detail as it is used by several field solvers (such as IE3D) for simulations.

3.5.1 Transmission Line Model

This model represents the microstrip antenna by two slots of width W and height h , separated by a transmission line of length L . The microstrip is essentially a non homogeneous line of two dielectrics, typically the substrate and air. Figure 3.8 illustrates this.

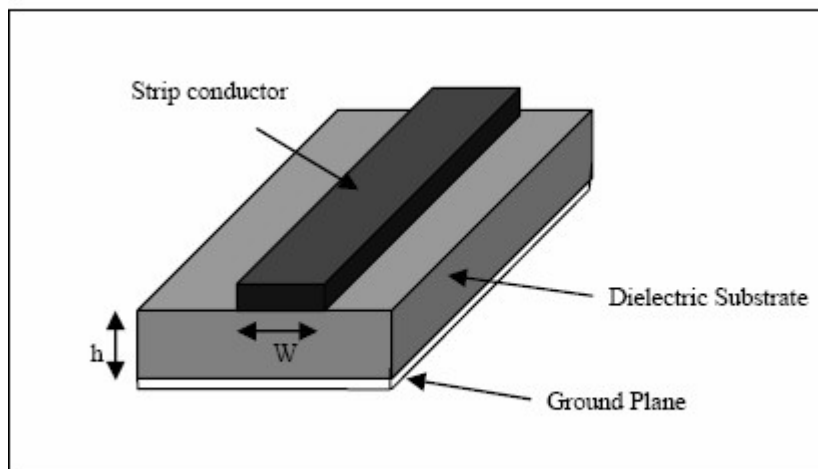


Figure – 3.8 – Microstrip Line

As seen from Figure 3.9, most of the electric field lines reside in the substrate and parts of some lines in air. As a result, this transmission line cannot support pure transverse electric-magnetic (TEM) mode of transmission, since the phase velocities would be different in the air and the substrate. Instead, the dominant mode of propagation would be the quasi-TEM mode. Hence, an effective dielectric constant (ϵ_{eff}) must be obtained in order to account for the fringing and the wave propagation in the line.

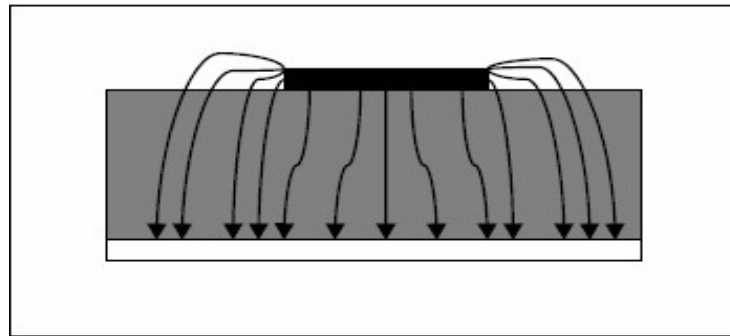


Figure – 3.9 – Electric Field Lines

The value of ϵ_{eff} is slightly less than ϵ_r because the fringing fields around the periphery of the patch are not confined in the dielectric substrate but are also spread in the air as shown in Figure 9. The expression for ϵ_{eff} is given as:

$$\epsilon_{\text{eff}} = (\epsilon_{\text{eff}} + 1)/2 + (\epsilon_{\text{eff}} - 1)/2[1+12h/W]^{-1/2}$$

Equation 3.1

Where ϵ_{eff} = Effective dielectric constant
 ϵ_r = Dielectric constant of substrate
 h = Height of dielectric substrate
 W = Width of the patch

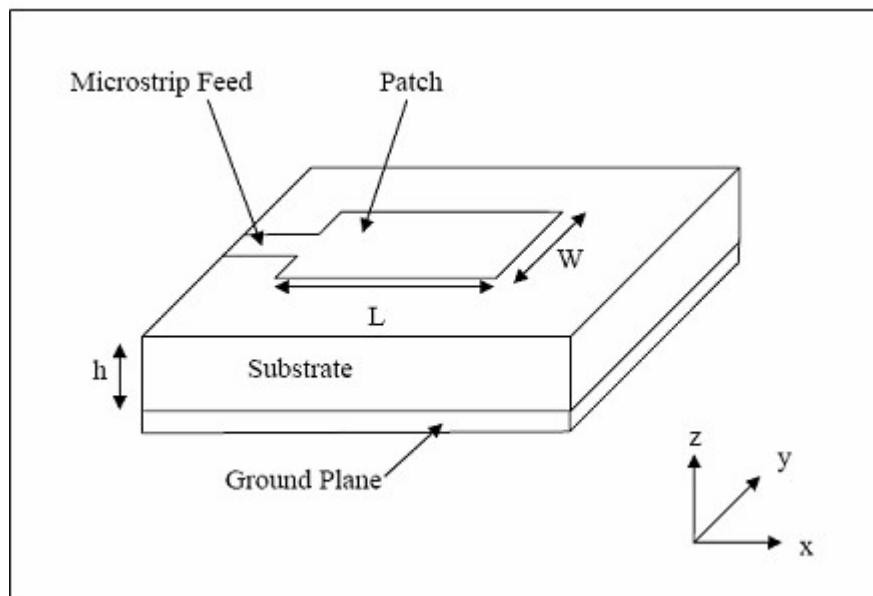


Figure - 3.10 – Microstrip Patch Antenna

Figure 3.10 shows a rectangular microstrip patch antenna of length L , width W resting on a substrate of height h . The co-ordinate axis is selected such that the length is along the x direction, width is along the y direction and the height is along the z direction. In order to operate in the fundamental TM mode, the length of the patch must be slightly less than $\lambda / 2$ where λ is the wavelength in the dielectric medium and is equal to $\lambda_0/\sqrt{\epsilon_{\text{eff}}}$ where λ_0 is the free space wavelength. The TM mode implies that the field varies one $\lambda / 2$ cycle along the length, and there is no variation along the width of the patch. In figure 3.11 the microstrip patch antenna is represented by two slots, separated by a transmission line of length L and open circuited at both the ends. Along the width of the patch, the voltage is maximum and current is minimum due to the open ends. The fields at the edges can be resolved into normal and tangential components with respect to the ground plane.

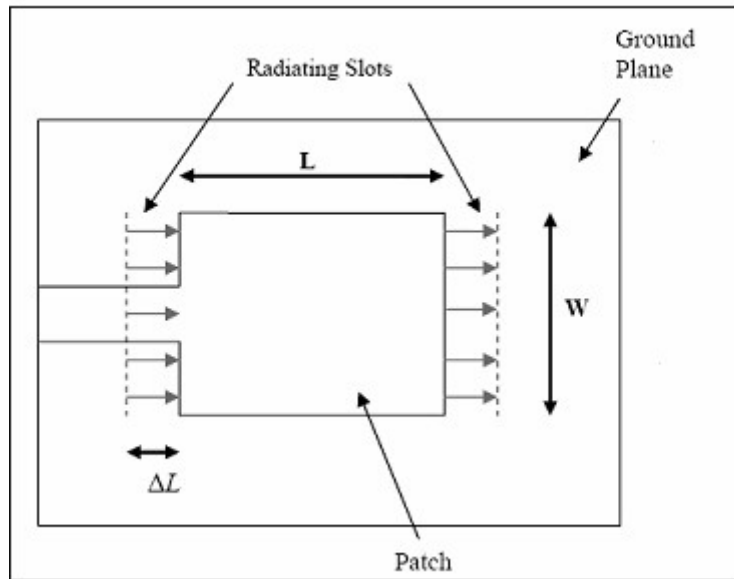


Figure – 3.11 – Top View of Antenna

It is seen from figure 3.12 that the normal components of the electric field at the two edges along the width are in opposite directions and thus out of phase since the patch is $\lambda/2$ long and hence they cancel each other in the broadside direction. The tangential components (seen in figure 11), which are in phase, means that the resulting fields combine to give maximum radiated field normal to the surface of the structure. Hence the edges along the width can be represented as two radiating slots, which are $\lambda / 2$ apart and excited in phase and radiating in the half space above the ground plane.

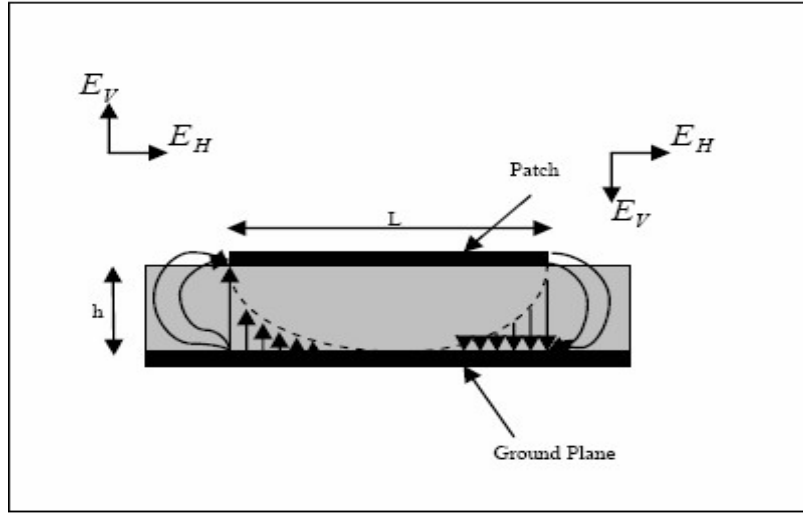


Figure – 3.12 – Side View of Antenna

The fringing fields along the width can be modeled as radiating slots and electrically the patch of the microstrip antenna looks greater than its physical dimensions. The dimensions of the patch along its length have now been extended on each end by a distance ΔL , which is given empirically by as:

$$\Delta L = 0.412h(\epsilon_{\text{reff}} + 0.3)(W/h + 0.264)/((\epsilon_{\text{reff}} - 0.258)(W/h + 0.8)) \quad \text{Equation 3.2}$$

The effective length of the patch L_{eff} now becomes:

$$L_{\text{eff}} = L + 2 \Delta L \quad \text{Equation 3.3}$$

For a given resonance frequency f_o , the effective length is given by as:

$$L_{\text{eff}} = c/(2f_o\sqrt{(\epsilon_{\text{reff}})}) \quad \text{Equation 3.4}$$

For a rectangular Microstrip patch antenna, the resonance frequency for any TM mode is given as:

$$f_o = c/(2\sqrt{(\epsilon_{\text{reff}})}[(m/L)^2 + (n/W)^2]^{1/2}) \quad \text{Equation 3.5}$$

Where m and n are modes along L and W respectively. For efficient radiation, the width W is given as:

$$W = c/(2f_o\sqrt{((\epsilon_r + 1)/2)}) \quad \text{Equation 3.6}$$

3.5.2 Cavity Model

Although the transmission line model discussed in the previous section is easy to use, it has some inherent disadvantages. Specifically, it is useful for patches of rectangular design and it ignores field variations along the radiating edges. These disadvantages can be overcome by using the cavity model. In this model, the interior region of the dielectric substrate is modeled as a cavity bounded by electric walls on the top and bottom. The basis for this assumption is the following observations for thin substrates ($h \ll \lambda$).

- 1) Since the substrate is thin, the fields in the interior region do not vary much in the z direction, i.e. normal to the patch.
- 2) The electric field is z directed only, and the magnetic field has only the transverse components H_x and H_y in the region bounded by the patch metallization and the ground plane. This observation provides for the electric walls at the top and the bottom.

3.5.3 Full Wave Solutions-Method of Moments

One of the methods, that provide the full wave analysis for the microstrip patch antenna, is the Method of Moments. In this method, the surface currents are used to model the microstrip patch and the volume polarization currents are used to model the fields in the dielectric slab. It has been shown by Newman and Tulyathan how an integral equation is obtained for these unknown currents and using the Method of Moments, these electric field integral equations are converted into matrix equations which can then be solved by various techniques of algebra to provide the result. A brief overview of the method of moments is given below.

The basic form of the equation to be solved by the method of moments is:

$$F(g) = h \quad \text{Equation 3.7}$$

where F is a known linear operator, g is an unknown function, and h is the source or excitation function. The aim here is to find g , when F and h are known. The unknown function g can be expanded as a linear combination of N terms to give:

$$g = \sum_{n=1}^N a_n g_n = a_1 g_1 + a_2 g_2 + \dots + a_N g_N \quad \text{Equation 3.8}$$

where a_n is an unknown constant and g_n is a known function usually called a basis or expansion function. Substituting equation 2 in 1 and using the linearity property of the operator F , we can write:

$$\sum_{n=1}^N a_n F(g_n) = h \quad \text{Equation 3.9}$$

The basis functions g_n must be selected in such a way, that each $F(g_n)$ in the above equation can be calculated. The unknown constants a_n cannot be determined directly because there are N unknowns, but only one equation. One method of finding these

constants is the method of weighted residuals. In this method, a set of trial solutions is established with one or more variable parameters. The residuals are a measure of the difference between the trial solution and the true solution. The variable parameters are selected in a way which guarantees a best fit of the trial functions based on the minimization of the residuals.

From the antenna theory point of view, we can write the Electric field integral equation as

$$E = f_e(J) \quad \text{Equation 3.10}$$

where E is the known incident electric field.

J is the unknown induced current.

f_e is the linear operator.

The first step in the moment method solution process would be to expand J as a finite sum of basis function given as:

$$J = \sum_{i=1}^M J_i b_i \quad \text{Equation 3.11}$$

where b_i is the i th basis function and J_i is an unknown coefficient. The second step involves the defining of a set of M linearly independent weighting functions, w_j . Taking the inner product on both sides and substituting equation 3.5 in equation 3.4 we get:

$$\langle w_j, E \rangle = \sum_{i=1}^M \langle w_j, f_e(J_i, b_i) \rangle \quad \text{Equation 3.12}$$

Where $j=1,2,\dots,M$

$$\text{In matrix form we get } [Z_{ij}][J] = [E_j] \quad \text{Equation 3.13}$$

Where $Z_{ij} = \langle w_j f_e(b_i) \rangle$

$E_j = \langle w_j, H \rangle$

J is the current vector containing the unknown quantities.

The vector E contains the known incident field quantities and the terms of the Z matrix are functions of geometry. The unknown coefficients of the induced current are the terms of the J vector. Using any of the algebraic schemes mentioned earlier, these equations can be solved to give the current and then the other parameters such as the scattered electric and magnetic fields can be calculated directly from the induced currents. IE3D is a powerful simulation software that uses the method of moments. It is an efficient field solver and this is why we used it for carrying out all our patch antenna simulations. The following section describes IE3D's uses and merits.

3.6 Simulation Software – IE3D

The software used to perform all simulations is Zealand Inc's IE3D. IE3D is a full-wave electromagnetic simulator based on the method of moments. It analyzes 3D and multilayer structures of general shapes. It has been widely used in the design of MICs, RFICs, patch antennas, wire antennas, and other RF/wireless antennas. It can be used to calculate and plot the S parameters, VSWR, current distributions as well as the radiation patterns. Some of IE3D's features are

- 1) Can model true 3D metallic structures in multiple dielectric layers in open, closed or periodic boundary
- 2) High efficiency, high accuracy and low cost electromagnetic simulation tool on PCs with windows based graphic interface
- 3) Automatic generation of non-uniform mesh with rectangular and triangular cells
- 4) Can model structures with finite ground planes and differential feed structures
- 5) Accurate modeling of true 3D metallic structures and metal thickness
- 6) Efficient matrix solvers
- 7) 3D and 2D display of current distribution, radiation patterns and near field.

For our purposes it is a very powerful tool as it allows for ease of design and accurate simulation results. The results obtained for each patch were 2D view of patch, 3D view of patch, RL curve, Directivity, gain, beam width and other such parameters, true 3D radiation pattern, mapped 3D radiation pattern and 2D polar radiation pattern. These terms are defined below.

True 3D Radiation Pattern- It is the pattern in the actual 3D space. The size of the pattern from the origin represents how strong the field at a specific (θ , ϕ) angle.

Mapped 3D Radiation Pattern - It is the pattern with the theta angle mapped to the radius of a cylindrical coordinate system. The radius in the cylindrical system represents value of the theta angle.

2D Polar Radiation Pattern - A polar pattern is basically a cut on the True 3D pattern at a specific phi angle.

2D Cartesian Radiation Pattern - A Cartesian pattern is basically a cut on the Mapped 3D pattern at a specific phi angle.

For our project IE3D was very useful as it ensured ease of patch design and comprehensive simulation results. This was the reason for the slowness of IE3D compared to other software like Sonnet. Typically IE3D took around 100s to generate a frequency point (we mostly used 20 such points for generation of all curves etc) and in some cases even 600s (10 min) depending on the patch dimensions, frequency range, degree of meshing etc. Sonnet on the other hand was slightly faster taking around 50s per frequency point for simple simulations but it only displayed the return loss curve while IE3D was used to determine 3D radiation patterns etc. This is why all simulations were carried out using IE3D only. The simulation results follow.

3.7 Design of a Simple Rectangular Patch Antenna

The software part of our project revolved around determination of the radiation pattern and return loss curve (s_{11} vs frequency) of several simple rectangular patch antennas. From the transmission line model of rectangular patch antennas it is clear that the three essential parameters for the design of a rectangular Microstrip Patch Antenna are:

- 1) Frequency of operation (f_0): The resonant frequency of the antenna must be selected appropriately.
- 2) Dielectric constant of the substrate (ϵ_r): A substrate with a high dielectric constant reduces the dimensions of the antenna.
- 3) Height of dielectric substrate (h): For the microstrip patch antenna to be used in certain applications (such as cell phones) it is essential that it is not bulky and to ensure this the height of the dielectric substrate can't be more than a few mm.

The effect of all the above 3 factors and the position of feed point on antenna performance was studied by simulating several rectangular patch antennas. The basic patch chosen for this purpose is shown in figure 3.13.

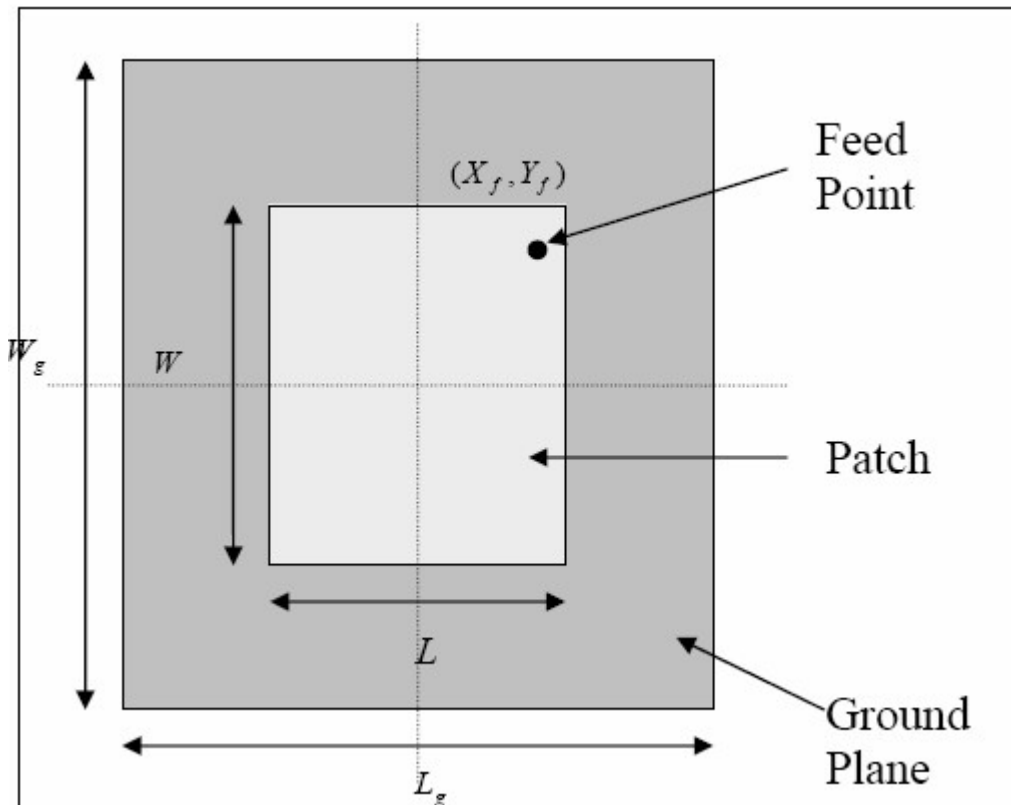


Figure – 3.13 – Top View of the rectangular patch

This patch is intended for cell phone applications and hence its frequency of operation was chosen to be 1.9 GHz (GSM frequency band). Its parameters are

$$f_o = 1.9 \text{ GHz}$$

$$\epsilon_r = 11.9$$

$$h = 1.5 \text{ mm}$$

Using the above parameters and the equations of the transmission line model we obtain

$$W = 31.1 \text{ mm}$$

$$\epsilon_{\text{refl}} = 10.7871$$

$$L_{\text{eff}} = 24 \text{ mm}$$

$$\Delta L = 0.63455 \text{ mm}$$

$$L = 22.8 \text{ mm}$$

The transmission line model is applicable to infinite ground planes only. However, for practical considerations, it is essential to have a finite ground plane. It has been shown that similar results for finite and infinite ground plane can be obtained if the size of the ground plane is greater than the patch dimensions by approximately six times the substrate thickness all around the periphery. Hence, for this design, the ground plane dimensions would be given as:

$$L_g = 6h + L = 31.8 \text{ mm}$$

$$W_g = 6h + W = 40.1 \text{ mm}$$

A simple MATLAB program that we used to perform these calculations is given in Appendix A.

A coaxial probe type feed is to be used in this design. As shown in Figure 3.13, the center of the patch is taken as the origin and the feed point location is given by the co-ordinates (X_f, Y_f) from the origin. The feed point must be located at that point on the patch, where the input impedance is 50 ohms for the resonant frequency. Hence, a trial and error method is used to locate the feed point. For different locations of the feed point, the return loss (RL) is compared and that feed point is selected where the R.L is most negative. There exists a point along the length of the patch where the RL is minimum. Hence in this design, Y_f was kept constant at zero and only X_f was varied to locate the optimum feed point.

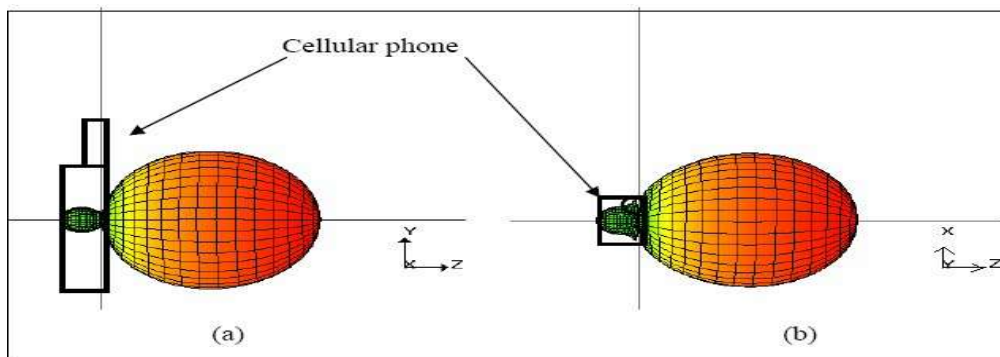


Figure – 3.14 (a) 3D view of radiation pattern for cellular phone orientation in the YZ plane (b) 3D view of radiation pattern for cellular phone orientation in the XZ plane

The first set of simulation results show the effect of feed point on the return loss curve and radiation pattern. When the microstrip patch antenna designed would be placed into a cellular phone, its orientation would be such that the z axis would be parallel to the surface of the earth. Figure 3.14 shows the 3D radiation pattern plots for this scenario. From the figure it became clear to us that the back lobe protruding into the cell phone had to be made as small as possible and the main lobe had to be expanded to ensure better transmission. To ensure this we varied h and ϵ_r until this occurred. In the process the effect of these parameters on patch dimensions, RL curve and radiation pattern was studied. These simulation results for this patch and 2 other patches are presented later in this report. First an introduction to the software used for the simulations is presented.

3.8 Simulation of a 1.9 GHz Patch Antenna

3.8.1 Introduction

One of the antennas that we simulated was the 1.9 GHz patch antenna. 1.9 GHz antenna is a commonly used frequency, used predominantly in GSM phones in United States. Our objective was to design a probe fed patch antenna that resonates at 1.9 GHz and then vary the parameters of the antenna such that the working of the patch is optimized. We divided the simulations into three basic groups-

- 1) Firstly, we varied the feed point of the patch. The gain of the antenna varies greatly as we vary the feed point. We get best gain when the probe is located at the 50 Ohm impedance line. In this case the return loss curve dips the maximum. Since there is no specific way of finding this line, we vary the feed point and try to get the best gain by trial and error.
- 2) We tried to ensure that the entire radiation due to the patch is in one direction. This is primarily because of the growing concern that cell phone signals are detrimental to human health. Hence we tried to design a patch such that the entire signal propagates

away from the user. This was achieved by varying the thickness of the patch. The catch here is that the patch cannot be made too thick, or it cannot be used in a cell phone
 3) We also varied the permittivity of the dielectric and observed its effects on the performance of the patch.

All the patches were designed with help of equations given previously. The simulation results for the patches are given in the following pages.

3.8.2 Effect of variation of probe feed on the patch

The centre of the patch is located at (0,0). The probe was fed at (2,0), (3,0), (4,0), (5,0), and (6,0) and its effect on various parameters of the patch, primarily, on the return loss curve was observed. Basic dimensions of the patch calculated were as follows.

Length of ground plane = 31.8 mm
 Width of ground plane = 40.1 mm
 Length of the patch = 22.8 mm
 Width of the patch = 31.1 mm
 Permittivity of substrate = 11.9
 Height of substrate = 1.5 mm
 Frequency = 1.9 GHz

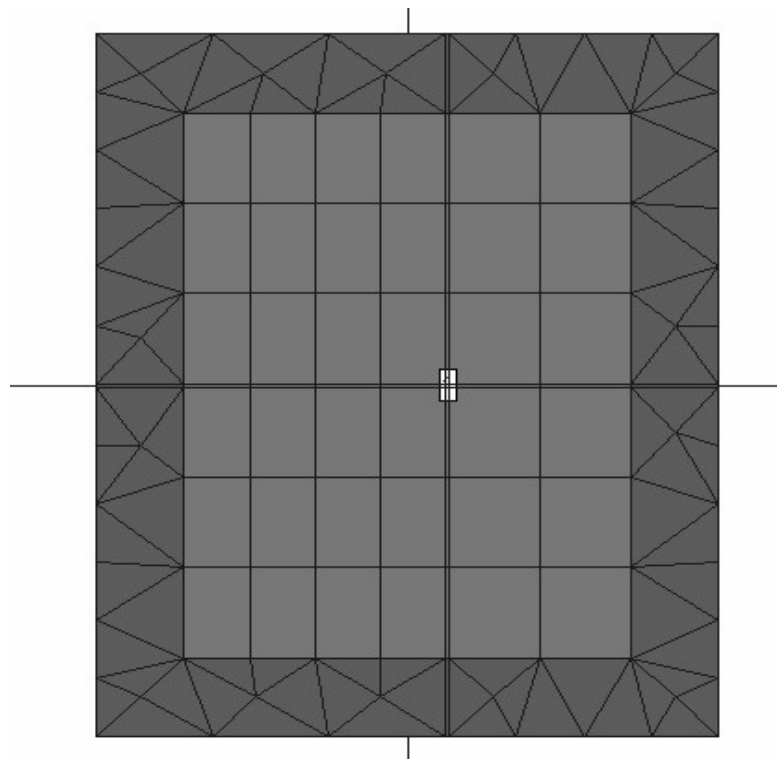


**Figure – 3.15 - The meshed patch designed in IE3D to resonate at 1.9GHz
 In this case the probe is located at (2,0)**

The above figure shows one of the patches simulated. A new patch was created for as the probe feed point was varied. A comparison of the results obtained in each case follows.

3.8.2.1 Return Loss Curves

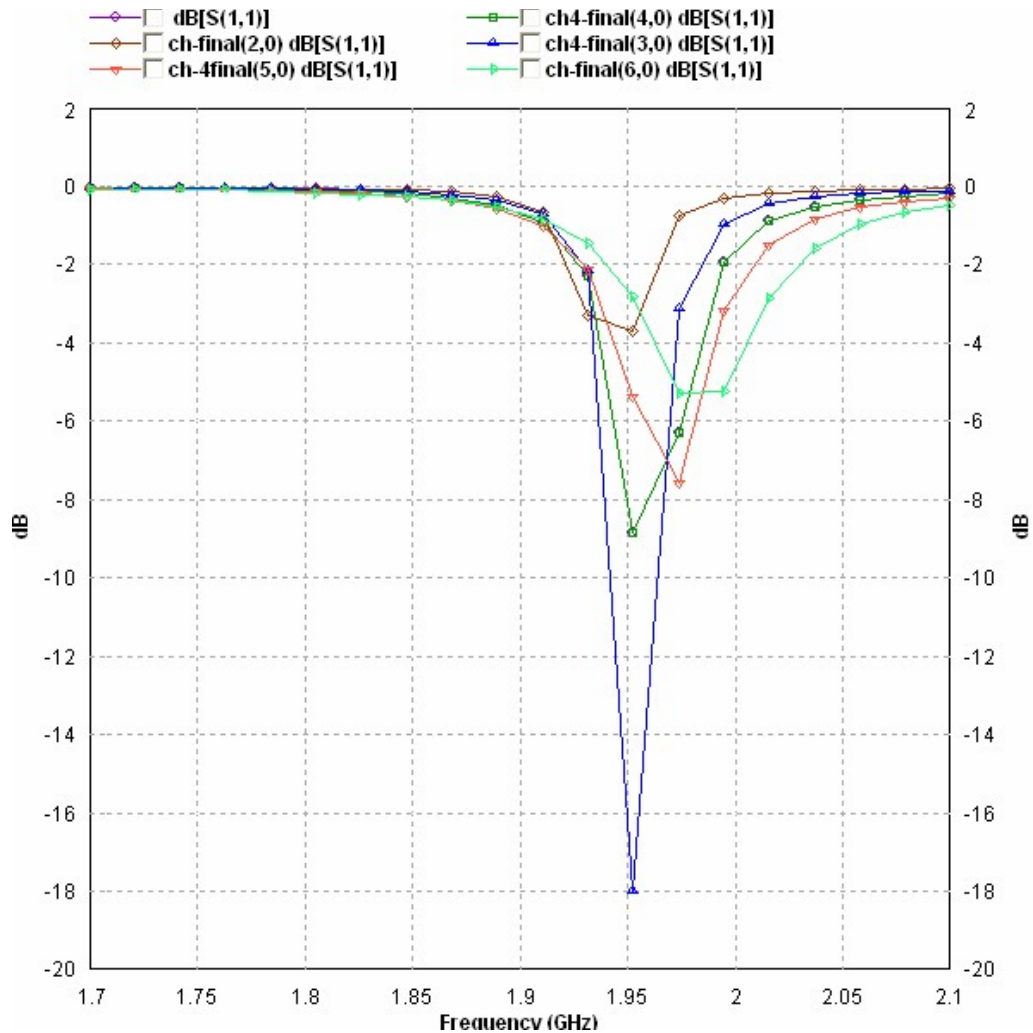


Figure – 3.16 – Return Loss curve for different feed points

As it can be seen from the above set of curves, we get best results when the probe is located (3,0), since the power reflected is minimum then.

3.8.2.2 Other Frequency Properties

Frequency	: 1.91053 (GHz)
Incident Power	: 0.01 (W)
Input Power	: 0.00139718 (W)
Radiated Power	: 0.000572898 (W)
Average Radiated Power	: 4.55898e-005 (W/s)
Radiation Efficiency	: 41.0038%
Antenna Efficiency	: 5.72898%
Conjugate Match Efficiency	: 20.5019%
Total Field Properties	:
Gain	: -9.11385 dBi
Directivity	: 3.30538 dBi
Maximum	: at (0, 90) deg.
3dB Beam Width	: (96.6573, 156.222) deg.
Conjugate Match Gain	: -3.57668 dBi

Table – 3.2 - Probe feed at (2,0) and f=1.9GHz

Frequency	: 1.91053 (GHz)
Incident Power	: 0.01 (W)
Input Power	: 0.00151214 (W)
Radiated Power	: 0.000625071 (W)
Average Radiated Power	: 4.97416e-005 (W/s)
Radiation Efficiency	: 41.3368%
Antenna Efficiency	: 6.25071%
Conjugate Match Efficiency	: 20.6684%
Total Field Properties	:
Gain	: -8.73455 dBi
Directivity	: 3.30615 dBi
Maximum	: at (0, 150) deg.
3dB Beam Width	: (96.6001, 156.159) deg.
Conjugate Match Gain	: -3.54078 dBi

Table – 3.3 - Probe feed at (3,0) and f=1.9GHz

Frequency	: 1.91053 (GHz)
Incident Power	: 0.01 (W)
Input Power	: 0.00200064 (W)
Radiated Power	: 0.000842743 (W)
Average Radiated Power	: 6.70633e-005 (W/s)
Radiation Efficiency	: 42.1236%
Antenna Efficiency	: 8.42743%
Conjugate Match Efficiency	: 21.0618%
Total Field Properties	:
Gain	: -7.42624 dBi
Directivity	: 3.31681 dBi
Maximum	: at (0, 80) deg.
3dB Beam Width	: (96.8584, 153.967) deg.
Conjugate Match Gain	: -3.44824 dBi

Table – 3.4 - Probe feed at (4,0) and f=1.9GHz

Frequency	: 1.91053 (GHz)
Incident Power	: 0.01 (W)
Input Power	: 0.00207797 (W)
Radiated Power	: 0.000882266 (W)
Average Radiated Power	: 7.02085e-005 (W/s)
Radiation Efficiency	: 42.4581%
Antenna Efficiency	: 8.82266%
Conjugate Match Efficiency	: 21.229%
Total Field Properties	:
Gain	: -7.22921 dBi
Directivity	: 3.3148 dBi
Maximum	: at (0, 260) deg.
3dB Beam Width	: (96.9764, 153.532) deg.
Conjugate Match Gain	: -3.4159 dBi

Table – 3.5 - Probe feed at (5,0) and f=1.9GHz

Frequency	:	1.91053 (GHz)
Incident Power	:	0.01 (W)
Input Power	:	0.00175946 (W)
Radiated Power	:	0.000746553 (W)
Average Radiated Power	:	5.94088e-005 (W/s)
Radiation Efficiency	:	42.4309%
Antenna Efficiency	:	7.46553%
Conjugate Match Efficiency	:	21.2154%
Total Field Properties	:	
Gain	:	-7.95669 dBi
Directivity	:	3.3127 dBi
Maximum	:	at (0, 330) deg.
3dB Beam Width	:	(97.0207, 153.505) deg.
Conjugate Match Gain	:	-3.42078 dBi

Table – 3.6 - Probe feed at (6,0) and f=1.9GHz

As can be seen from the above tables, other parameters such as gain, directivity and 3dB beamwidth are nearly the same as we vary the feed points.

3.8.2.3 True 3D patterns

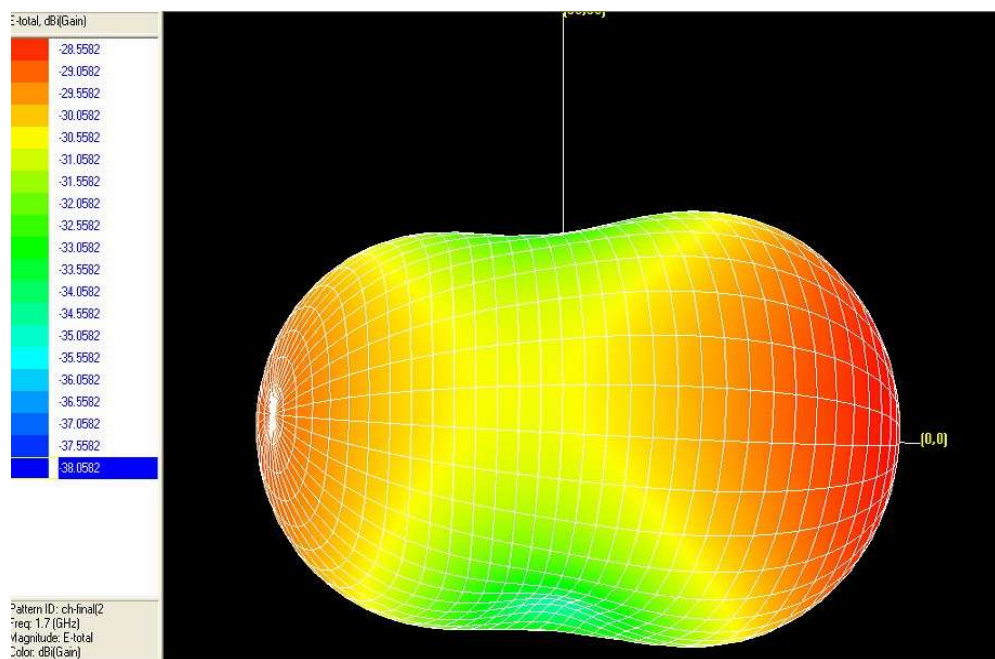


Figure – 3.17 - Probe feed at (2,0)

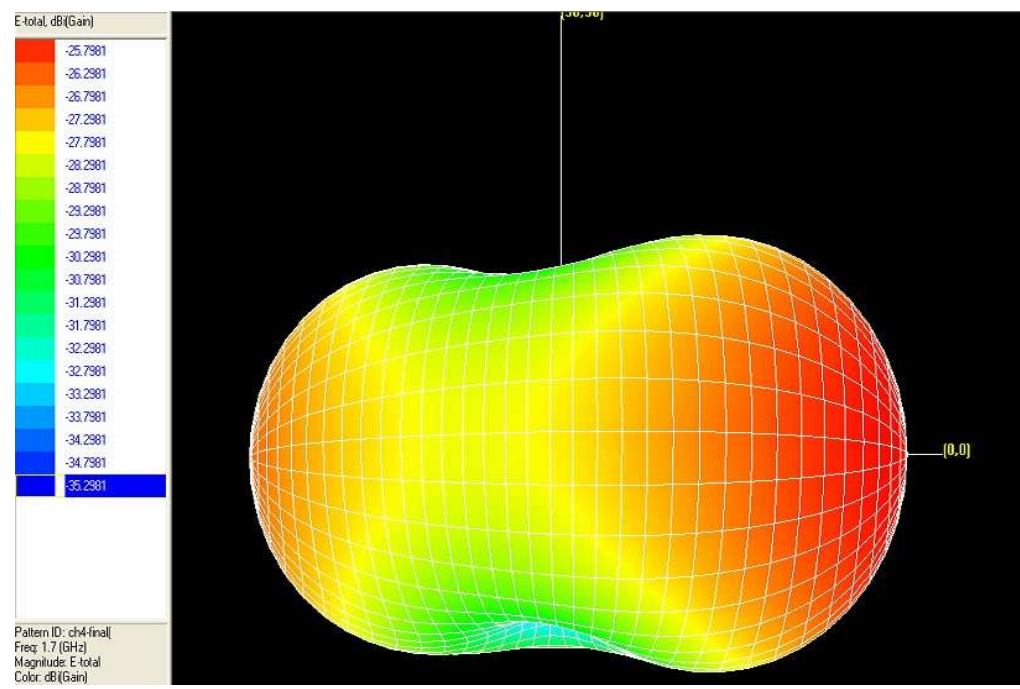


Figure – 3.18 - Probe feed at (3,0)

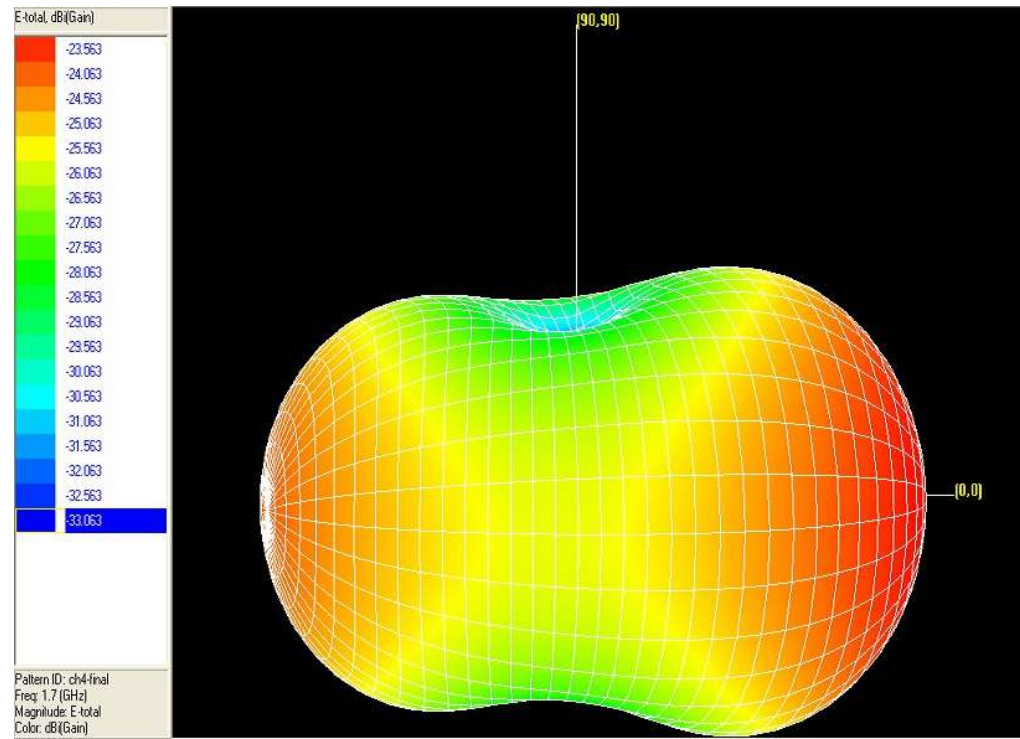


Figure – 3.19 - Probe feed at (4,0)

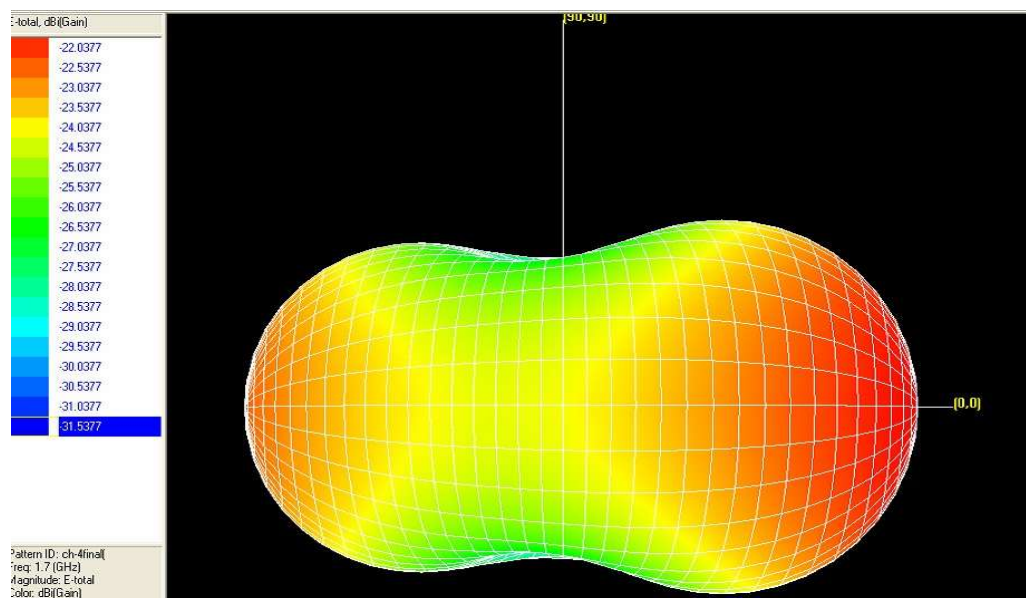


Figure – 3.20 - Probe feed at (5,0)

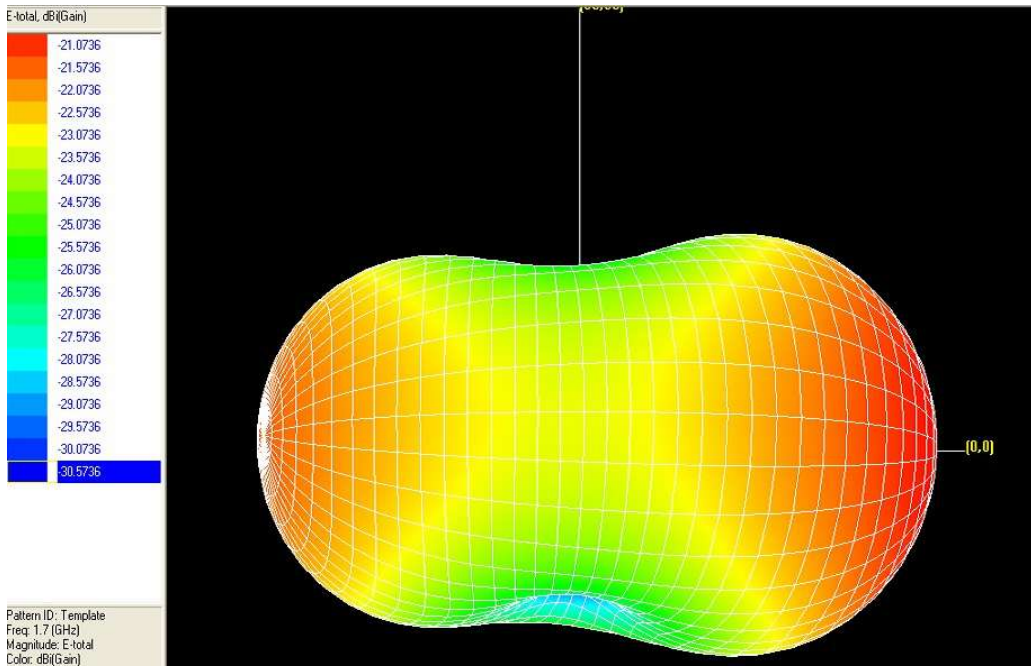


Figure – 3.21 - Probe feed at (6,0)

3.8.2.4 Mapped 3D Patterns

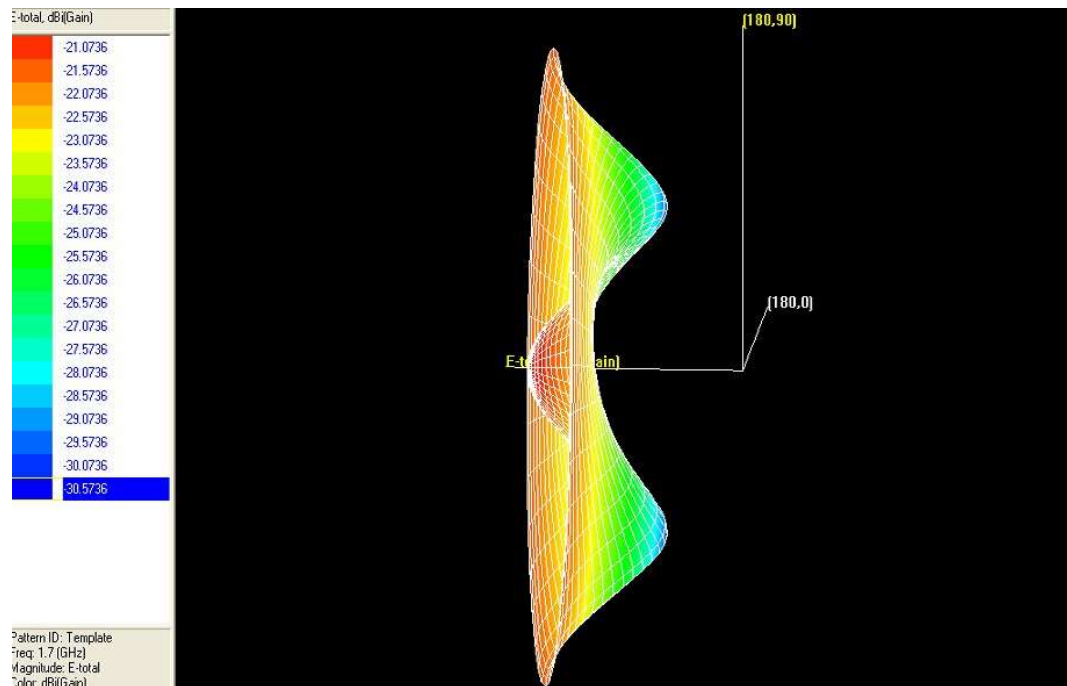


Figure – 3.22 - Probe feed at (2,0)

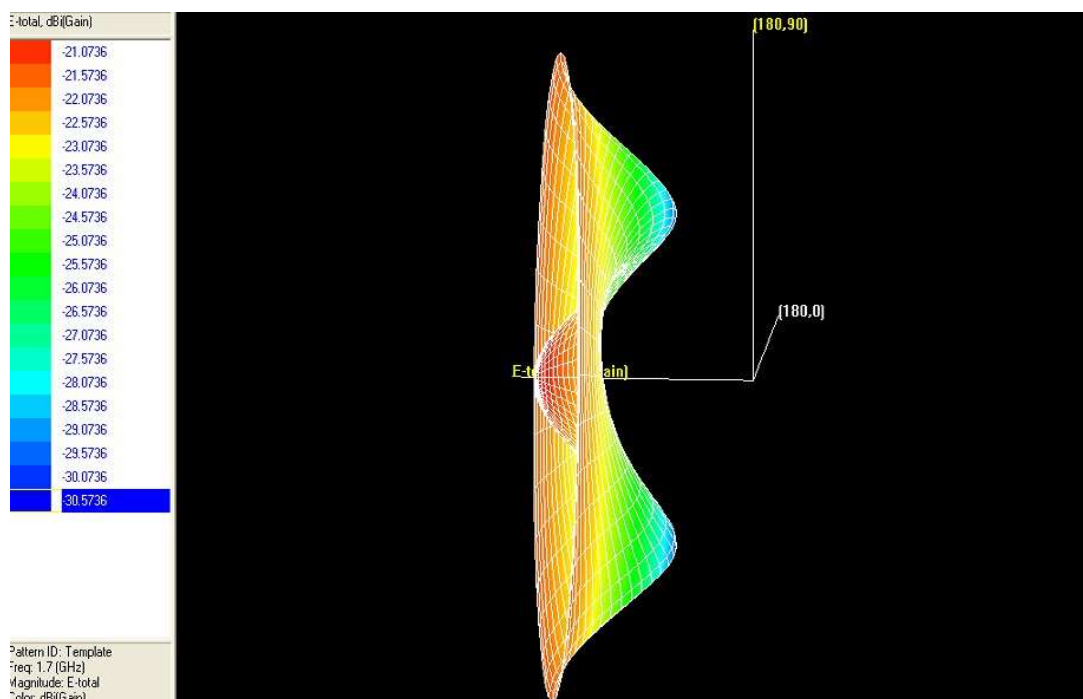


Figure – 3.23 - Probe feed at (3,0)

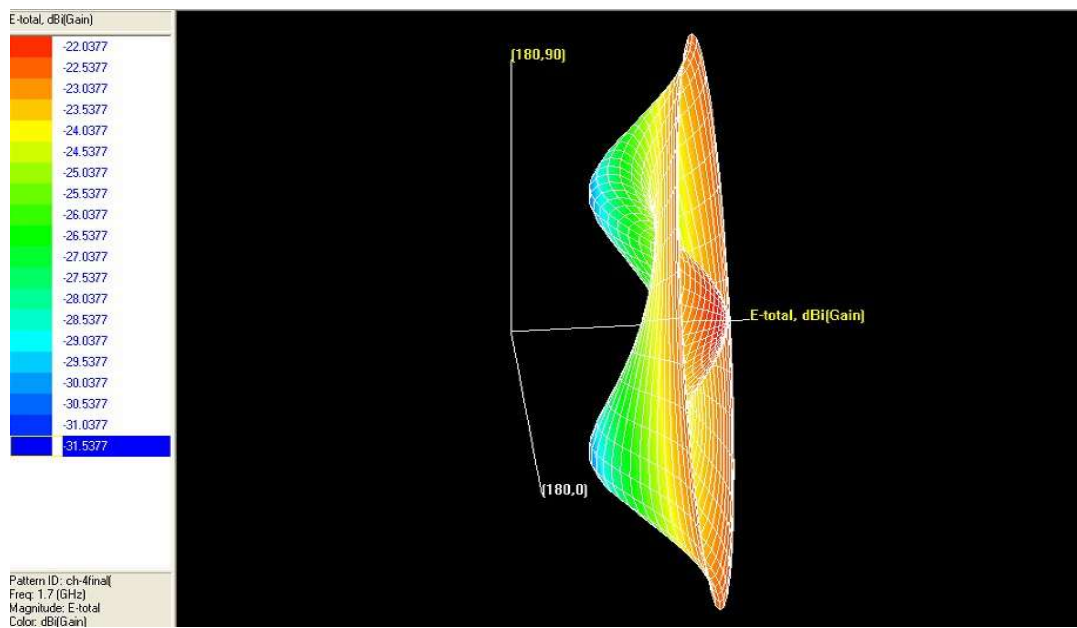


Figure – 3.24 - Probe feed at (5,0)

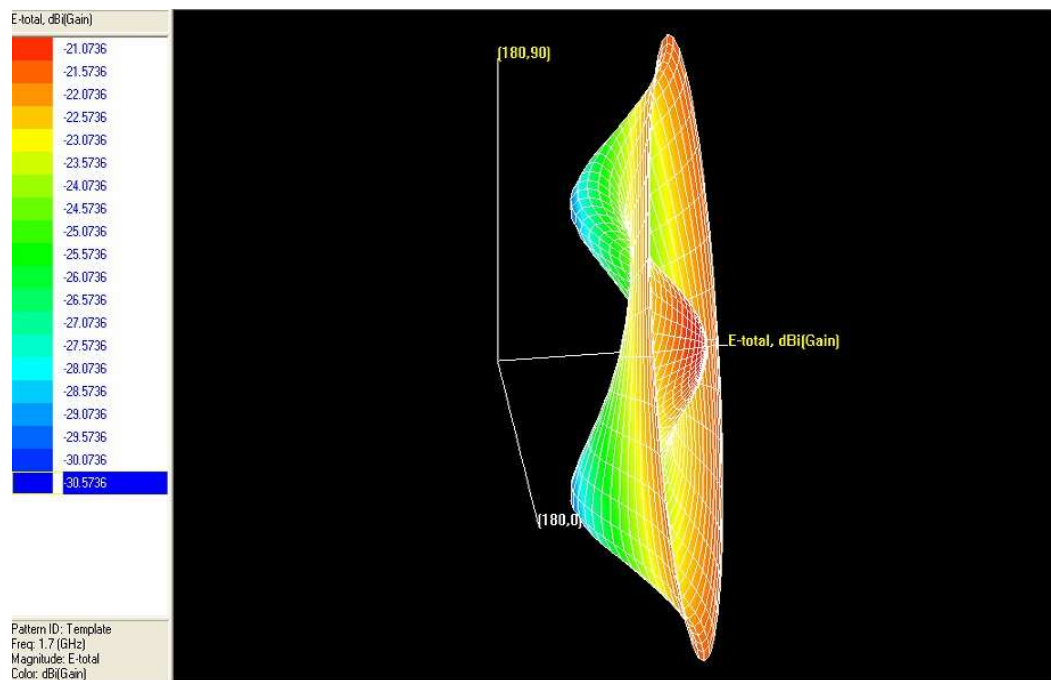


Figure – 3.25 - Probe feed at (6,0)

As seen from above figures, the shape of the true 3D pattern and the mapped 3D pattern remain almost invariant as the feed point is varied. The 2D polar plot obtained for probe feed at (2,0) is shown in figure 3.26. Like the 3D pattern remained invariant, the 2D pattern for probe feed at other points also remained almost invariant, and hence has not been shown.

3.8.2.5 2D Polar Plot (Radiation Pattern)

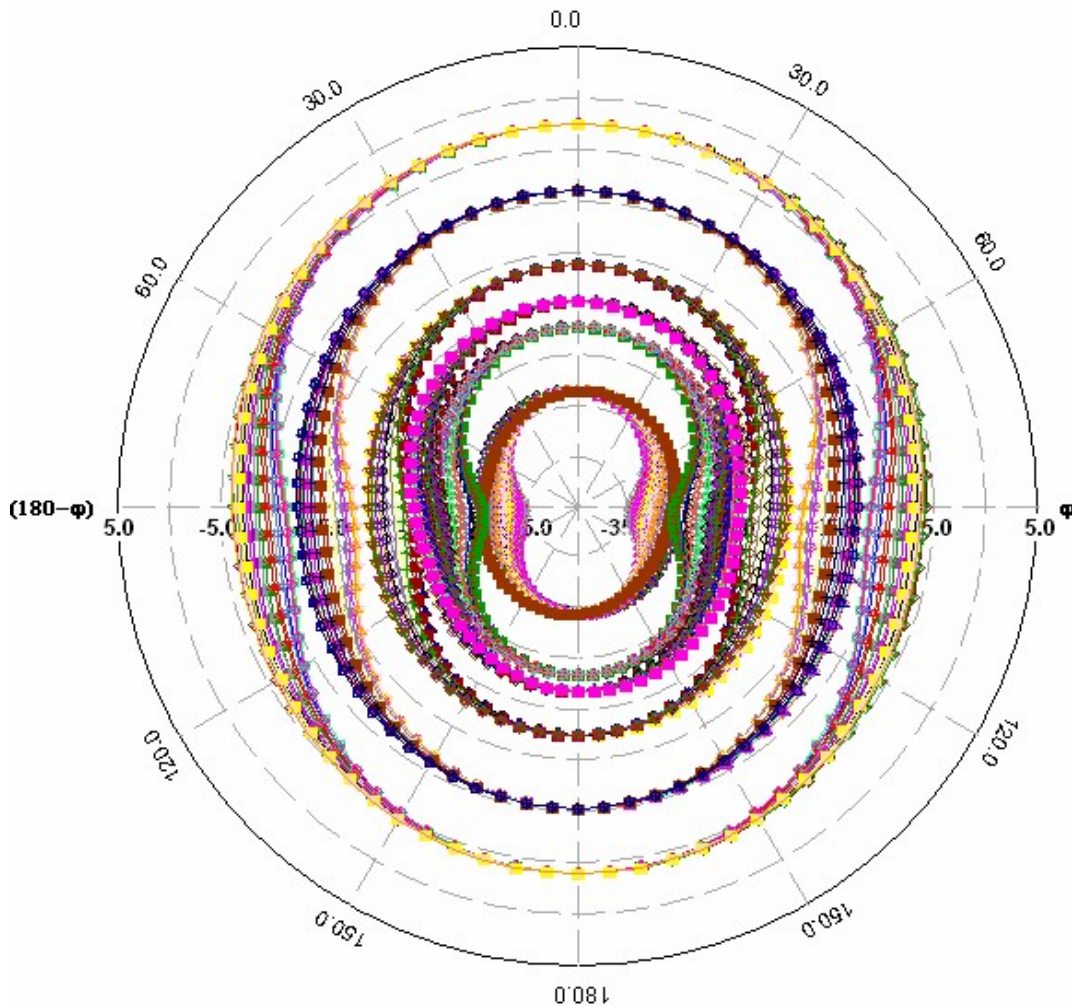


Figure – 3.26 – 2D Polar Plot for different frequencies and angle (ϕ) for feed point at (2,0)

3.8.3 Effect of variation of height of the patch on the patch characteristics

The height of the patch, or in other words the thickness of the substrate was varied, and its effect on the various parameters of the patch antenna was observed. The primary objective of these simulations was to ensure, bulk of the signal propagates in a single direction. It was expected, that as the substrate is made thicker, the signal propagating through the substrate would reduce. Three set of simulations were performed.

With substrate height= 0.5mm

With substrate height= 2mm

With substrate height= 10mm

The results obtained follow.

The dimension of the patches simulated are as follows

Height of substrate = 0.5 mm
Length of ground plane = 25.9 mm
Width of ground plane = 34.1 mm
Length of the patch = 22.9 mm
Width of the patch = 31.1 mm
Permittivity of substrate = 11.9
Frequency = 1.9 GHz

Height of substrate = 2 mm
Length of ground plane = 34.6 mm
Width of ground plane = 43.1 mm
Length of the patch = 22.6 mm
Width of the patch = 31.1 mm
Permittivity of substrate = 11.9
Frequency = 1.9 GHz

Height of substrate = 10 mm
Length of ground plane = 78.9 mm
Width of ground plane = 91.1 mm
Length of the patch = 18.9 mm
Width of the patch = 31.1 mm
Permittivity of substrate = 11.9
Frequency = 1.9 GHz

Figure – 3.27 shows the meshed patches

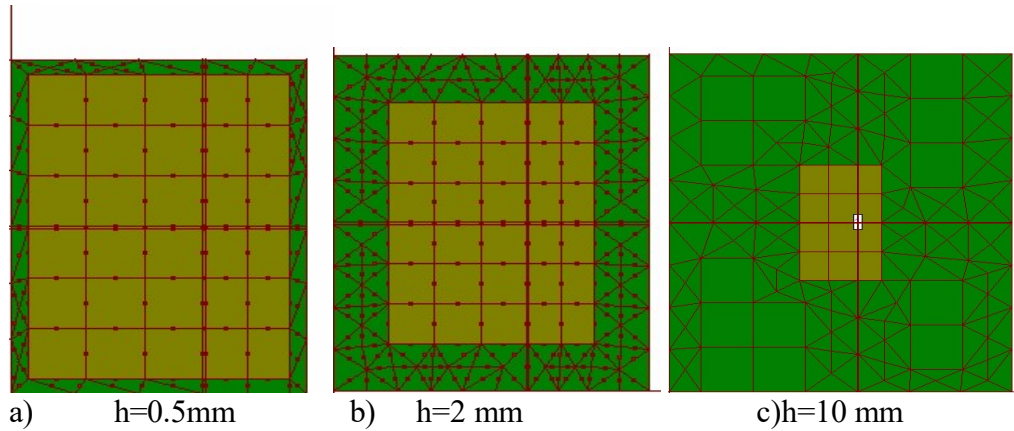


Figure – 3.27 – Meshed patches for different values of h

The simulation results for all three cases follow.

3.8.3.1 True 3D patterns

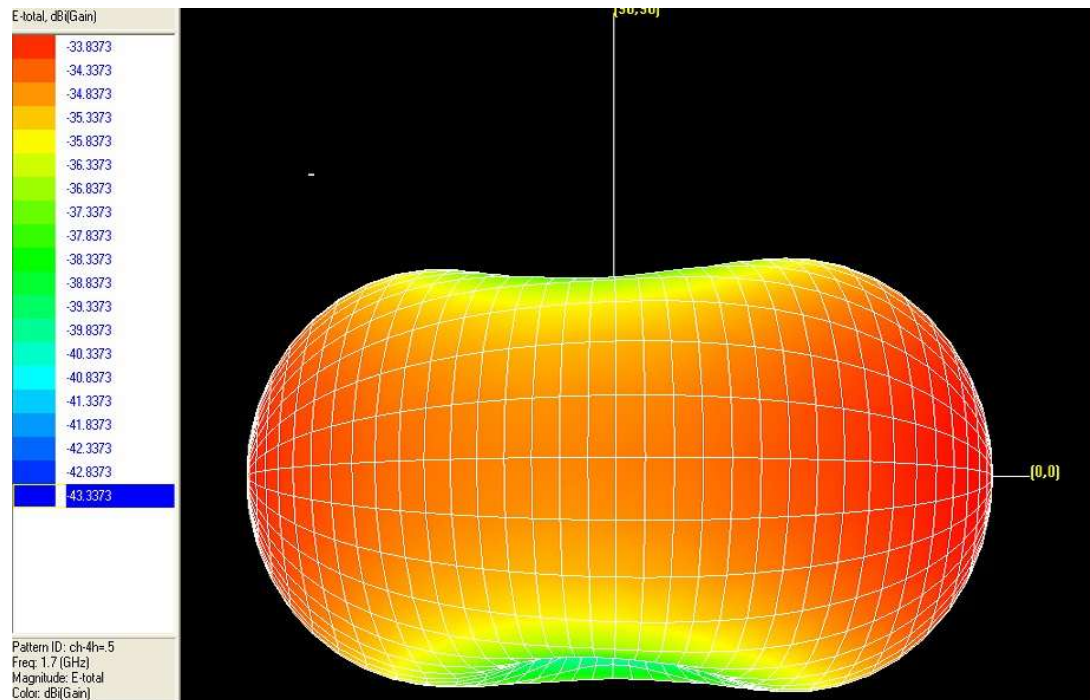


Figure – 3.28 - For substrate height = 0.5mm

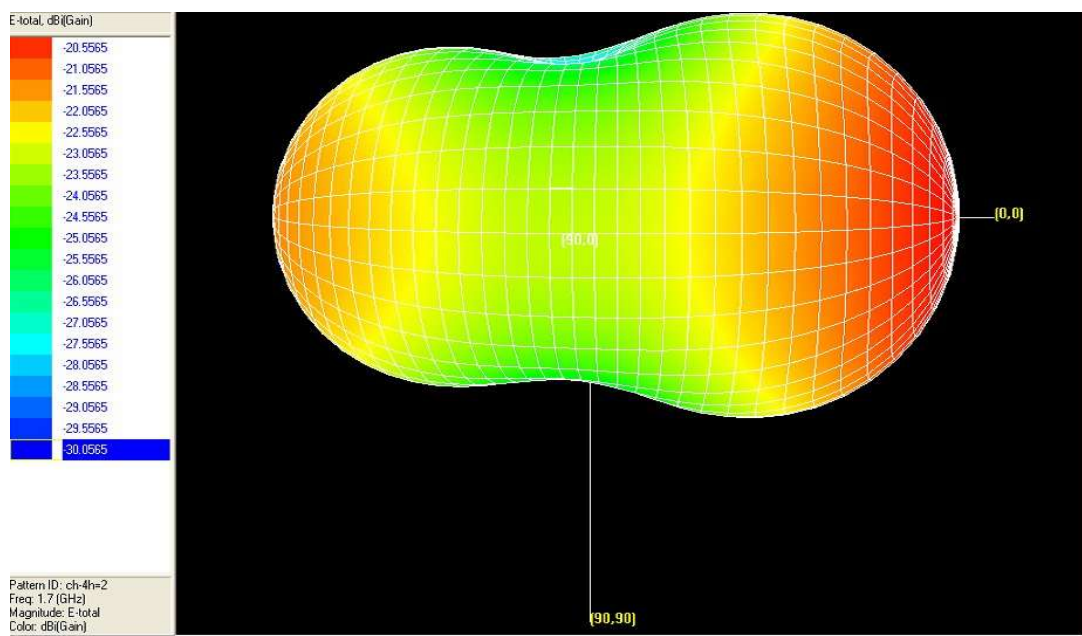


Figure – 3.29 - For substrate height = 2mm

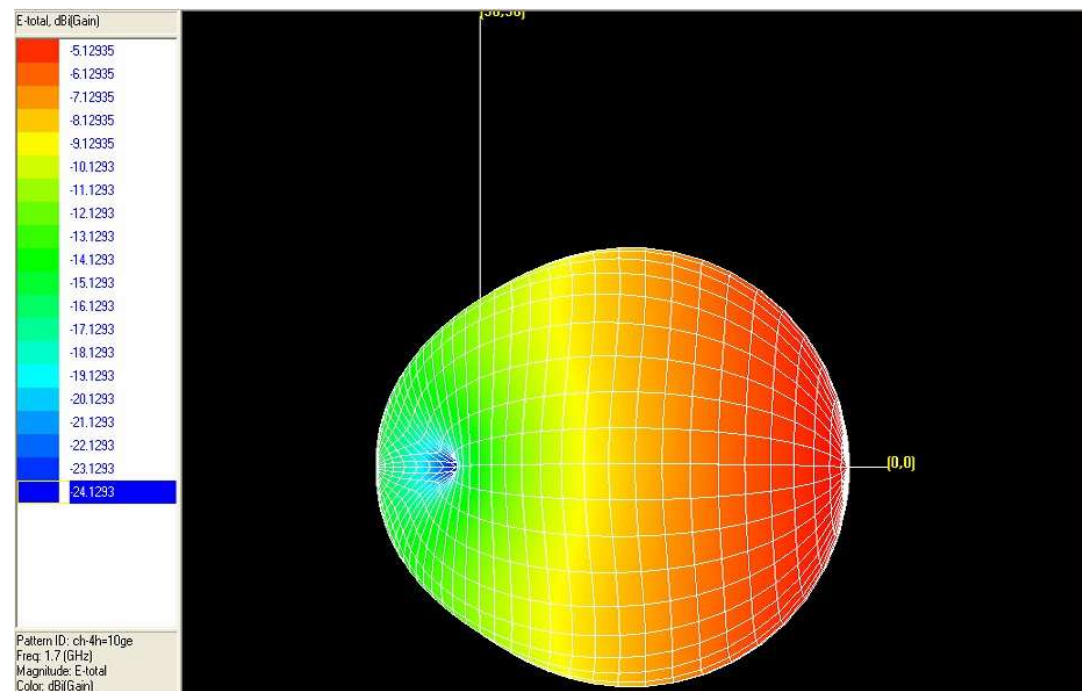


Figure – 3.30 - For substrate height = 10mm

As expected, as the height is increased, the signal propagated through the substrate reduces. This fact becomes clearer from the mapped 3D patterns shown in the following figures.

3.8.3.2 Mapped 3D patterns

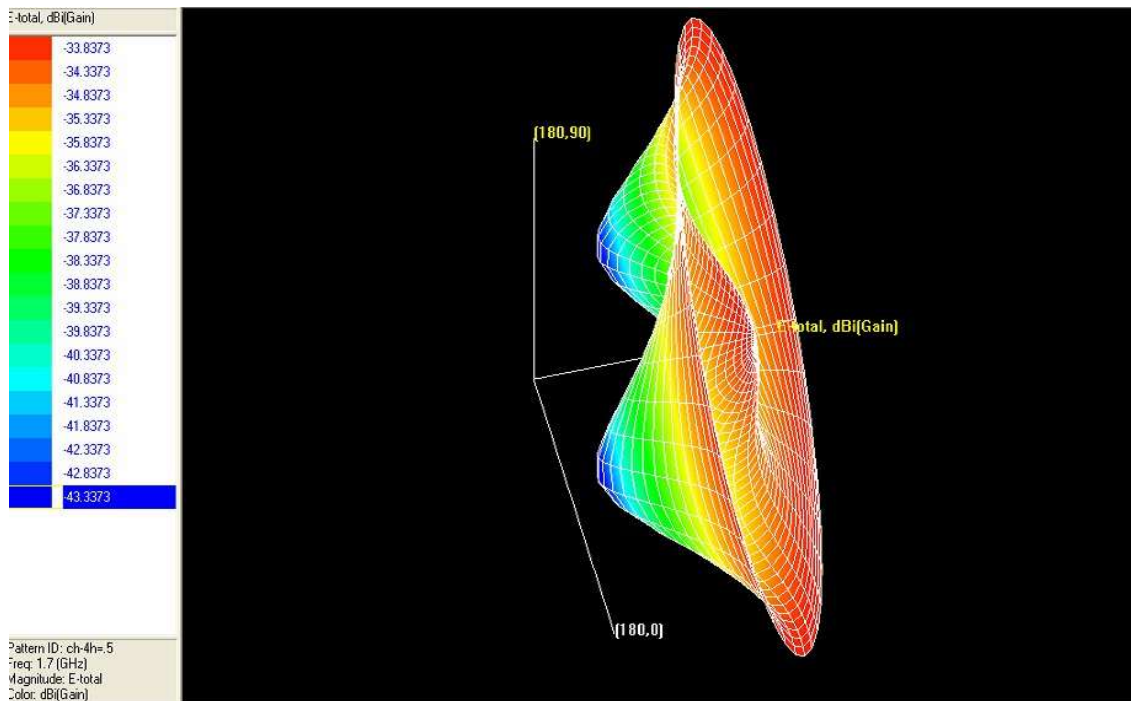


Figure – 3.31 - For Substrate height = 0.5 mm

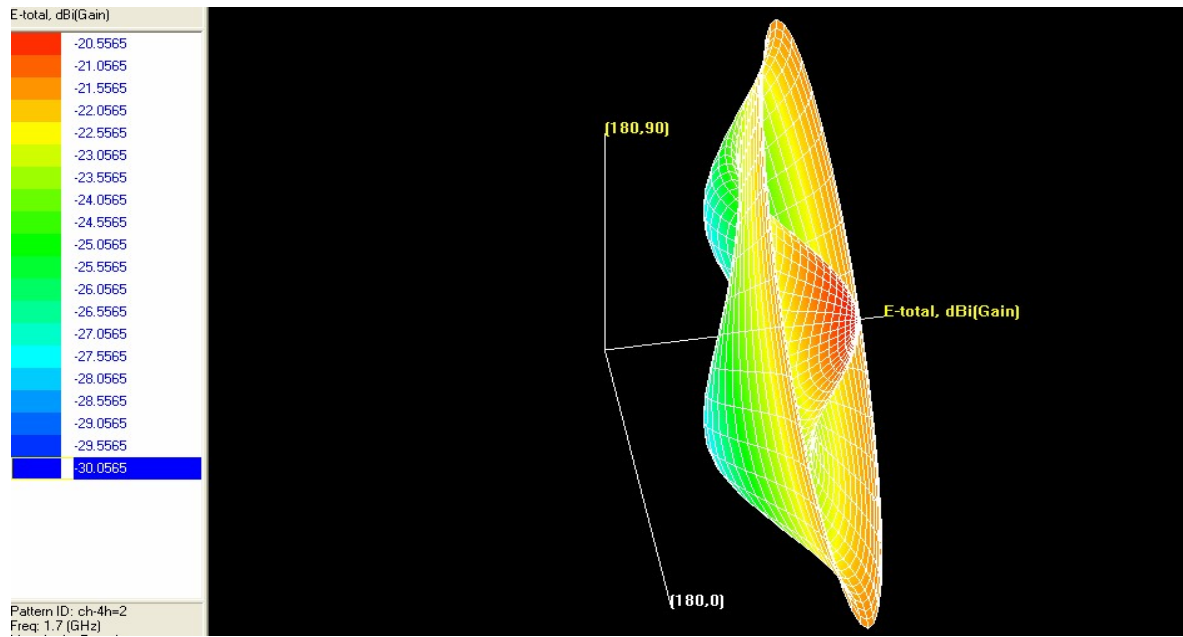


Figure – 3.32 - For Substrate height = 2 mm

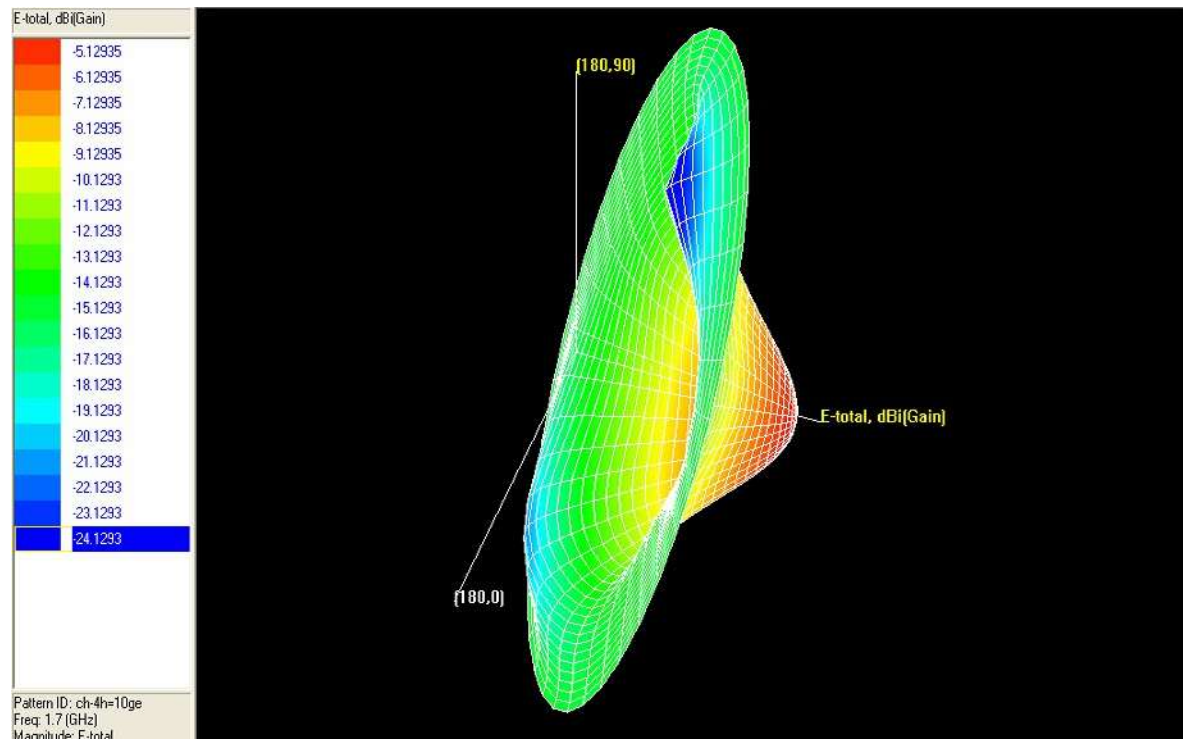


Figure – 3.33 - For Substrate height = 10 mm

It can be seen that as the height of the substrate is increased, the gain in dBi in backward direction decreases. Hence, the expected objective was achieved. The effect of variation of height on other parameters is given in the following pages.

3.8.3.3 Return Loss Curves

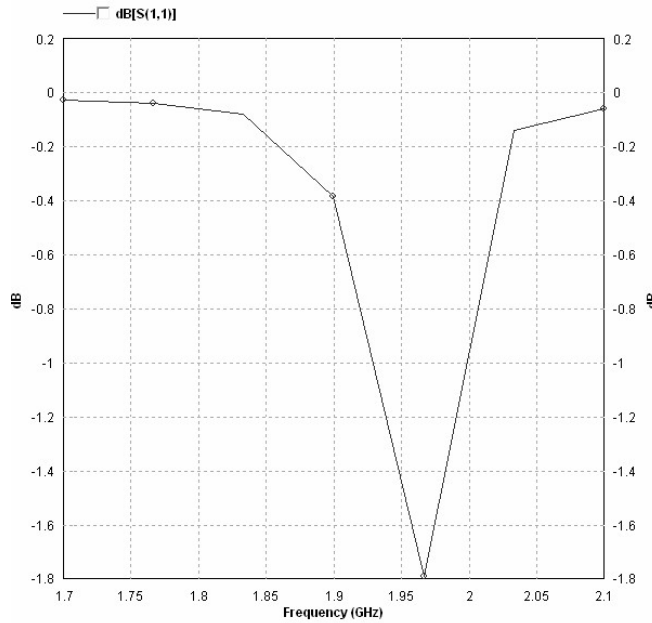


Figure – 3.34 – RL curve for substrate height = 0.5 mm

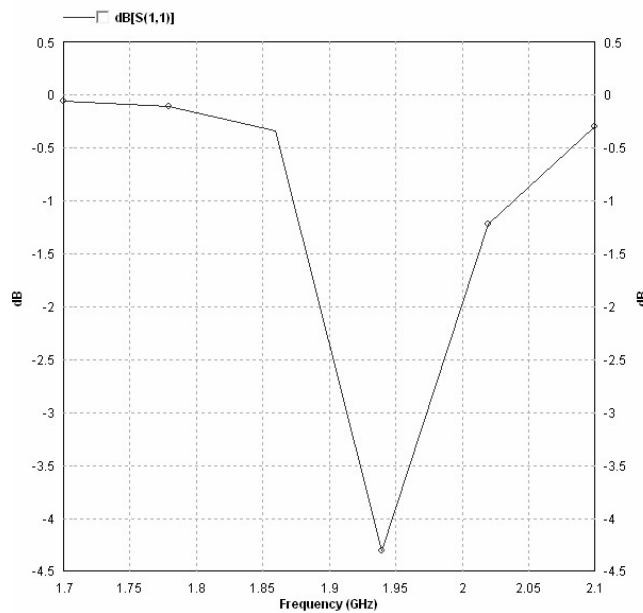


Figure – 3.35 – RL curve for Substrate height = 2 mm

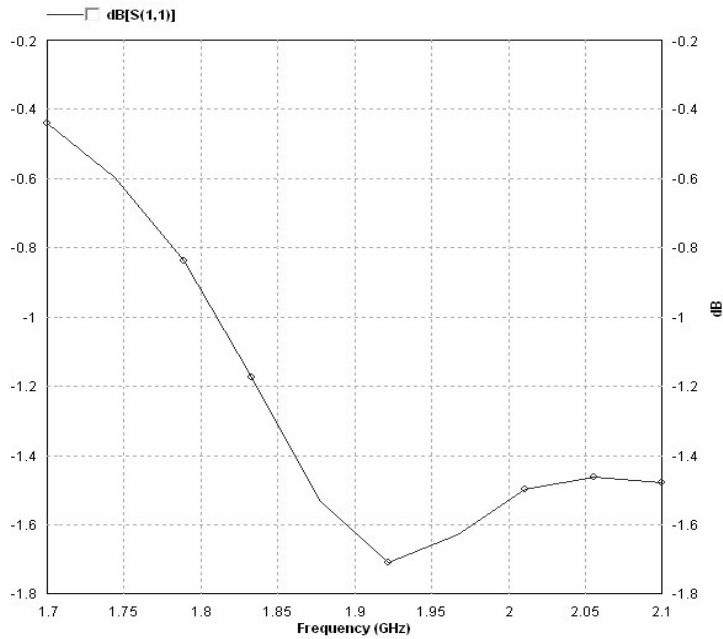


Figure – 3.36 - RL curve for Substrate height = 10 mm

The return loss curve is seen to improve initially and then deteriorate as height is increased.

3.8.3.4 Other Frequency Properties

Frequency	: 1.9 (GHz)
Incident Power	: 0.01 (W)
Input Power	: 0.000849249 (W)
Radiated Power	: 9.09267e-005 (W)
Average Radiated Power	: 7.23572e-006 (W/s)
Radiation Efficiency	: 10.7067%
Antenna Efficiency	: 0.909267%
Conjugate Match Efficiency:	5.35336%
Total Field Properties	:
Gain	: -17.7599 dBi
Directivity	: 2.65322 dBi
Maximum	: at (0, 10) deg.
3dB Beam Width	: (89.5577, 184.065) deg.
Conjugate Match Gain	: -10.0605 dBi

Table – 3.7 - For height= 0.5mm at frequency=1.9GHz

Frequency	:	1.94 (GHz)
Incident Power	:	0.01 (W)
Input Power	:	0.00628805 (W)
Radiated Power	:	0.00359769 (W)
Average Radiated Power	:	0.000286295 (W/s)
Radiation Efficiency	:	57.2146%
Antenna Efficiency	:	35.9769%
Conjugate Match Efficiency	:	28.6073%
Total Field Properties	:	
Gain	:	-0.696194 dBi
Directivity	:	3.74357 dBi
Maximum	:	at (0, 200) deg.
3dB Beam Width	:	(99.771, 129.61) deg.
Conjugate Match Gain	:	-1.69166 dBi

Table – 3.8 - For height= 0.5mm at frequency =1.9GHz

Frequency	:	1.92222 (GHz)
Incident Power	:	0.01 (W)
Input Power	:	0.00325512 (W)
Radiated Power	:	0.00298394 (W)
Average Radiated Power	:	0.000237455 (W/s)
Radiation Efficiency	:	91.6691%
Antenna Efficiency	:	29.8394%
Conjugate Match Efficiency	:	45.8346%
Total Field Properties	:	
Gain	:	0.127792 dBi
Directivity	:	5.37989 dBi
Maximum	:	at (0, 40) deg.
3dB Beam Width	:	(95.0533, 112.184) deg.
Conjugate Match Gain	:	1.99182 dBi

Table – 3.9 - For height= 10mm at frequency =1.9GHz

As seen from the above figures, the radiation efficiency and the gain increase significantly, while other parameters vary slightly, as the height is increased

3.8.4 Effect of variation of permittivity of the substrate on the patch

We observed the effect of variation of permittivity of the substrate on the characteristics of the patch. We performed two sets of simulations.

- 1) With substrate permittivity =2.2
- 2) With substrate permittivity =15

We coupled these simulations with simulations done at substrate permittivity=11.9 (given previously) to analyze the effect of variation permittivity on the substrate. The patch dimensions for the two permittivity values of the substrate are given below.

Permittivity of substrate = 2.2

Height of substrate = 1.5 mm

Length of ground plane = 61.5 mm

Width of ground plane = 71.4 mm

Length of the patch = 52.5 mm

Width of the patch = 62.4 mm

Frequency = 1.9 GHz

Permittivity of substrate = 11.9

Height of substrate = 1.5 mm

Length of ground plane = 31.8 mm

Width of ground plane = 40.1 mm

Length of the patch = 22.8 mm

Width of the patch = 31 .1 mm

Frequency = 1.9 GHz

Permittivity of substrate = 15

Height of substrate = 1.5 mm

Length of ground plane = 29.3 mm

Width of ground plane = 36.9 mm

Length of the patch = 20.3 mm

Width of the patch = 27.9 mm

Frequency = 1.9 GHz

The figures of the meshed patches are given below followed by the simulation results.

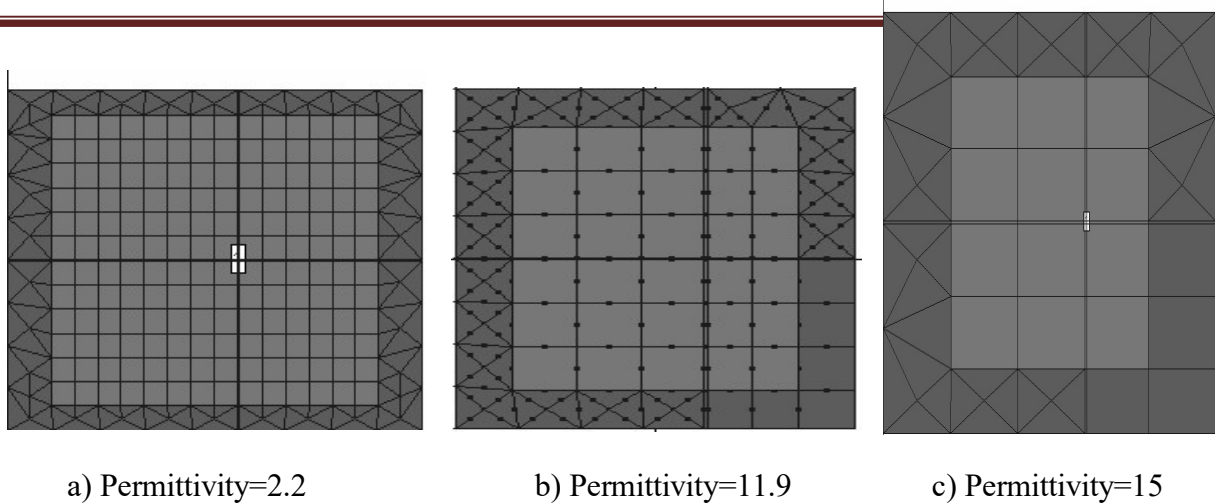


Figure – 3.37 – Meshed patches for varying dielectric constant

3.8.4.1 Return Loss Curves

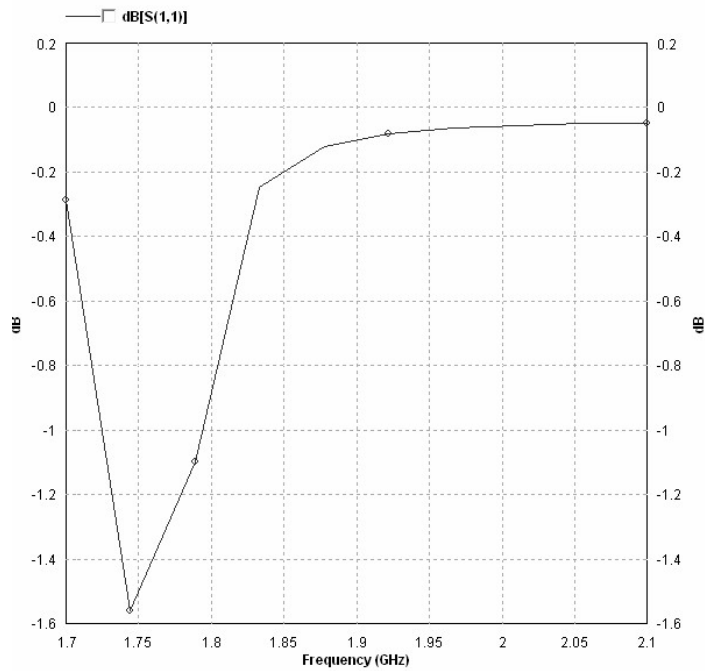


Figure – 3.38 – RL curve for permittivity = 2.2

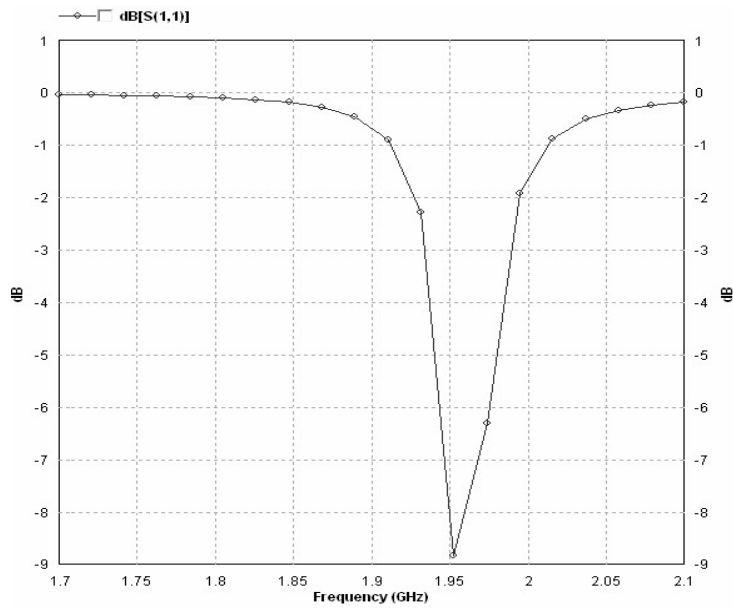


Figure – 3.39 – RL curve for permittivity = 11.9

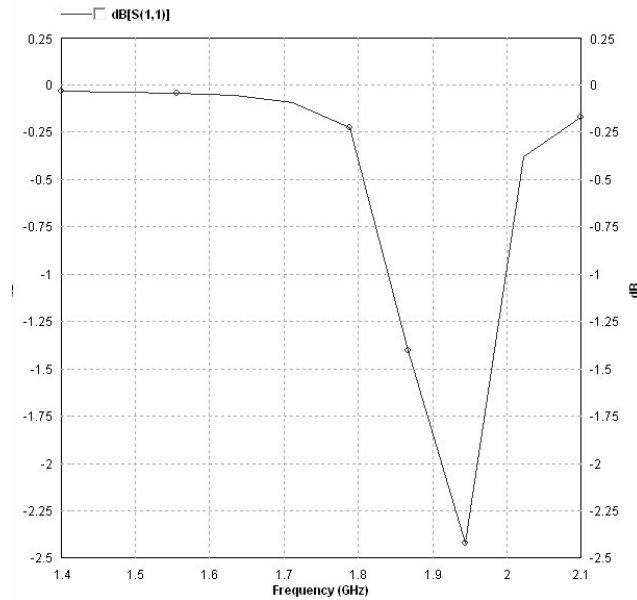


Figure – 3.40 – RL curve for permittivity = 15

It was observed from the return loss curves that the best performance was obtained at permittivity=11.9 because for this value s11 at the operating frequency was minimum.

3.8.4.2 True 3D Patterns

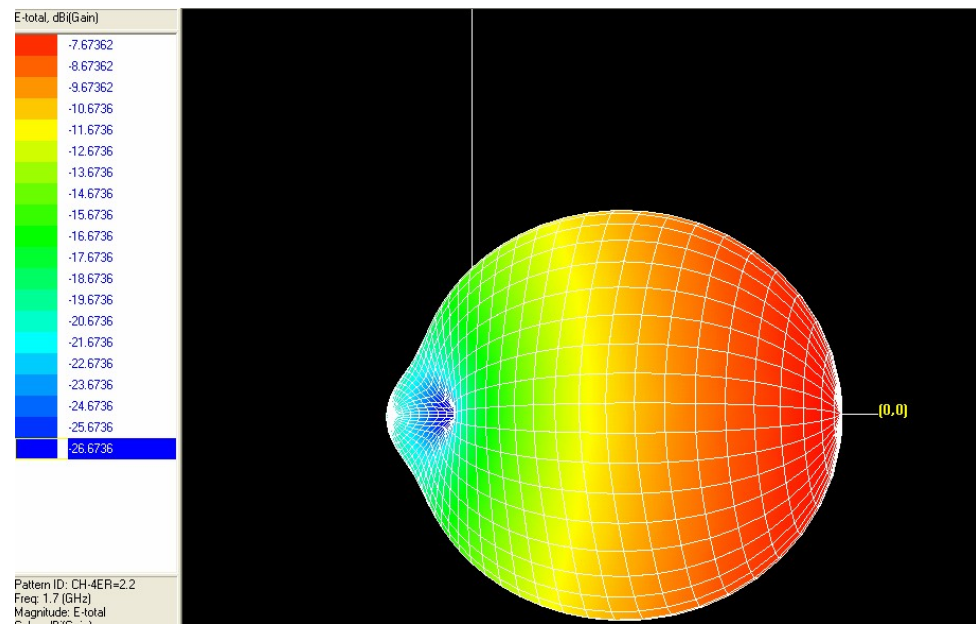


Figure – 3.41 - Permittivity = 2.2

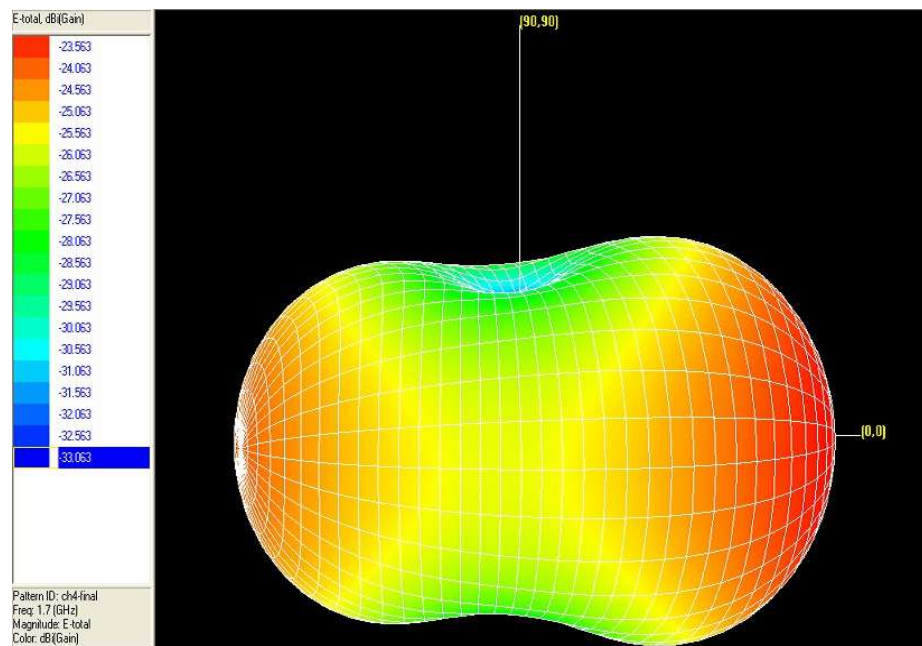


Figure – 3.42 - Permittivity = 11.9

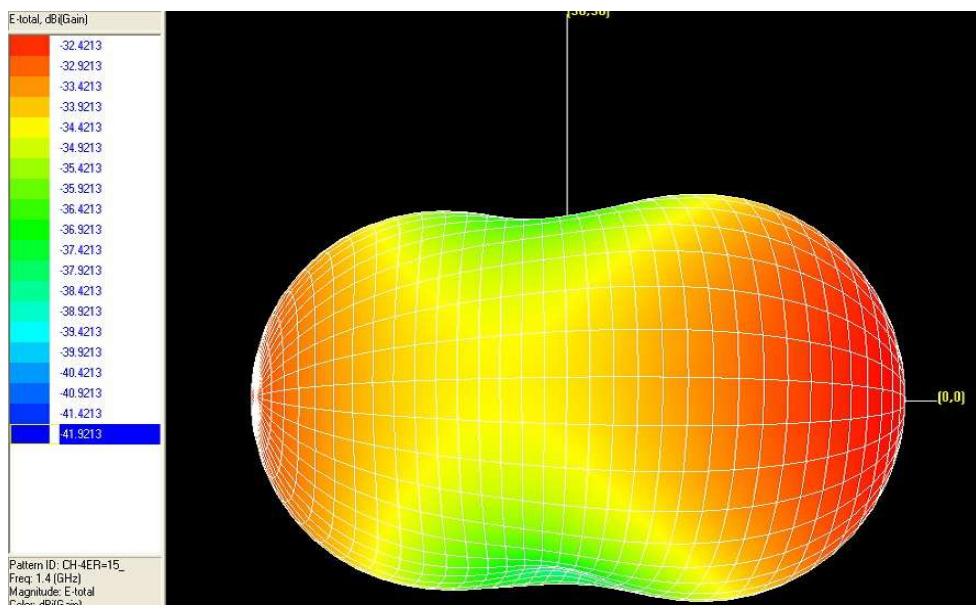


Figure – 3.43 - Permittivity = 15

As permittivity increases, it was observed that the radiation through the substrate (backward direction) increased. This can also be observed from the Mapped 3D pattern. It is also clear that changes in h and permittivity have the opposite effect on the true and mapped 3D radiation patterns.

3.8.4.3 Mapped 3D Patterns

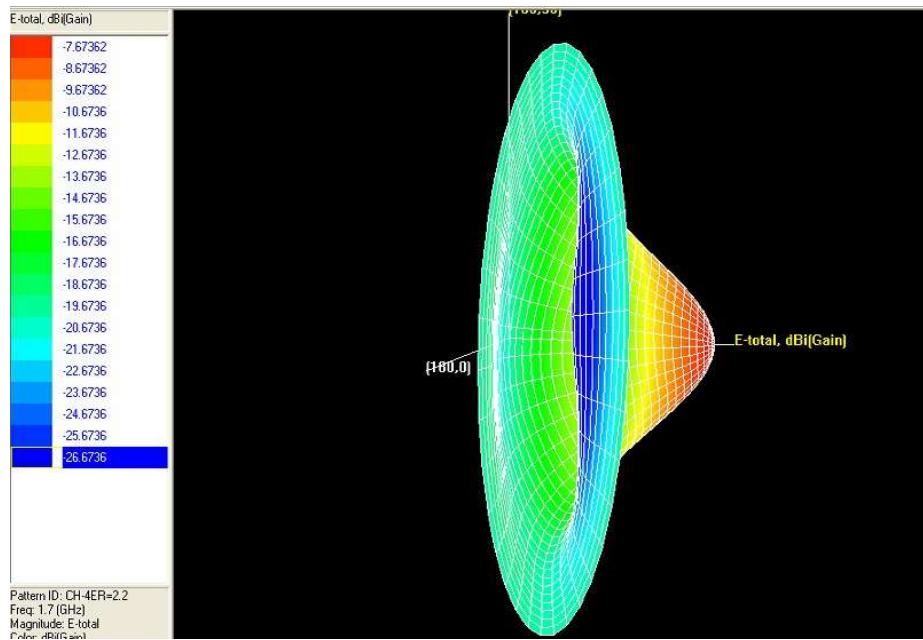


Figure – 3.44 - Permittivity= 2.2

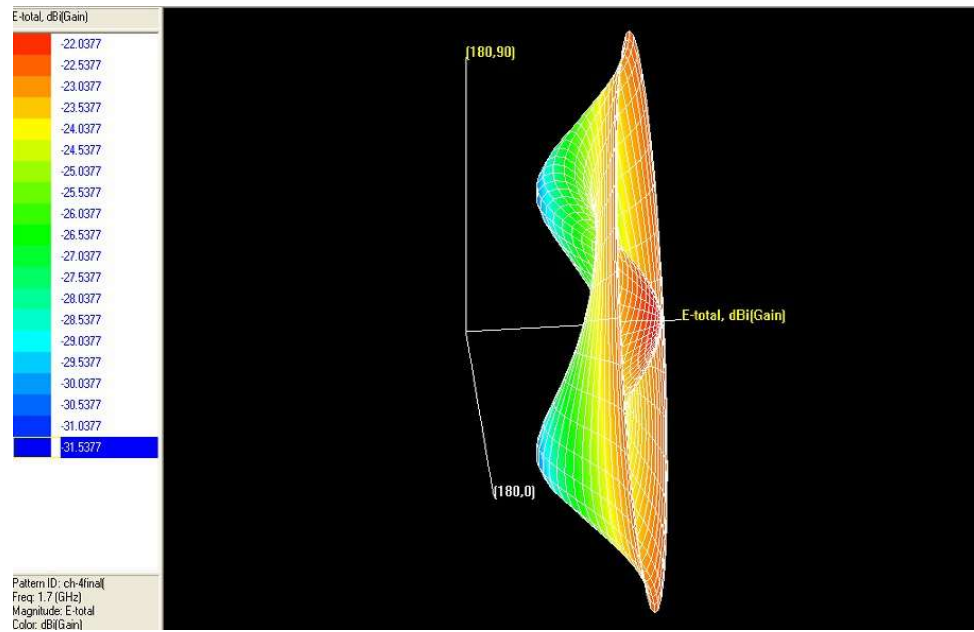


Figure – 3.45 - Permittivity= 11.9

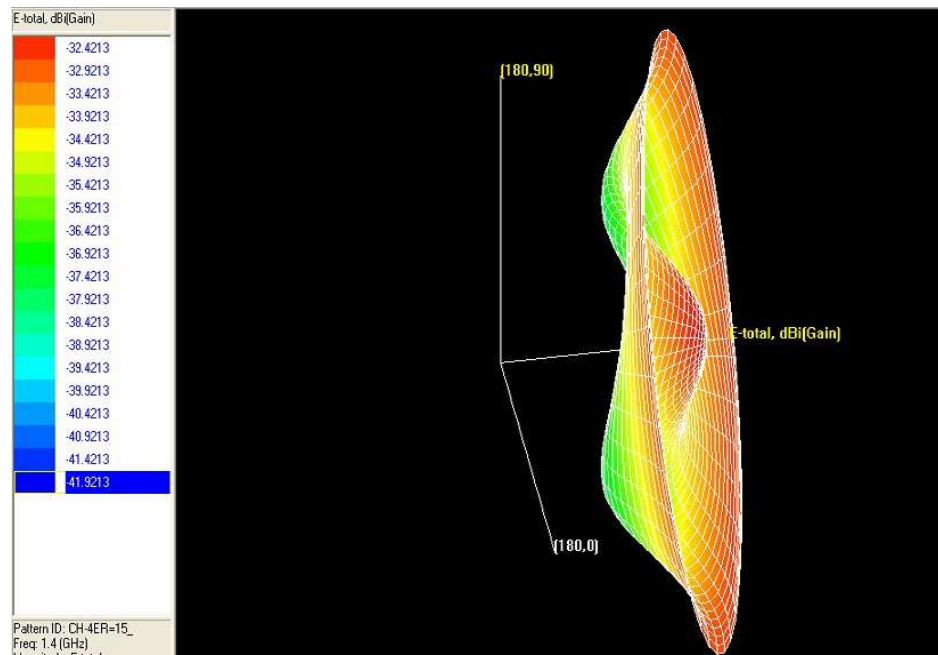


Figure – 3.46 - Permittivity= 15

3.8.4.4 Other Frequency Properties

Frequency	: 1.92222 (GHz)
Incident Power	: 0.01 (W)
Input Power	: 0.000185371 (W)
Radiated Power	: 0.000103529 (W)
Average Radiated Power	: 8.23856e-006 (W/s)
Radiation Efficiency	: 55.8495%
Antenna Efficiency	: 1.03529%
Conjugate Match Efficiency	: 27.9247%
Total Field Properties	:
Gain	: -13.8382 dBi
Directivity	: 6.01117 dBi
Maximum	: at (5, 180) deg.
3dB Beam Width	: (44.3396, 102.652) deg.
Conjugate Match Gain	: 0.471063 dBi

Table – 3.10 - Permittivity = 2.2

Frequency	: 1.91053 (GHz)
Incident Power	: 0.01 (W)
Input Power	: 0.00200064 (W)
Radiated Power	: 0.000842743 (W)
Average Radiated Power	: 6.70633e-005 (W/s)
Radiation Efficiency	: 42.1236%
Antenna Efficiency	: 8.42743%
Conjugate Match Efficiency	: 21.0618%
Total Field Properties	:
Gain	: -7.42624 dBi
Directivity	: 3.31681 dBi
Maximum	: at (0, 80) deg.
3dB Beam Width	: (96.8584, 153.967) deg.
Conjugate Match Gain	: -3.44824 dBi

Table – 3.11 - Permittivity = 11.9

It was observed that for a given frequency the antenna efficiency decreased and the gain increased, as permittivity was increased.

3.8.5 Conclusions based on simulation results

Based on our simulation results we were able to clearly see the effect of changing h and ϵ_r on antenna dimensions and performance. These results are presented in a lucid manner in table 3.13 assuming a fixed frequency of operation.

Parameter Variation	L_g (Length of ground plane)	W_g (Width of ground plane)	L (Length of metal patch)	W (Width of metal patch)
h increased	Increases	Increases	Decreases	Remains Constant
h decreased	Decreases	Decreases	Increases	Remains Constant
ϵ_r increased	Decreases	Decreases	Decreases	Decreases
ϵ_r decreased	Increases	Increases	Increases	Increases

Table – 3.13 – Effect of variation of h and ϵ_r on patch dimensions

Simulation of a 5GHz Patch Antenna

3.8.6 Introduction

One of the experiments in our RF laboratory course required us to obtain the s_{11} curve of a microstrip fed patch antenna. We decided to simulate this antenna, so that students will have not only the s_{11} curve of the antenna, but also its radiation patterns and other parameters such as its directivity, which will help them understand the working of the patch better. The dimensions of the patch and a figure of the meshed patch are given below.

Permittivity of substrate	= 3.2
Height of substrate	= 0.762 mm
Length of ground plane	= 51.0 mm
Width of ground plane	= 51.0 mm
Length of the patch	= 15.0 mm
Width of the patch	= 20.685 mm
Frequency	= 5 GHz
Width of microstrip	= 1.836 mm
Length of microstrip	= 30.45 mm

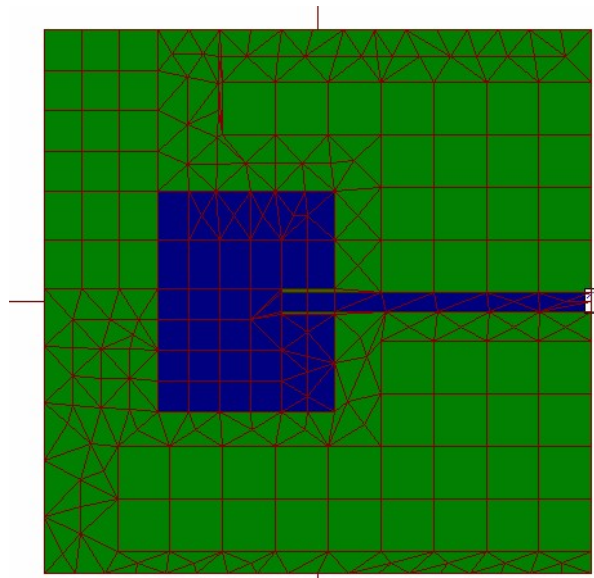


Figure – 3.47 – Meshed Patch

The simulation results follow

3.8.7 True 3D Pattern

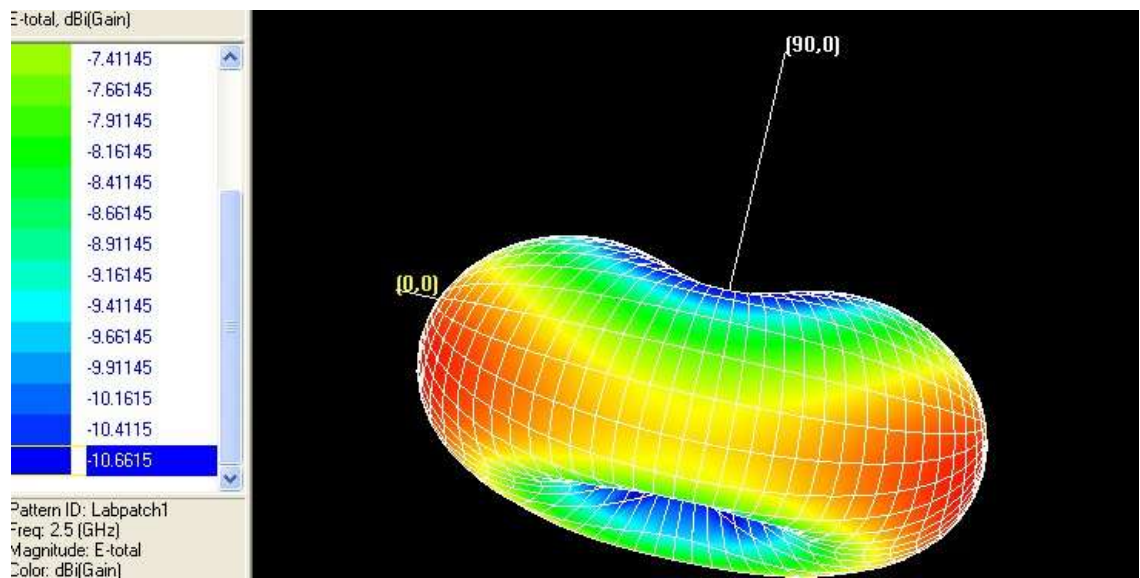


Figure – 3.48 – True 3D Radiation Pattern of the 5 GHz Patch

3.8.8 Mapped 3D Pattern

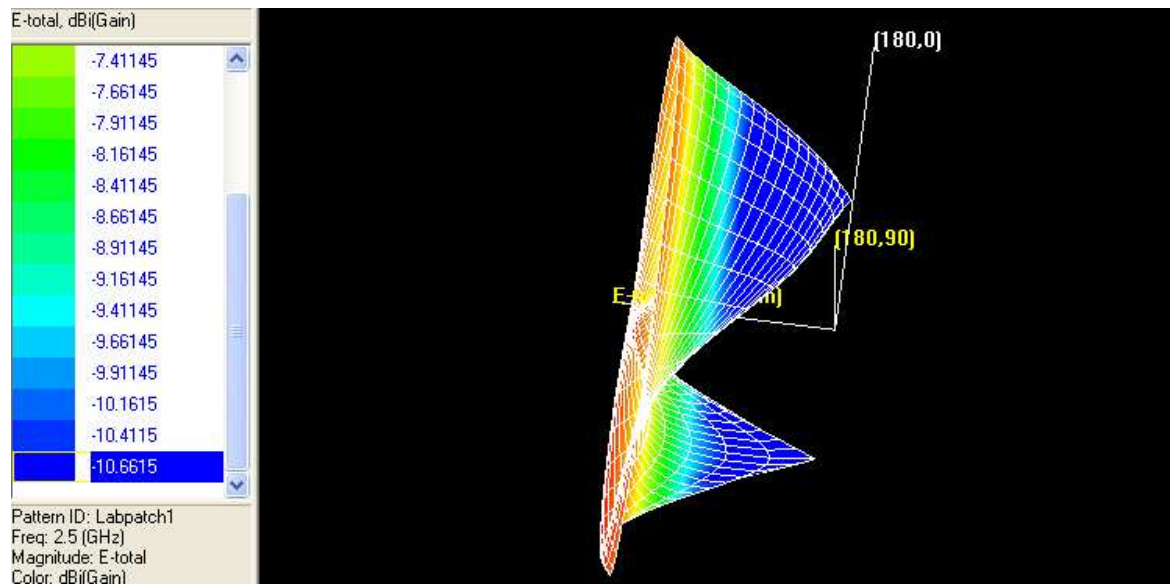


Figure – 3.49 – Mapped 3D Radiation Pattern of the 5 GHz Patch

3.8.9 2D Polar Plot

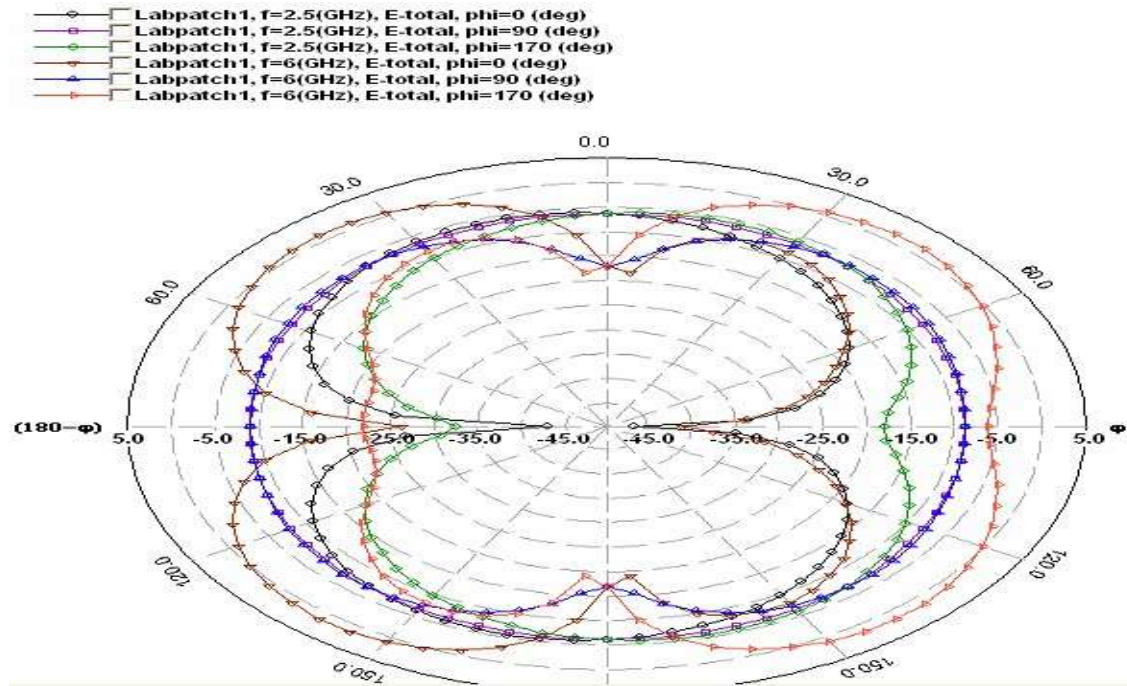


Figure – 3.50 – Polar plot for the antenna for three values of ϕ at $f=2.5\text{GHz}$ and $f=6\text{GHz}$

3.8.10 Other Frequency Properties

Frequency	: 3.5 (GHz)
Incident Power	: 0.01 (W)
Input Power	: 0.00520864 (W)
Radiated Power	: 0.00185641 (W)
Average Radiated Power	: 0.000147728 (W/s)
Radiation Efficiency	: 35.6409%
Antenna Efficiency	: 18.5641%
Conjugate Match Efficiency	: 17.8205%
Total Field Properties	:
Gain	: -3.03168 dBi
Directivity	: 4.28158 dBi
Maximum	: at (40, 220) deg.
3dB Beam Width	: (56.8323, 183.477) deg.
Conjugate Match Gain	: -3.20923 dBi

Table 3.14 – Other parameters for the 5 GHz antenna

3.8.11 Return Loss Curve

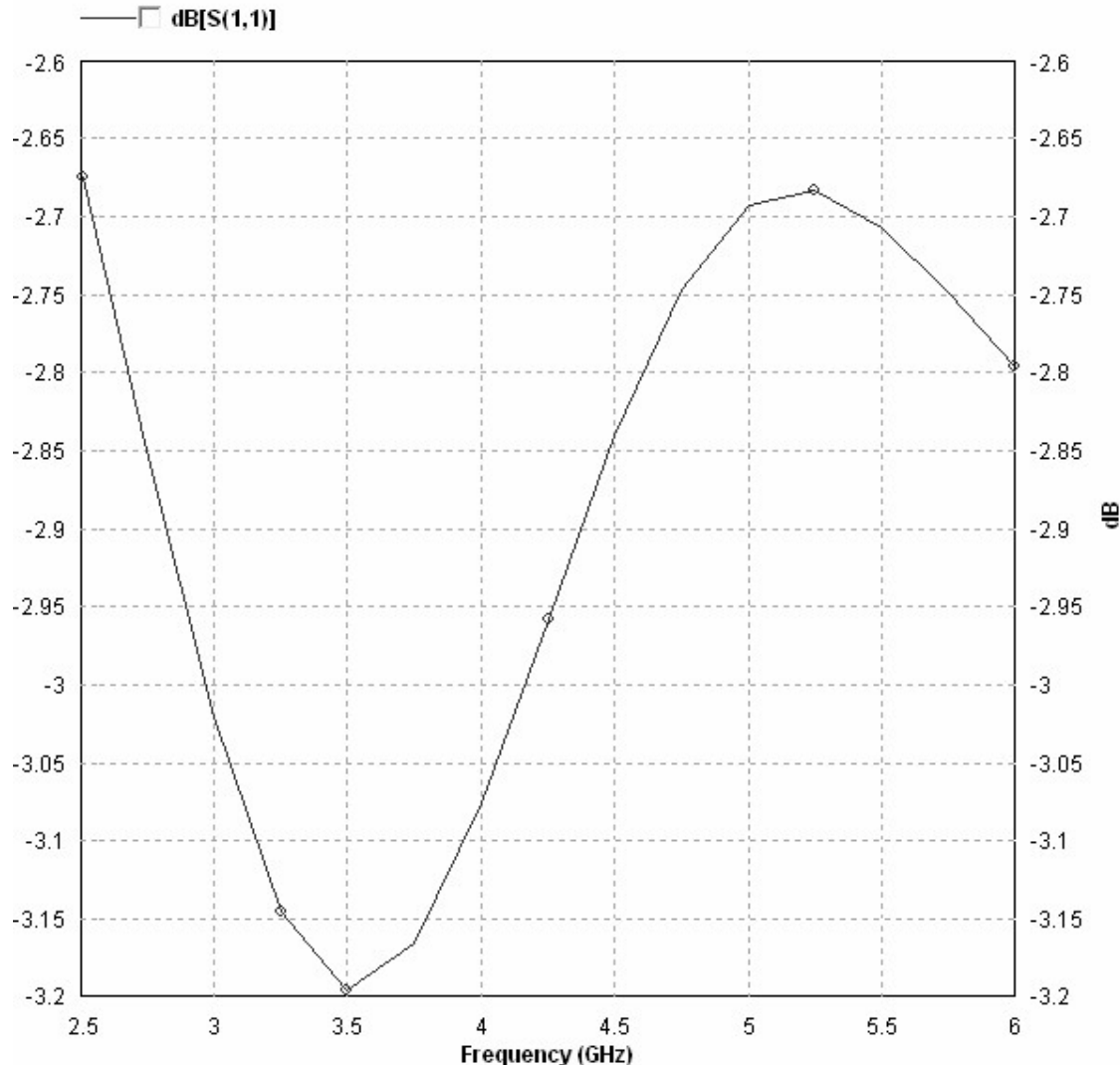


Figure – 3.51 – RL curve for the patch antenna

It can be seen from the return loss curve that the antenna resonates at 3.5GHz. However, this value differs from the expected value of 5GHz. Reasons for the deviation could be that we didn't have all the dimensions of the patch, and data on type of material used for metal and dielectric. Since, we had to manually measure some dimensions, this is a cause for the errors. Another reason is that when we are actually testing the patch, we do so by placing it on a metallic jig. The jig, should act as a ground. When we are doing the simulations, we do not consider the effect of the jig. This too could have brought about the variation.

3.9 Simulation of Dual Band Patch antennas

3.9.1 Antenna 1

3.9.1.1 Introduction

The following patch antenna is a dual band antenna that uses two rectangular patches with bridges connecting them. It shows two minima in its return loss curve unlike all simple patches that only show one such point. The first dual band we simulated was composed of two rectangular patches, which configure 2.4 and 5.5GHz connected to each other using 4-briges. Bridges have a role of connection of each rectangular patch to operate antenna in dual frequency band. In addition, bridges have a role of tuning the frequency bands by changing bridge width. It has an advantage on conversion of frequency band by simply changing the bridge width (BW). The configuration of the patch is shown in figure 52 (a and b).

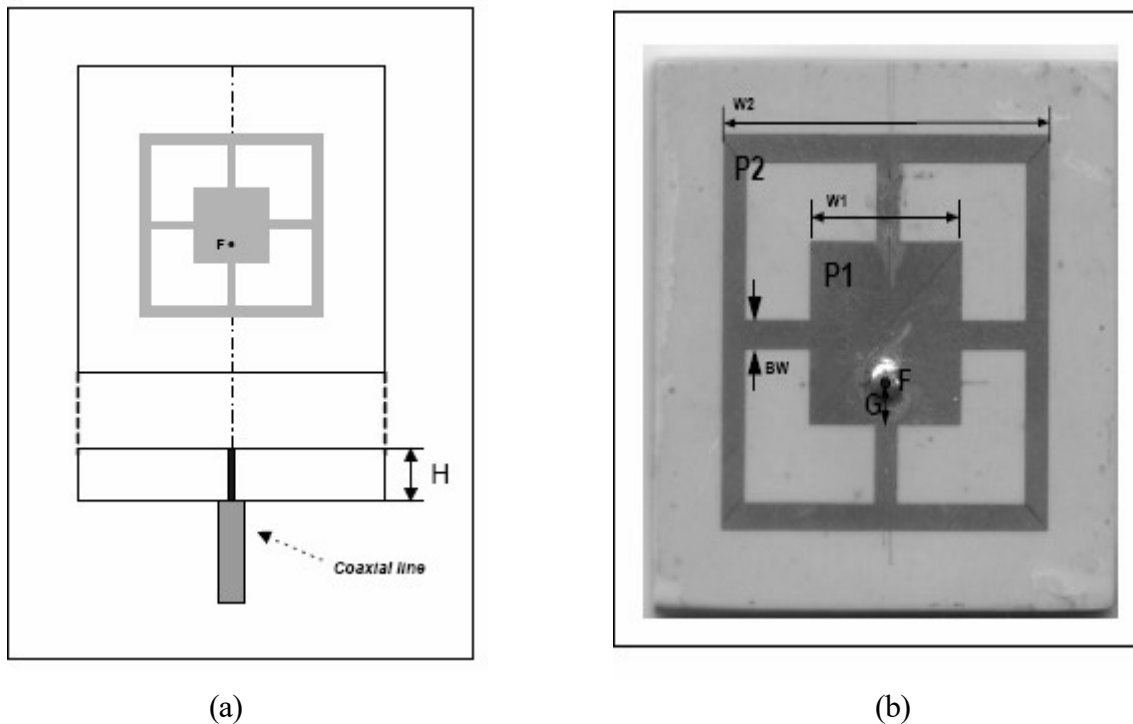


Figure – 52 – Configuration of the dual band patch

The dimensions of the patch are as follows

Ground plane $L_g = W_g = 40$ mm (Square ground plane)
Outer Patch $L = W = w_2 = 28$ mm (Square outer patch)
Inner Patch $L = W = w_1 = 13$ mm (Square inner patch)
Permittivity of substrate = 3.27
Height of substrate = 3.175 mm
Frequency = 2.4 GHz (due to outer patch)
= 5.5 GHz (due to inner patch)
Bridge width = 2 mm

Variation of Bridge Width (BW) affects the frequency of operation thus changing the return loss curve of the antenna, however the simulation of such antennas took nearly four hours to complete so this variation in RL curve due to changes in BW could not be studied by us and only the effect of BW = 2 mm was considered. Location of feeding point (F) is determined by input impedance. It is located at 2.5mm with gap (G) between the nearest edge of inner patch and feeding point. The simulation results follow.

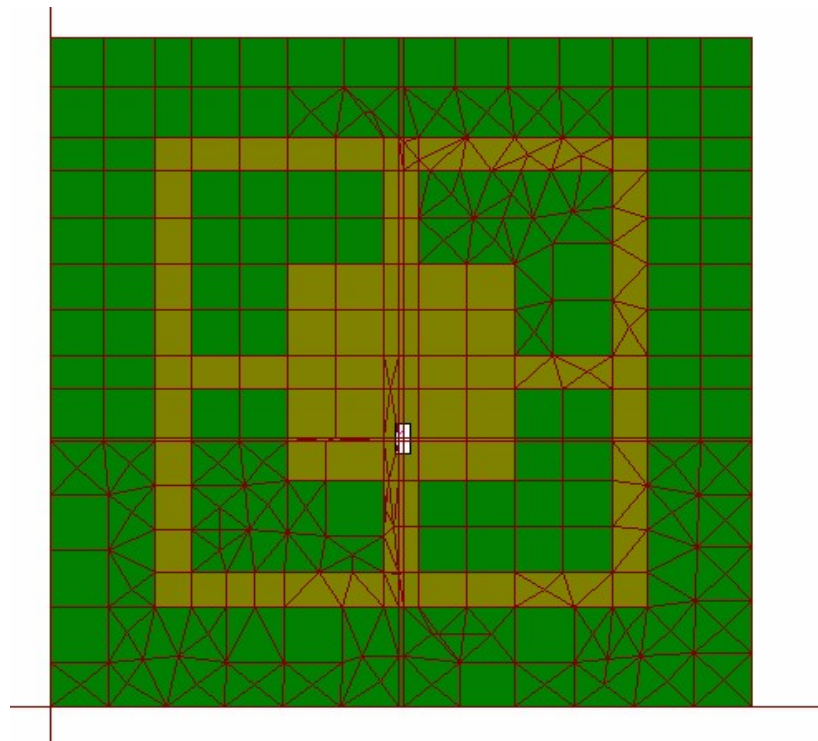


Figure – 3.53 – Meshed dual band patch antenna 1

3.9.2 True 3D Radiation Pattern

The true 3D radiation pattern obtained after simulation is shown in figure 54.

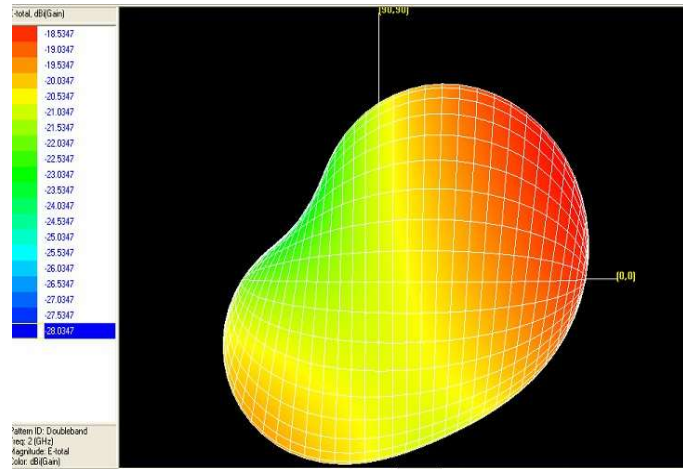


Figure – 3.54 – True 3D Radiation Pattern for dual band antenna 1

3.9.3 Mapped 3D Radiation Pattern

The mapped 3D radiation pattern obtained after simulation is shown in figure 55.

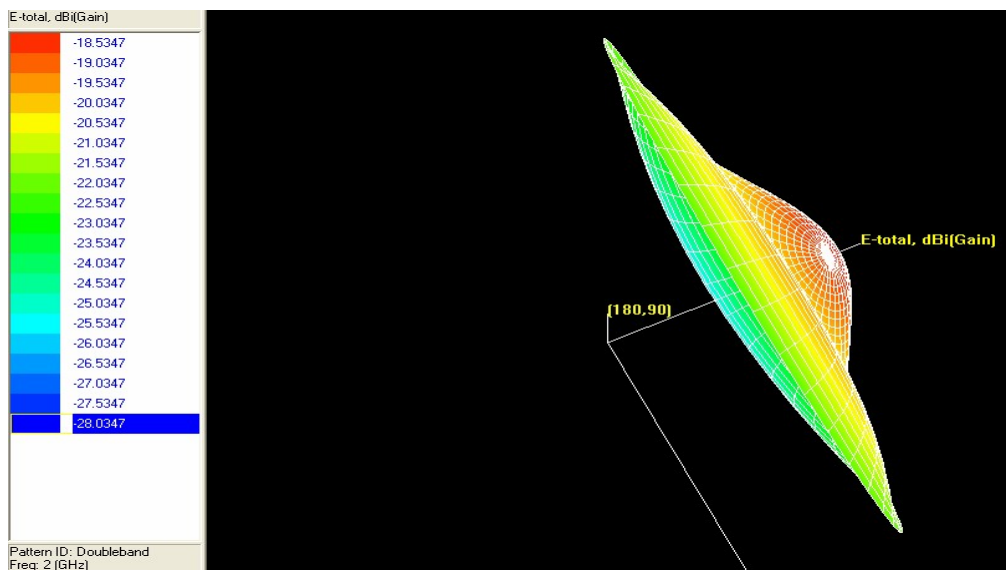


Figure – 3.55 – Mapped 3D Radiation Pattern for dual band antenna 1

3.9.4 2D Polar plot

The 2D polar plot obtained after the simulation is shown in figure 56. It has been plotted for only three frequencies (2 GHz, 3.67 GHz and 5.9 GHz) for three values of φ (0, 90 and 170 degrees).

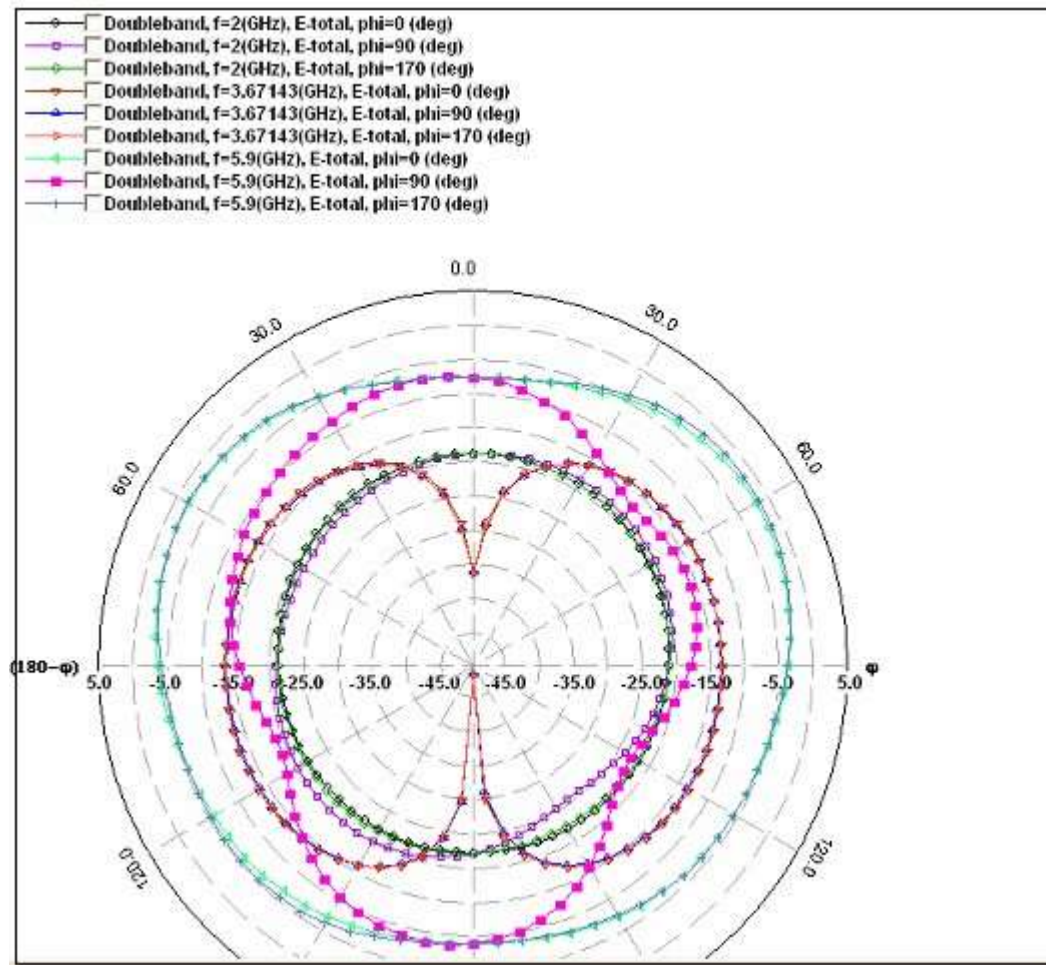


Figure – 3.56 – 2D Polar Plot for dual band antenna 1

3.9.5 Other Frequency Properties

Frequency: 2.27857 (GHz)
Incident Power: 0.01 (W)
Input Power: 0.000356354 (W)
Radiated Power: 0.000255574 (W)
Average Radiated Power: 2.03379e-005 (W/s)
Radiation Efficiency: 71.719%
Antenna Efficiency: 2.55574%
Conjugate Match Efficiency: 35.8595%
Total Field Properties:
Gain: -11.5476 dBi
Directivity: 4.37724 dBi
Maximum: at (5, 90) deg.
3dB Beam Width: (56.0092, 117.71) deg.
Conjugate Match Gain: -0.0767216 dBi
Theta Field Properties:
Gain: -11.5477 dBi
Directivity: 4.37717 dBi
Maximum: at (5, 90) deg.
3dB Beam Width: (9.98227, 56.0093) deg.
Conjugate Match Gain: -0.0767929 dBi

Table – 3.15 – Frequency properties of antenna 1 at 2.27857 GHz

Frequency: 5.34286 (GHz)
Incident Power: 0.01 (W)
Input Power: 0.000785845 (W)
Radiated Power: 0.000561573 (W)
Average Radiated Power: 4.46886e-005 (W/s)
Radiation Efficiency: 71.461%
Antenna Efficiency: 5.61573%
Conjugate Match Efficiency: 35.7305%
Total Field Properties:
Gain: -8.28596 dBi
Directivity: 4.21998 dBi
Maximum: at (65, 230) deg.
3dB Beam Width: (51.5497, 95.0348) deg.
Conjugate Match Gain: -0.249627 dBi
Theta Field Properties:
Gain: -9.33806 dBi
Directivity: 3.16788 dBi
Maximum: at (55, 220) deg.
3dB Beam Width: (46.5382, 89.8729) deg.
Conjugate Match Gain: -1.30173 dBi

Table – 3.16 – Frequency properties of antenna 1 at 5.34286 GHz

3.9.6 Return Loss Curve

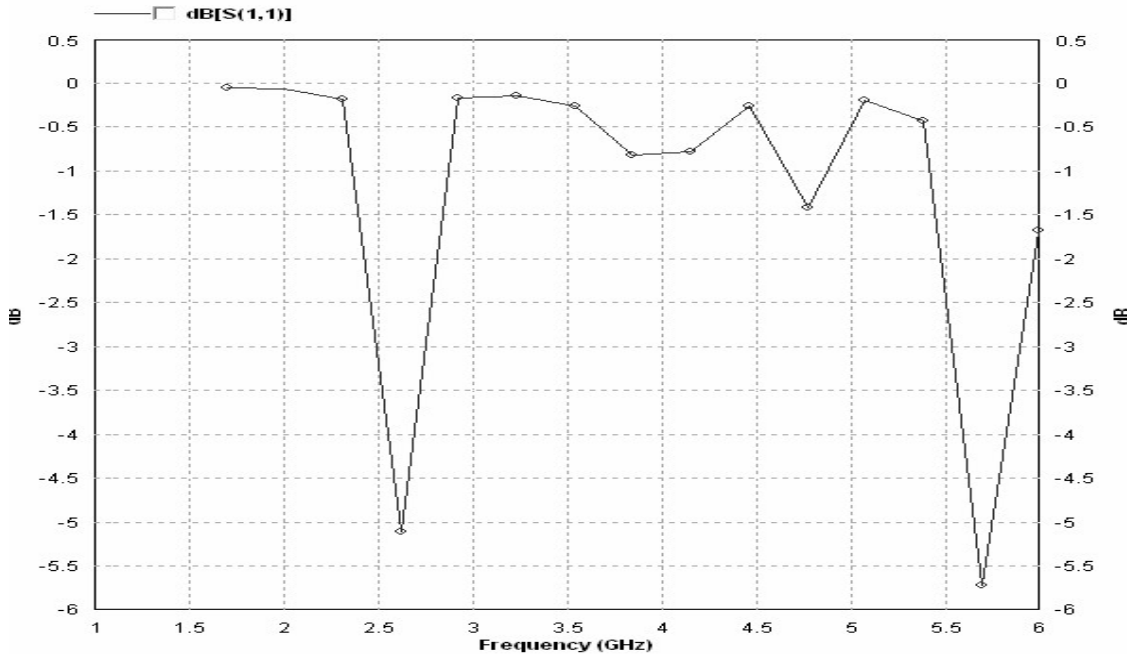


Figure – 3.57 – Return Loss Curve of dual band patch antenna 1

From the return loss curve it is clear that the simulated results match with those theoretically predicted and the antenna does have operating frequencies at 2.4 GHz and 5.5 GHz.

3.10.2 Antenna 2

3.10.2.1 Introduction

We constructed a new dual band antenna with different patch dimensions to observe the shift in operating frequencies caused due to this. It was our intention to construct a patch with operating frequencies at 0.9 GHz and 1.9 GHz (the GSM frequencies used in India and the U.S) so that a theoretical cell phone patch antenna that could be used at two different frequencies could be constructed. By increasing the patch dimensions we were able to lower both operating frequencies, as shown by the simulation results. However, we were unable to lower them to the required values again due to the large simulation time required and trial and error involved. We also noticed that though the theory behind our efforts was correct the resulting patch would be of very large size (greater than 10cm by 10 cm) which wouldn't be practical for a cell phone. Nevertheless, the results for a dual band antenna that operates at 2.3 GHz and 4.6 GHz are presented in the following pages.

The dimensions of the patch are as follows

Ground plane $L_g = W_g = 77$ mm (Square ground plane)
Outer Patch $L = W = w_2 = 56$ mm (Square outer patch)
Inner Patch $L = W = w_1 = 42$ mm (Square inner patch)
Permittivity of substrate = 3.27
Height of substrate = 3.175 mm
Frequency = 2.3 GHz (due to outer patch)
= 4.6 GHz (due to inner patch)
Bridge width = 2 mm

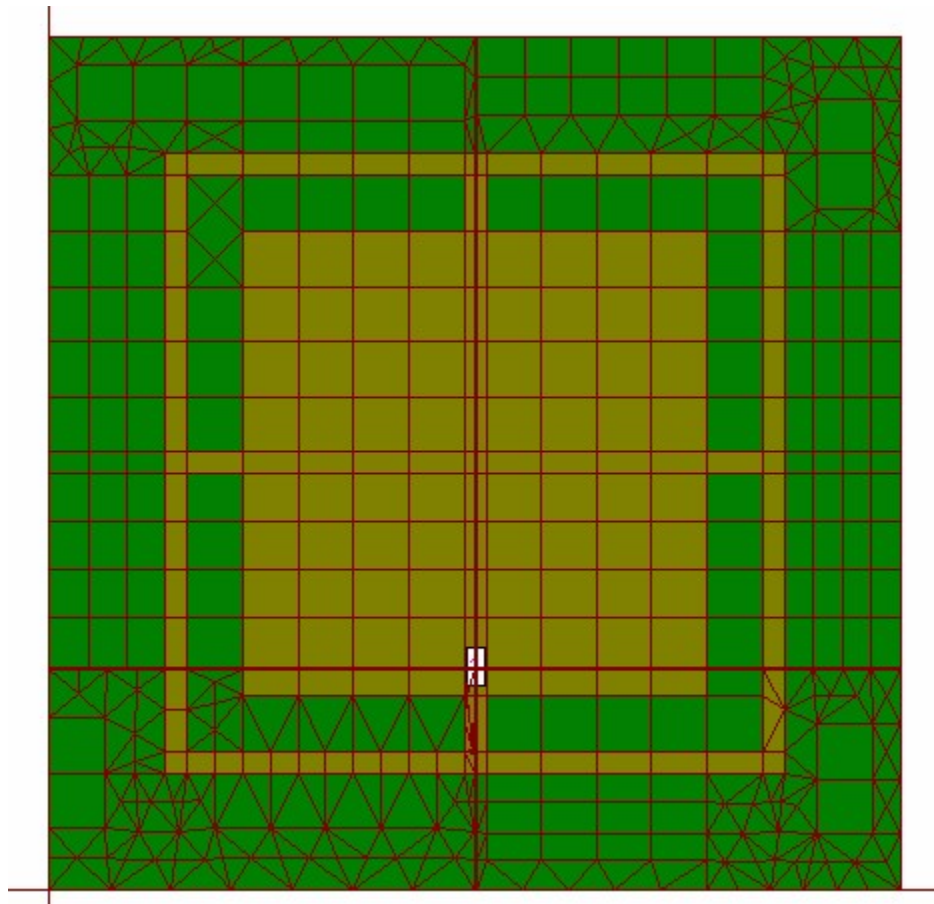


Figure – 3.58 - Meshed dual band patch antenna 2

3.10.2.2 True 3D Radiation Pattern

The true 3D radiation pattern obtained after simulation is shown in figure 3.59.

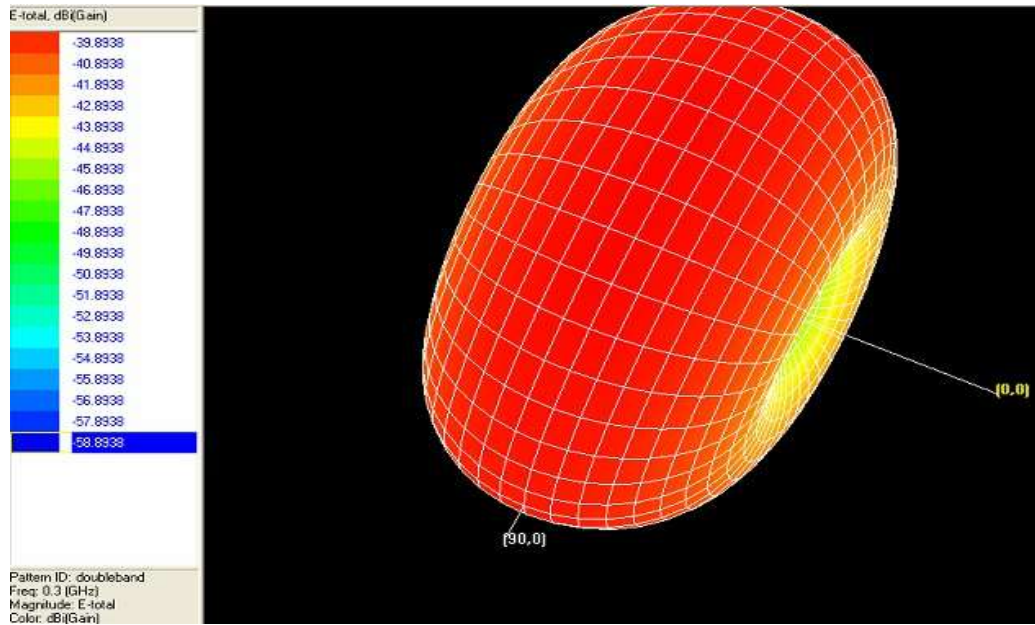


Figure – 3.59 – True 3D Radiation Pattern for Dual Band Antenna 2

3.10.2.3 Mapped 3D Radiation Pattern

The mapped 3D radiation pattern obtained after simulation is shown in figure 3.60.

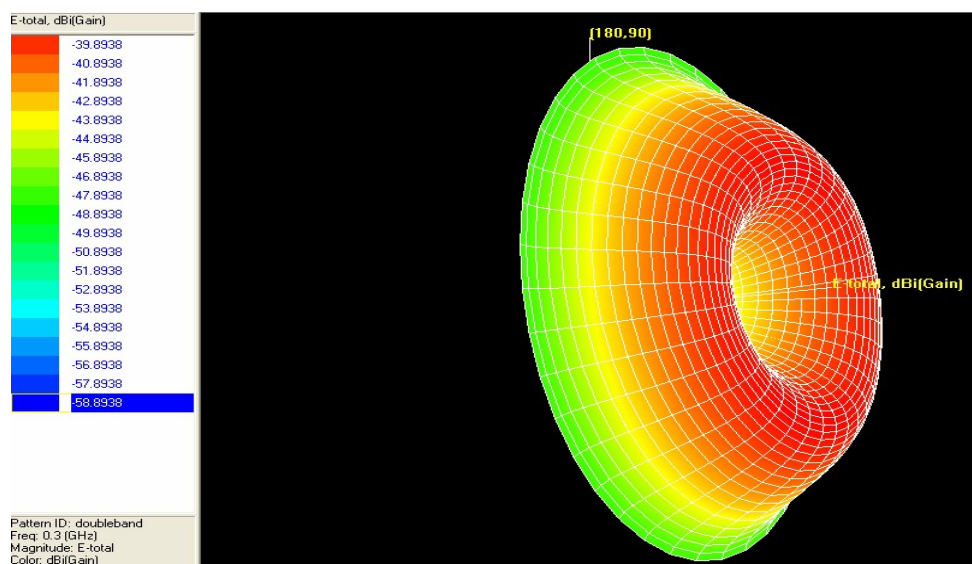


Figure – 3.60 – Mapped 3D Radiation Pattern for Dual Band Antenna 2

3.10.2.4 2D Polar plot

The 2D polar plot obtained after the simulation is shown in figure 3.61. It has been plotted for only three frequencies (0.3 GHz, 5.014 GHz and 5.407 GHz) for three values of ϕ (0, 90 and 170 degrees).

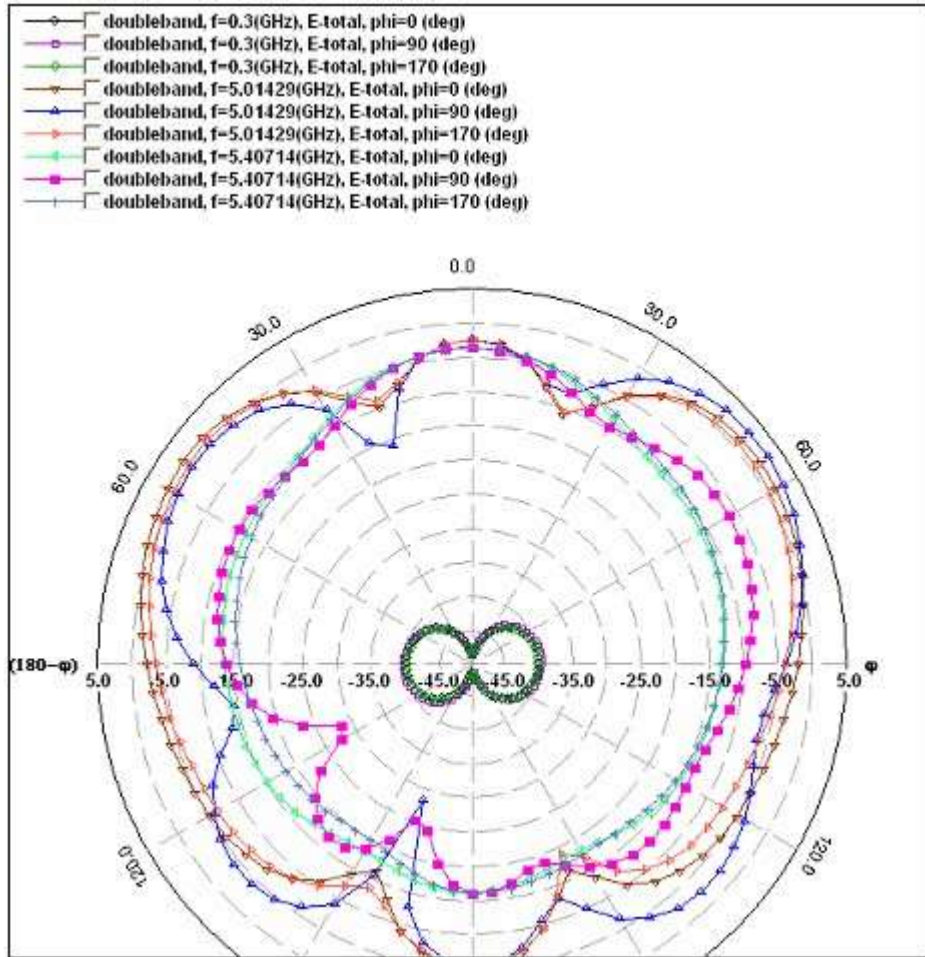


Figure – 3.61 – 2D Polar Plot for Dual Band Antenna 2

Other Frequency Properties

Frequency: 2.26429 (GHz)
Incident Power: 0.01 (W)
Input Power: 0.00757225 (W)
Radiated Power: 0.00529582 (W)
Average Radiated Power: 0.000421428 (W/s)
Radiation Efficiency: 69.9372%
Antenna Efficiency: 52.9582%
Conjugate Match Efficiency: 34.9686%
Total Field Properties:
Gain: 3.92592 dBi
Directivity: 6.6866 dBi
Maximum: at (0, 20) deg.
3dB Beam Width: (88.0808, 91.6176) deg.
Conjugate Match Gain: 2.12338 dBi
Theta Field Properties:
Gain: 3.92485 dBi
Directivity: 6.68552 dBi
Maximum: at (0, 90) deg.
3dB Beam Width: (0, 0) deg.
Conjugate Match Gain: 2.1223 dBi

Table – 3.17 – Frequency properties of antenna 2at 2.26429 GHz

Frequency: 4.62143 (GHz)
Incident Power: 0.01 (W)
Input Power: 0.0090008 (W)
Radiated Power: 0.00746423 (W)
Average Radiated Power: 0.000593984 (W/s)
Radiation Efficiency: 82.9285%
Antenna Efficiency: 74.6423%
Conjugate Match Efficiency: 41.4642%
Total Field Properties:
Gain: 3.74383 dBi
Directivity: 5.01399 dBi
Maximum: at (50, 230) deg.
3dB Beam Width: (48.3662, 121.301) deg.
Conjugate Match Gain: 1.19072 dBi
Theta Field Properties:
Gain: 2.54818 dBi
Directivity: 3.81834 dBi
Maximum: at (55, 270) deg.
3dB Beam Width: (44.816, 95.3565) deg.
Conjugate Match Gain: -0.00492768 dBi

Table – 3.18 – Frequency properties of antenna 2 at 4.62143 GHz

Return Loss Curve

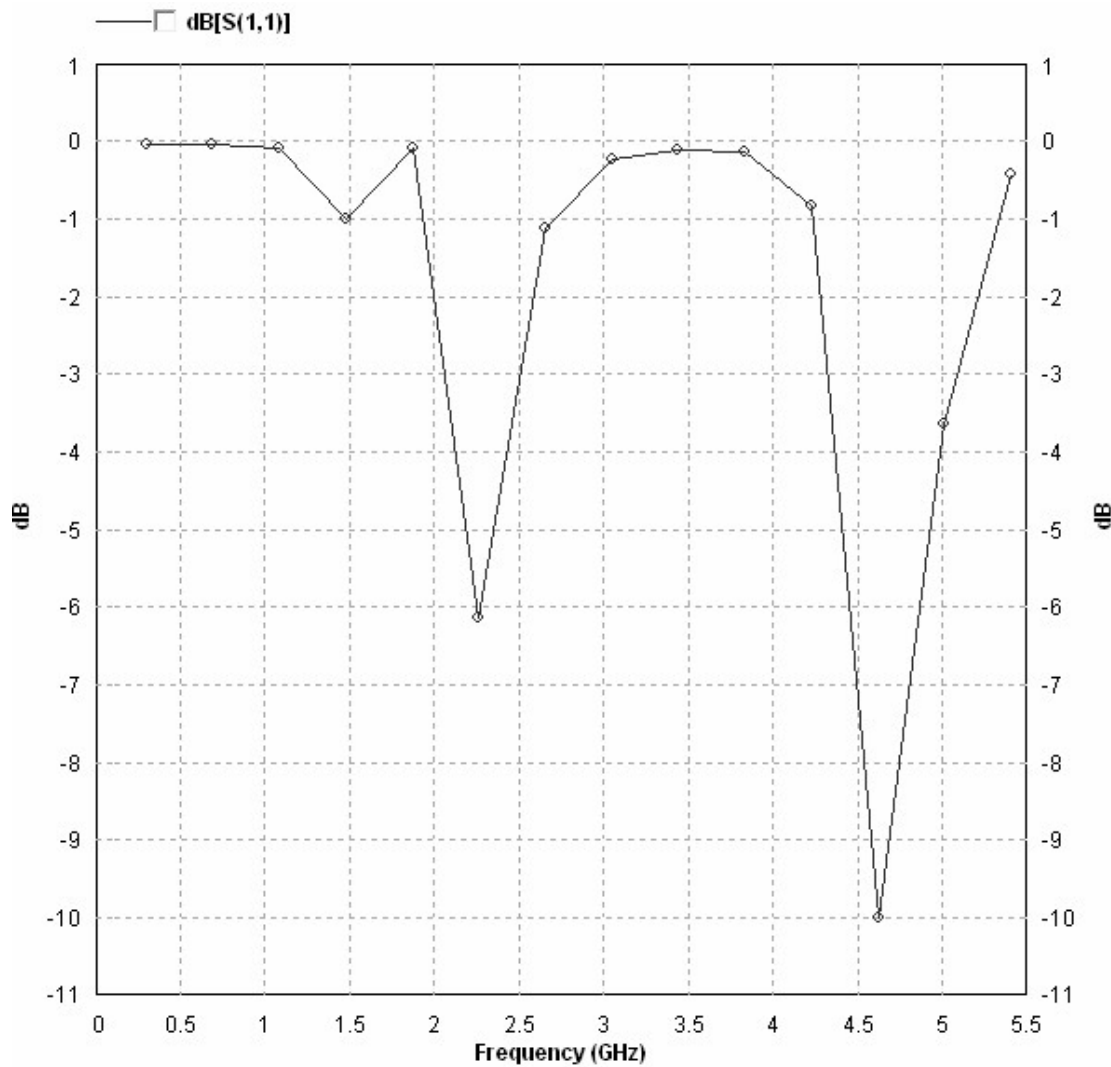


Figure – 3.62 – Return Loss Curve of dual band patch antenna 2

From the return loss curve it is clear that the antenna has operating frequencies at 2.4 GHz and 5.5 GHz.

Chapter 4

Conclusions and Scope for Improvement

4.1 Conclusions

Upon the conclusion of our project we made the following assessment of our work:

The overall working of antennas was understood. The major parameters (such as Return Loss curves, Radiation Patterns, Directivity and Beamwidth) that affect design and applications were studied and their implications understood. The constructed slotted waveguide and biquad antennas operated at the desired frequency and power levels. Several patch antennas were simulated (using IE3D) and the desired level of optimization was obtained. It was concluded that the hardware and software results we obtained matched the theoretically predicted results.

4.2 Scope for Improvement

There were some areas we felt we did not address. They were

- The experimental radiation patterns of the constructed antennas could not be obtained and compared with the theoretical patterns
- Though we were able to simulate several patch antennas, we were unable to fabricate one and compare the practical and simulated results.
- A more complete study of different field solvers and simulators (such as Sonnet, AWR, HFSS etc) could not be made. We were only able to focus on IE3D.

References

Books

Modern Antenna Design by Thomas Milligan (2nd edn – Thomas Wiley and Sons)

Antenna Theory and Design by Robert S. Elliot (Wiley Publications)

Antennas for all Applications by John Krauss (Third edition TMH)

Electromagnetic Waves and Radiating Systems – Edward C. Jordan and Keith G. Balmain (2nd edn – PHI Publishers)

Research Papers

A Dual band antenna for WLAN applications by double rectangular patch with 4 bridges – Chang Won Jung and Franco De Flaviis

Design and analysis of an Electrically Steerable Microstrip Antenna for Ground to Air Use – Johan Lagerqvist

A High-Performance Dual Frequency Microstrip Antenna for GPS
Luigi Boccia, Giandomenico Amendola and Giuseppe Di Massa

Analysis and Design of Equilateral Triangle Microstrip Patch Antenna with Microstrip Feed – V. Sarala and V. M. Pandharipande

Websites

www.ingecom.ch

www.zealand.com

www.wikipedia.com

www.howstuffworks.com

www.sonnetsoftware.com